Bioactive Materials 24 (2023) 197–235

Contents lists available at ScienceDirect

Bioactive Materials

journal homepage: www.keaipublishing.com/en/journals/bioactive-materials

Review article

Structural and biological engineering of 3D hydrogels for wound healing

Mohammad Hadi Norahan [a,b], Sara Cristina Pedroza-González [a,b], Mónica Gabriela Sánchez-Salazar [b,c], Mario Moisés Álvarez [b,c,**], Grissel Trujillo de Santiago [a,b,*]

[a] Escuela de Ingeniería y Ciencias, Tecnológico de Monterrey, Monterrey, NL, 64849, Mexico
[b] Centro de Biotecnología-FEMSA, Tecnológico de Monterrey, Monterrey, Nuevo León, CP, 64849, Mexico
[c] Departamento de Bioingeniería, Tecnológico de Monterrey, Monterrey, Nuevo León, CP, 64849, Mexico

ARTICLE INFO

Keywords:
Wound healing
Wound dressing
Hydrogel
Tissue engineering
3D culture

ABSTRACT

Chronic wounds have become one of the most important issues for healthcare systems and are a leading cause of death worldwide. Wound dressings are necessary to facilitate wound treatment. Engineering wound dressings may substantially reduce healing time, reduce the risk of recurrent infections, and reduce the disability and costs associated. In the path of engineering of an ideal wound dressing, hydrogels have played a leading role. Hydrogels are 3D hydrophilic polymeric structures that can provide a protective barrier, mimic the native extracellular matrix (ECM), and provide a humid environment. Due to their advantages, hydrogels (with different architectural, physical, mechanical, and biological properties) have been extensively explored as wound dressing platforms. Here we describe recent studies on hydrogels for wound healing applications with a strong focus on the interplay between the fabrication method used and the architectural, mechanical, and biological performance achieved. Moreover, we review different categories of additives which can enhance wound regeneration using 3D hydrogel dressings. Hydrogel engineering for wound healing applications promises the generation of smart solutions to solve this pressing problem, enabling key functionalities such as bacterial growth inhibition, enhanced re-epithelialization, vascularization, improved recovery of the tissue functionality, and overall, accelerated and effective wound healing.

1. Introduction

The skin is the biggest organ in the body, and its major role is to protect the body from external elements. A wound is known as an injury or disintegration of skin tissue, which could happen due to different causes, including thermal injury, trauma, and chronic ulcerations derived from diabetes mellitus, pressure, and venous stasis [1]. Chronic wounds are becoming increasingly common. Venous ulcers, whether active or healed, affect 1% of the population in the United States [2]. Pressure ulcers will affect 0.75% of the population. Every year, one million of the 30 million + diabetic individuals in the United States will develop a foot ulcer, and another 6 to 7 million will develop ulcers over their lifetimes [2], many requiring amputations. Another 3 million people in the United States suffer from pressure and leg ulcers, including venous ulcers, with yearly treatment expenditures of up to $8 billion [1]. Although recent therapeutic interventions, including skin substitutes, have improved skin healing in the clinic, they are still very perfectible and have not fully shown the ability to effectively restore normal skin structure and function. Despite the advances in wound healing, the ultimate purpose would be to engineer tissues that could provide appropriate biological and structural features to effectively regenerate the wounded area [1,3]. In this regard, it is critical to investigate the nature of wound healing and its underlying mechanisms in order to follow and mimic them as closely as possible.

Inflammation, proliferation, and remodeling are three major phases of wound healing that overlap significantly. Clot development is the initial tissue response to a wound to prevent bleeding. At the same time, inflammatory cytokines that control blood flow to the wound bed are released, and lymphocytes and macrophages are recruited to fight infection. Subsequent to the primary inflammatory response, the

Peer review under responsibility of KeAi Communications Co., Ltd.
* Corresponding author. Escuela de Ingeniería y Ciencias, Tecnológico de Monterrey, Monterrey, NL, 64849, Mexico.
** Corresponding author. Centro de Biotecnología-FEMSA, Tecnológico de Monterrey, Monterrey, Nuevo León, CP, 64849, Mexico.
E-mail addresses: mario.alvarez@tec.mx (M.M. Álvarez), grissel@tec.mx (G. Trujillo de Santiago).

https://doi.org/10.1016/j.bioactmat.2022.11.019
Received 9 August 2022; Received in revised form 7 November 2022; Accepted 25 November 2022

proliferation phase takes place with angiogenesis, fibroblast proliferation, and collagen deposition [4]. Later, granulation tissue, a tissue with a high content of cells and blood capillaries, is formed. Ultimately, during remodeling, the proliferation and migration of keratinocytes are induced by myofibroblasts and factors such as TGF-β, to replace granulation tissue with scar tissue and to reconstruct the epidermal structure. A chronic wound can occur if any of these healing processes is continued for an extended period.

Chronic wounds are frequently linked to basic medical disorders that impede wound healing (Fig. 1). Subsequently, these abnormalities may be associated with a loss of tissue viability, suboptimal local tissue permeability, and an elevated and sustained inflammatory response [4]. One of the key differences between acute and chronic wounds is that the ordered phases associated with acute wound healing are not identical to the asynchrony of the healing process occurring in chronic human wounds [5]. Within the chronic wound, several phases of the wound repair process may be occurring simultaneously or out of sequence [5]. Nonhealing wounds are plagued by bacterial and, in rare circumstances, fungal colonization or infection [5]. These features include a lack of epithelium and its barrier capabilities, continuous wound exudation caused by bacterial products and inflammation, inadequate blood flow, and hypoxia [6]. Growth factor imbalances have been linked to the inadequate healing response seen in chronic wounds [7]. Another problem is that all chronic wounds have reduced angiogenesis, which exacerbates the tissue damage already caused by persistent hypoxia and poor nutrient supply [6]. For instance, impaired angiogenesis in diabetics leads to inadequate blood vessel creation and a reduced entry of inflammatory cells and their growth factors [8]. Experimental diabetic wound models have shown lower levels of growth factors, such FGF-2 and PDGF, which are crucial for wound healing [9–11]. Topical injection of high concentrations of glucose into wounds in rat models was demonstrated to impede the normal angiogenic process, demonstrating that high glucose levels had a direct and negative impact on angiogenesis [12]. In addition, increased protease activity has the potential to damage granulation tissue and degrade growth factors.

An imperative requirement for a wound dressing is protecting the wound bed while also stimulating skin regeneration to speed up wound healing. Many issues must be considered when selecting a wound dressing product for a wounded individual, including the condition of the existing wound, the frequency of dressing replacement, the expense of treatment, and the need for other supplies (such as antibiotics and sedatives) [13]. An ideal construct for wound healing applications must be biocompatible, non-sensitizing, and display suitable physiochemical properties (i.e., appropriate viscosity and/or mechanical properties). An ideal wound dressing should be able to absorb the tissue fluid that has been secreted (exuded) and exchange gases in a timely manner. It must also protect the wound from bacterial infection and preserve a humid environment in interaction with the wound bed to allow the cells to adhere and proliferate appropriately, aiding wound healing. The rate and extent of biodegradation is another issue that should be considered in fabricating wound dressings. Ideally, the wound dressing should progressively free up space for newly formed ECM and proliferated cells. In a parallel fashion, the degradation products must be metabolically eliminated from the body to prevent inflammation [14]. An additional consideration for wound dressings should be the minimization of discomfort upon removal [15,16]. For example, conventional wound dressings, such as gauze, may solidify into a clot-gauze composite that sticks to the wound bed, causing further pain and bleeding [15,17,18]. An ideal wound dressing should not cause secondary damage during its removal [15,16].

Hydrogels have shown great promise in various applications in the fields of tissue engineering and wound dressings [19]. Hydrogels are hydrophilic three-dimensional polymeric network structures that can hold a considerable amount of water in their networks while maintaining their structure. Hydrogels can be biocompatible and undergo biodegradation, while also exhibiting desirable properties, such as similar elasticity to native tissue, providing a humid environment, the ability to absorb wound exudates, presenting a porous structure suitable for gas exchange, playing a key role as a barrier to bacterial infections, and providing a suitable environment for improving cellular functions, such as migration and proliferation [20]. Further, hydrogels should hydrate wounds to provide a moist environment and facilitate wound scab removal via autolysis [16]. Due to the weak adhesion of hydrogels, they do not attach to the wound bed and can be removed without pain or without damaging the newly formed tissue [16,18].

Moreover, hydrogels could be incorporated with different additives to tailor their structural and biological properties. Several bioactive components, such as anti-biotics and anti-inflammatory molecules, and living cells, could be easily encapsulated into hydrogels to promote wound healing. Hydrogels can also be injected into the defect site, which can be helpful to fill wounds with irregular geometry and provide adhesiveness to the wound bed [21]. All these features make hydrogels a great platform for wound healing and skin regeneration. However, several issues related to their structure, mechanical stability, and biological characteristics limits hydrogels to be a standard wound treatment in the clinic. In the last decade, many researchers have shown the great wound healing and skin regeneration potential of 3D hydrogel constructs with different polymer precursors, crosslinkers, biomolecules, nanoparticles, and living cells [22–24].

In this review, we will highlight a selection of recently published

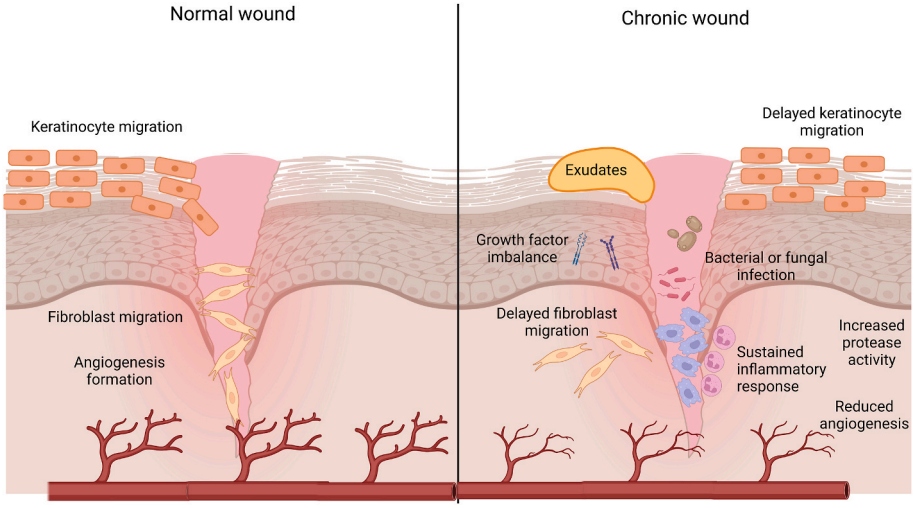

Fig. 1. Differences between normal and chronic wounds. Created with BioRender.com

papers that illustrate the design, characterization, and evaluation of hydrogels for wound-healing applications. Excellent reviews have been written on this topic [13,18,20,25]. Our aim was to provide a fresh and relevant perspective; therefore, the focus of our discussion is on the engineering of hydrogel constructs that, through the fabrication process and the incorporation of additives, provide enhanced functionalities for wound-healing applications. Arguably, the fabrication process is not the major determinant of the hydrogel structure. However, we firmly believe that the fabrication method, as well as the set of additives used during fabrication to impart or enhance particular properties of a wound dressing, are fundamental to the design/customization of ideal mechanical and biological performance of wound dressings.

Firstly, we will discuss the desired structural characteristics of 3D hydrogel wound dressing and the results of the corresponding papers based on the method of fabrication. Later, we will comprehensively review the biological engineering of 3D hydrogels via bioactive components that have been used efficiently to promote wound healing.

2. Engineering the architecture and structure through fabrication

The structure and architecture of the hydrogel constructs for wound healing applications should favor the creation of an environment that fosters proper regeneration (Fig. 2A). A 3D structure seems to be very beneficial, acting as a framework for regeneration and healing processes. Mechanical strength should match the native tissue to provide a bio-mimicked environment for cell attachment, spreading, and proliferation [26]. For cell function, morphological characteristics and porosity are also essential to be helpful not only to mimic the morphology of ECM compounds but also to have suitable porosities and pore sizes for cell infiltration and enhanced nutrient transport. Degradability is also an important principle for any tissue engineering application, permitting native tissue to be generated as the scaffold degrades. Water retention capability is another factor which is crucial specifically for wound dressings. Cells need a humid environment to display their normal behavior, such as attachment and proliferation, to restore the damaged area. Despite their water-retaining properties, wound dressings should absorb excessive wound exudates that could otherwise provide an environment for microorganisms, such as bacteria, to thrive [27].

A wide range of hydrogels have been investigated for wound healing applications, exhibiting different ranges of mechanical properties. Hydrogels could be categorized into three classes: natural, synthetic, and semi-synthetic polymers. Aside from the chemical nature of each polymer and its concentration, the fabrication method and crosslinking method may also influence structural properties. Thus, hydrogels could exhibit a wide spectrum of properties, including various morphological, mechanical, rheological, degradation, and water retention features. Furthermore, according to the application, different additives can be incorporated into hydrogel 3D structures, which can alter and adjust the structural characteristics of the 3D hydrogels.

A deep wound is a highly complex and dynamic environment in which many stimuli occur sequentially or simultaneously, both from the host cells (e.g., inflammatory or healing responses) and the environment

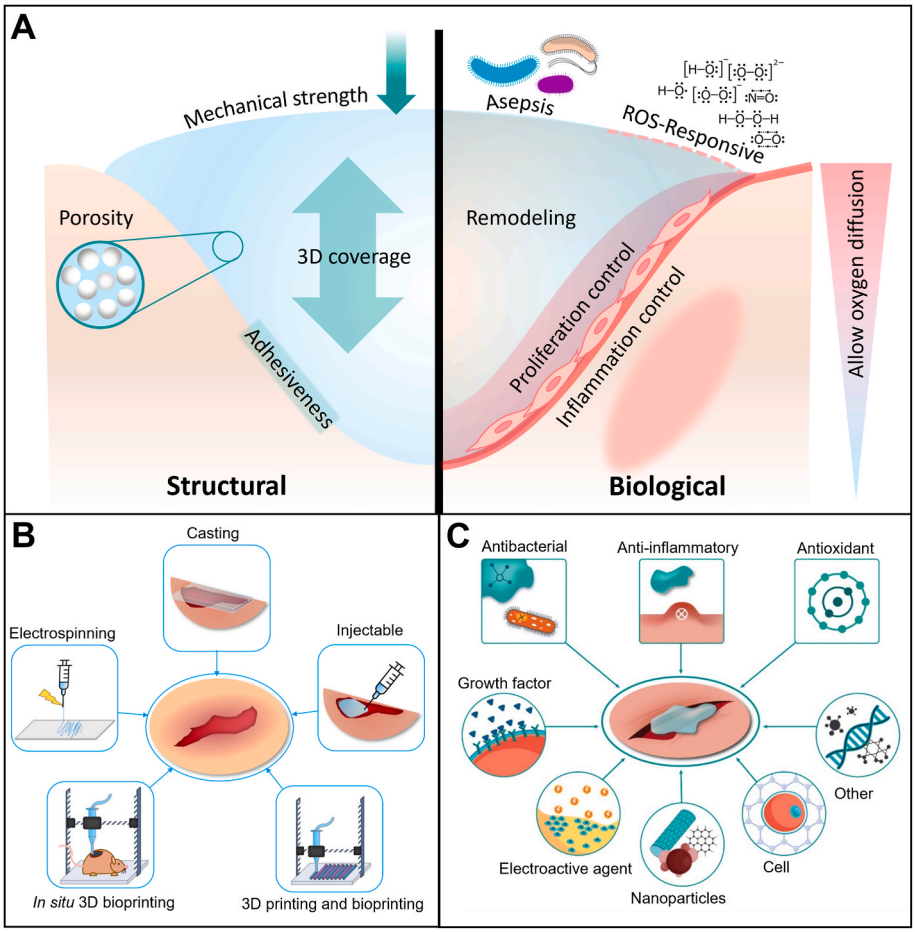

Fig. 2. Structural and biological engineering of 3D hydrogels for wound healing applications. (A) Structural and biological features of hydrogels, necessary for wound healing improvement. (B) Different fabrication methods which are reported for wound healing applications. (C) Different bioactive agents that could be loaded within hydrogels to promote wound healing.

(e.g., infection, dehydration). Therefore, stimuli-responsive hydrogels have a wide spectrum of applications and advantages in wound healing.

In this section, we will review representative studies in which hydrogels have been structurally engineered for wound healing applications. We have categorized studies based on the method of fabrication (Fig. 2B) and elaborated on their structural characteristics.

2.1. Casting/molding

The simplest and cheapest method to fabricate a hydrogel for wound dressing application is casting. This method is based on molding the polymeric solution and inducing the solidification by different possible mechanisms. This gelation could take place through different crosslinking routes, including chemical or physical. The wound bed itself can be considered as the mold for injectable hydrogels capable of being crosslinked *in situ*. Thus, in the following discussion, we subdivide the molding of hydrogels used for wound healing into two categories. First, we describe applications in which the wound healing construct is fabricated and then applied to the wound site (i.e., casting outside the wound). Then, we discuss reports in which the wound dressing hydrogels are directly cast into the wound site (i.e., *in situ* molding).

2.1.1. Casting outside the wound

The most obvious advantage of casting is its ease of use in creating structures that will later be applied to deep wounds. The process of fabrication can be entirely and carefully controlled in the lab or manufacturing facility. This can lead to the integrated use of sophisticated resources to tune the performance of the hydrogel construct. In this category of wound dressings, hydrogel precursor solutions, either cell-laden or not, will be placed in the molds and then solidified by a specific crosslinking mechanism. In particular, photo-crosslinkable hydrogels, hydrogels that can be crosslinked by light stimulus (e.g., ultraviolet [UV] light or visible light), are extensively used in wound healing due to their numerous advantages. Additional crosslinking mechanisms of hydrogels for wound healing and different tissue engineering applications have been discussed in several review papers [13,20,28,29].

Among photo-crosslinkable hydrogels, gelatin methacryloyl (GelMA) is the most extensively used. GelMA [30] is a gelatin derivative, very attractive to researchers due to its high affinity for native mammalian ECM and ease of crosslinking. GelMA contains a high amount of methacrylamide groups and a minority of methacrylate groups which could be crosslinked through radical polymerization, in the presence of photo-initiator upon UV exposure [30]. Based on its wavelength and exposure time, UV light could be hazardous for living cells and the skin. Despite the investigations which have shown the safety of UV lights with particular wave length and specifications [31], the long-term clinical side effects are still not evident. Moreover, patients might not tend to expose UV to their skin. Thus, molding hydrogels could be an ideal choice to manipulate characteristics of photo-crosslinkable hydrogel wound dressings, without direct exposure of risky irradiations to living tissue. Many examples of use of photo-crosslinked hydrogels used for casting wound healing dressings can be found in recent literature. We have chosen only a few of them to illustrate some representative characteristics of the casting of photo-sensitive hydrogels for wound healing.

Zhao et al., investigated a GelMA hydrogel (75% of methacrylation) with adjustable mechanical and degradation features based on different concentrations (5%–20%), for wound healing (Fig. 3A). Mechanical analyses were performed after injecting the polymer in a PDMS mold and UV crosslinking. The compressive and elastic moduli were 3 kPa and 5 kPa, respectively, for 5% GelMA. The compressive and elastic moduli were significantly enhanced by increasing the concentration of GelMA to 20%, and reached ≈110 kPa and ≈200 kPa, respectively. This observation was expected due to a higher degree of crosslinking by increasing the concentration of GelMA. Reaching these high values of moduli is relevant in the context of wound healing applications; compressive moduli in the range of 100 kPa are advantageous for keratinocyte growth [32]. The high elastic moduli and tensile strength of 20% GelMA hydrogels are also sufficient to withstand stretching and bending forces applied throughout wound healing [33]. The authors also observed that cell adhesion and proliferation were significantly higher in 20% GelMA hydrogels than in softer GelMA hydrogels. Furthermore, immortalized human keratinocytes grown on 20% GelMA were able to differentiate and stratify after being lifted to the air-liquid interface [34]. Skin tissue is the exterior layer of the body that is exposed to a vast range of mechanical stresses, including compression, tension, shear, torsion, and bending. Different studies with different testing methods have reported a wide range of elastic moduli for human skin, ranging from 0.001 to 57 MPa [35]. Mimicking this range of values is ideal for wound dressings not only to induce appropriate skin cell behavior but also to tolerate the external stresses. An increase in GelMA concentration (and therefore crosslinking densities), also decreased degradability. Degradation tests using collagenase showed complete degradation of 5% GelMA in less than 72 h. However, this degradation happened for 20% GelMA after 8 weeks, which is desirable for long-term wound healing and prevention of secondary bacterial infection [34].

Arguably, due to the simplicity of the casting method, the researchers can focus on other aspects of the engineering, such as designing more sophisticated chemistry. Methods such as 3D printing and *in situ* application of polymeric solutions restrict scientists to using a limited number of components which exhibit desired characteristics compatible with these methods (such as being shear thinning and having good fidelity after injection and printing). Therefore, using a wider range of materials and reagents is one of the main advantages of preparing hydrogels by casting. Illustratively, heparin, as a natural highly sulfated glycosaminoglycan which is capable of binding to growth factors, has been used as a photo-crosslinkable wound dressing hydrogel [36]. One study reported the use of a thiol-ene reaction to connect thiolated heparin (Hep-SH) to polyethylene glycol diacrylate (PEG-DA) to create a heparin-based hydrogel sheet using UV irradiation [36]. Heparin-based and pristine PEG hydrogel sheets were characterized after lyophilization and rehydration in phosphate-buffered saline (PBS) [36]. The swelling capacities of both hydrogels were similar, suggesting equal degrees of chemical crosslinking. However, when compared to heparin gel sheets, it took longer for PEG gel sheets to equilibrate. This result suggests that heparin-based hydrogel is capable of quicker absorption of exudate from the wound bed and is appropriate for use as a wound dressing. The storage modulus (G′) of both samples was in the same range before swelling (i.e., nearly 14 kPa), comparable to that of human skin, demonstrating a desirable mechanical property as a wound dressing [37,38]. The water vapor transmission rate (WVTR) of the heparin-based hydrogel and the PEG hydrogel, were 1010 ± 100 and 1080 ± 50 g/m^2/day, respectively. These values are in the appropriate range to absorb enough extrude and prevent wound dehydration (2000–2500 g/m^2/day) [39]. Interestingly, while both hydrogels exhibited a similar swelling ratio, they greatly differed in their capacity to release proteins. Human epidermal growth factor (hEGF) embedded in hydrogels showed a gradual release over 21 days for heparin-based hydrogels, while a complete release in 5 days was observed for PEG hydrogels. This result was attributed to the interaction of a heparin-based hydrogel sheets with hEGF, which finally improved wound healing *in vivo* as compared to the PEG hydrogel [36]. Goh et al. also performed *in vivo* wound healing experiments in mice, and the results showed that hEGF loaded heparin-based hydrogel sheets improved wound closure as compared to PEG-based hydrogel sheets, which was evident from day 7 after injury. Such wounds achieved up to 90% closure in two weeks, whereas other treatments only achieved 50%–60%. These results were attributed to the slower hEGF release from the heparin hydrogel, which protects it from proteases and allows continuous stimulation for the proliferation and differentiation of keratinocytes and other cells [36].

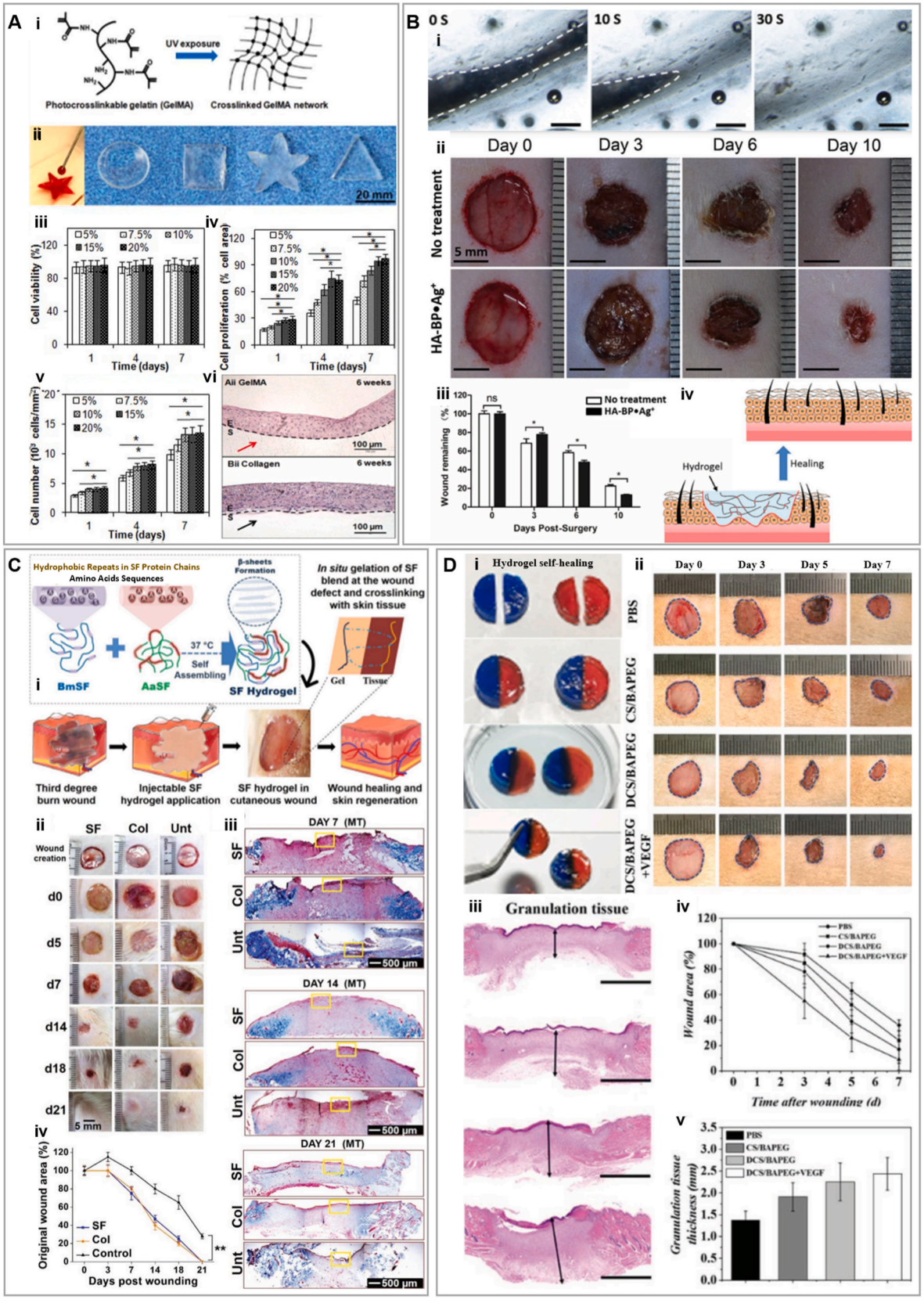

(caption on next page)

Fig. 3. Casted hydrogels for wound healing applications (A) Casted gelatin methacryloyl (GelMA) (i) Schematic formation of GelMA hydrogel network. (ii) Injection of 20% GelMA solution into the molds with different shapes to form hydrogels upon UV exposure. Cell viability (ii), proliferation (iii), and number of cells cultured on surfaces with different GelMA concentrations. (v) Hematoxylin and eosin (H&E) stained sections of reconstructed epidermis on GelMA (top) and control collagen (bottom) scaffolds after 6 weeks of culture at air-liquid interface (ALI). Reprinted and adapted with permission from Zhao et al., 2015 [34]. (B) Self-healing hydrogel (i) Micrographs of hydrogel self-healing at 0, 10, and 30 s after the hydrogel cut. (ii) Images of wounds treated with hyaluronic acid (HA) chains were modified with pendant bisphosphonate (BP) ligand, incorporated with silver (Ag^{+}) ions (HA-Bp Ag^{+}) or untreated at different time points. (iii) Percentage of remaining wound size relative to day 0, asterisks show statistical differences between treatment and control. (iv) Schematics of HA-Bp Ag^{+} hydrogel filling the wound without the need for premolding. Reprinted and adapted with permission from Shi et al., 2018 [50]. (C) Silk fibroin (SF) and collagen hydrogels (i) Schematic of *in situ* formation of SF blend hydrogel at 37 °C in wound bed. (ii) Images of wounds implanted with SF, collagen (Col) or left untreated (Unt) on excised third-degree burn wounds showing the healing process through time. (iii) Masson's trichrome (MT) staining of full wound biopsy sections at 4x magnification. (iv) Percentage of original wound area calculated at different time points using ImageJ. Reprinted and adapted with permission from Chouhan et al., 2018 [51]. (D) Benzaldehyde-terminated polyethylene glycol (BAPEG) and dodecyl-modified chitosan (DCS) hydrogels. (i) BAPEG/DCS hybrid hydrogels in blue and red, were cut into two parts, one piece of each was coupled together and they were kept in integral blended disks for 20 min, and the integrated healed hydrogel disks were maintained for 2 h in PBS. (ii) Images of skin wounds treated with PBS, CS/BAPEG, DCS/BAPEG, and vascular endothelial growth factor (VEGF)-loaded DCS/BAPEG. (iii) H&E staining of the wounds at day 7 post-injury. Mean wound area (iv) and quantification of granulation tissue thickness (v). Reprinted and adapted with permission from Chen et al., 2018 [56].

Engineers can easily combine hydrogels with solid materials like mats and gauze by casting them together. This enables the fabrication of hybrid structures that can be used for various purposes, such as reinforcing the wound dressing, improving functionality, etc. In a study by Anjum et al., a wound dressing was fabricated by coating a cotton fabric with a blend of chitosan (CS), PEG, and polyvinyl pyrrolidone (PVP) [40] and freeze drying. The authors observed that the pores of the CS/PEG/PVP-coated cotton fabric (CPPC) were more spherical than the elongated porous structures in the samples without PVP. This observation could be related to the phase separation that limited interaction between chitosan and PEG, which could be changed upon the addition of PVP that may have enabled a stronger hydrogen bonding with chitosan [41]. In addition, adding PVP (50%) decreased porosity (from 68% to 58%) and increased water absorption as the swelling rate improved from ~400%–1210%. The WVTR of cotton fibers coated with CS, CS/PEG, and CS/PEG/PVP blends was measured ≈2600, ≈3380, and ≈2230 g/m^2/day, respectively. Moreover, the air permeability of the samples was also altered by adding PVP, from ≈8.65 cc/cm^2/sec for the CS/PEG coating to 5 cc/cm^2/sec for 50% PVP. These experiments also showed that PVP could significantly increase the tensile strength of the composite. The tensile strength of CS/PEG/PVP blends (i.e., 16 MPa) was an order of magnitude higher than the tensile strength of CS/PEG-coated cotton fabric (i.e., 1.6 MPa). The CPPC composite showed an initial burst release over 8 h and then a more gradual release of 60%–78% of Tetracycline (TC) by 48 h. These results suggest the potential of this fabrication strategy for the early-stage antibacterial treatment of wounds. *In vivo* wound healing studies carried out in Wistar rats demonstrated that CPPC-TC-based wound dressings promoted faster and better wound healing (with 76% and 98% wound contraction by days 4 and 12, respectively) than the control (which only achieved 20% and 66% wound contraction on the same days). In addition, the amount of scar tissue was lower with CPPC-TC wound dressings (only 0.33%) than in the control group (10.67%) [40].

Self-healing hydrogels have been an interesting class of materials for biomedical applications. These hydrogels have the ability to repair their repeated structural defects and restore their original function through reversible interactions, such as hydrogen bonds, charge interactions, host−guest interactions, and coordination bonds [42]. For example, Tian et al. developed a self-healing hydrogel made of hyaluronic acid (HA) and capable of an on-demand release of antibacterial agents. HA is a non-sulfated glycosaminoglycan (GAG) and the main component of skin ECM. The hydrogel was fabricated via reversible supramolecular interactions, providing self-healing ability using a dynamic coordinate bond between the ethylene-diamine-tetra-acetic acid (EDTA)−Fe^{3+} complex and HA. In the presence of bacterial infection, the hyaluronidase (HAase) secreted by the microorganisms degrades HA, leading to the local release of Fe^{3+} which consequently kills bacteria (via reduction to Fe^{+2} and reaction with H_2O_2 to form a hydroxyl radical). The authors conducted an extensive characterization of this active system. Rheological analysis showed higher storage modulus (G′) than loss modulus (G″) for different ratios of Fe^{3+}−EDTA complexes (4:1, 5:1, and 6:1), indicating self-standing hydrogel formation [42]. At day 7, mass spectrometry (MS) spectra revealed degradation of the hydrogels by the bacteria secreted HAase, which is required to release Fe^{3+}. Atomic absorption spectroscopy showed that Fe^{3+} in the HA-Fe-EDTA hydrogel gradually lowers with increasing treatment time *in vivo*, indicating the efficient release of Fe^{3+} from the hydrogel to the infection environment, which is consistent with MS data. Continuously produced Fe^{3+} can kill bacteria, inhibiting infection and reducing infection-related microbial/skin metabolites. Complete wound closure was achieved in a 10 day period whilst also avoiding infection by *Escherichia coli (E. coli)* and *Staphylococcus aureus (S. aureus)* [42].

Adding nanoparticles is one of the most common strategies not only to improve structural properties but also to enhance the bioactivity of hydrogels in tissue engineering. Casting as a simple method of fabrication enables researchers to easily fabricate hydrogel composites containing micro/nano particles. Producing homogenous suspensions of nanoparticles for casting may post a challenge. However, including particles in pregel solutions for *in situ* injection and 3D printing methods may be even more challenging. Nanoparticles may disturb the rheology of the suspension and make them more difficult to design/implement in *in situ* injection applications. For instance, not all the combinations of micro/nano particles with polymeric solutions are injectable and printable. Moreover, including additives might impede the crosslinking mechanism, which needs to take place instantly after injection or printing. An illustrative example of the fabrication of nano-particulated hydrogels for wound healing and fabricated by casting methods follows. Gan et al. fabricated a plant derived hydrogel consisting of lignin-coated Ag nanoparticles (NPs), and an interpenetrating network of pectin into the poly-acrylic acid (PAA) [43]. The NPs-P-PAA hydrogel exhibited resilience and stretchability up to 26 times its preliminary length, demonstrated by load–unload tensile stress–strain curves. Compression analysis also indicated complete deformation and complete recovery after 2 min. Typical tensile stress–strain curves showed maximum tensile strain of 2660% for the highest mass of NPs (0.03 gr), compared to 860% and 380% for P-PAA and PAA, respectively. The 0.03 NPs-P-PAA hydrogel also showed the highest strength and ductility (300 MPa%). Moreover, the fracture energy of 0.03NPs sample was measured at 5500 Jm^{-2} which is much higher compared to the amount for human skin, which is ≈ 2000 Jm^{-2}. These results are associated with the interpenetrated network and reinforcing the hydrogels by Ag-Lignin NPs, which through noncovalent interactions with polymers can dissipate energy, leading to an improved mechanical property. The adhesiveness of the hydrogel was quantified using tensile adhesion test. Adhesion strengths to porcine skin was measured for NPs-P-(poly acrylamide) PAM, NPs-P-P poly (acrylic acid-co acrylamide) (AA-co-AM) and NPs-P-PAA hydrogels 12 kPa, 15 kPa, and 25 kPa, respectively. These findings indicated that carboxyl groups of PAA and catechol groups of Ag-Lignin NPs could enhance the adhesiveness of the hydrogel. *In vivo* performance was better for the NPs-P-PAA hydrogel as compared to the

control and the P-PAA hydrogel in a wound healing assay. The NPs-P-PAA hydrogel treated wounds reached a healing ratio of 90%, whereas the control group and the P-PAA hydrogel only reached 59% and 78%, respectively. The authors also evaluated the quality of the regenerated tissue by hematoxylin and eosin (H&E) staining, which showed collagen fibers in the NPs-P-PAA hydrogel-treated sample, whereas there were still many granulation tissues in the controls [43].

Casting is the easiest and simplest way to fabricate wound dressing hydrogels; however, it normally produces an isotropic, monolithic hydrogel construct. With this method, the structural properties, such as pore size and mechanical properties, are usually determined by the type and concentration of polymer, the choice of crosslinkers, the type of additives, etc. In addition, a relatively wide variety of polymers, components, and additives could be used in casting methods without concerns such as altering the rheology and fidelity of the pregel solution/suspension. Furthermore, during the molding process, it will be possible to add solid compartments such as 2D sheets to make a hybrid wound dressing. Besides, molding hydrogels before applying them to the skin tissue prevents exposing the skin of patients to UV light and enables scientists to even consider crosslinking mechanisms that might release toxic byproducts. On the other hand, the main disadvantages of prefabricating hydrogels by casting could be the limited geometrical complexity that the method provides which translates in difficulties in adapting to irregular wound beds, difficulty of handling, and poor engraftment with the wounded area.

2.1.2. *In situ* molding

Compared to traditional hydrogel casting, the *in situ* application of hydrogels has the important advantage of completely filling the wound bed in three dimensions. The fluidity of injectable hydrogels allows them to fill deep wound cavities with irregular dimensions, which cannot be done by prefabricated hydrogels. Furthermore, when compared to prefabricated hydrogels, *in situ* crosslinking can result in a more appropriate integration and attachment of the wound dressing to the wound site. However, the other side of the coin is that not all types of hydrogels are injectable. This limits the *in situ* application of the hydrogels in tissue engineering. Injectable hydrogel solutions have to exhibit non-Newtonian characteristics of shear-thinning fluids, leading to a decreased viscosity when exposed to shear strain [44]. This will ensure cell survival throughout syringe-needle flow [45]. Another aspect to consider is the gelation time of the injectable solutions. If gelation happens very slowly, there may be significant solution and cell loss from the injected site [44]. Thus, the application of micro/nano additives that may impede shear-thinning properties and/or rapid sol–gel transition is also limited in injectable systems. The crosslinking mechanism is another important consideration. Although chemically-crosslinked hydrogels are rather strong and stable in terms of mechanical properties, physical crosslinking is more appropriate for *in situ* application of hydrogels due to safety considerations [46].

Many examples of the *in situ* application of hydrogel-based wound dressings can be found in recent literature. Here we discuss some illustrative reports. Lazurko et al. designed a thermosensitive hydrogel suitable for wound healing, made of different compositions of collagen type I, poly-D-Lysine (PDL), and chondroitin sulfate [47]. Gelation time was reported to be less than 5 min for the samples containing no chondroitin sulfate, whereas including this polymer in the matrix extended the gelation time up to 1 h. This result was possibly related to alterations in the conformation of the collagen which impaired inter-chain crosslinking. All the hydrogels (Collagen type I, Collagen/PDL, Collagen/chondroitin sulfate, and Chondroitin sulfate/PDL) denaturate at an average temperature of 50 °C, which is far from 41 °C, the highest possible fever temperature [48]. All samples showed a water content in the 94%–96% range, and CRYO-scanning electron microscope (SEM) images of PDL-containing ones exhibited fibrous architecture, indicating that the collagen and the poly-peptide formedan interpenetrated-network-like-structure [49]. Additionally, the pore size of collagen and collagen/PDL hydrogels was reported to be 16 μm and 10 μm, respectively. However, when air microbubbles were added to the matrix during its preparation, the pore size increased in both samples and reached up to ≈30 μm–40 μm. Having this range of pore size, collagen hydrogel could support migration of cells from mouse microscopic skin tissue column (MSTC) up to 21 days, suggesting the regenerative potential of this collagen-based hydrogel as a wound healing platform. Wounds in diabetic mice closed two times faster after treatment with the MSTC/collagen matrix than those treated with collagen matrix alone. Meanwhile, untreated diabetic mice showed impaired wound healing [47].

A moldable self-healing HA supramolecular hydrogel was fabricated by dynamic metal–ligand coordination bonds (Fig. 3B) [50]. HA chains were modified with pendant bisphosphonate (BP) ligands via carbo-di-imide coupling and "click" reactions. Upon silver (Ag^+) addition to the solution, the reversible crosslinking occurred. The precursor concentrations used in the hydrogel were 3% (w/v) and 15×10^{-3} M for HA-BP and Ag^+, respectively. Rheology analysis showed G′ of ≈400 Pa and G″ of ≈100 Pa confirming the hydrogel formation. Morphology of the hydrogels after freeze drying was assessed by SEM. No fibrous architecture was observed for these hydrogels, which could be associated with Ag^+ ion crosslinkers with low-molecular weight, which usually cannot form fibrils with polymeric macromolecules. The HA-BP Ag^+ hydrogels were tested in a rat full-thickness wound model to determine the remaining wound rates. The remaining wound rates for treated samples with HA-BP Ag^+ hydrogels were 13%, while the controls exhibited remaining rates of 22.6%, ten days post-injury. Wounds treated with HA-BP Ag^+ hydrogels also developed a thicker and more complete epithelium (144 μm) than the control wounds (63 μm) as observed by H&E staining on day 10 [50].

In a study by Chouhan et al., a thermosensitive silk fibroin (SF) hydrogel capable of self-assembly was developed using a mixture of two types of SF extracted from silkworms of *Bombyx mori* (BmSF) and *Antheraea assama* (AaSF) (Fig. 3C) [51]. SEM micrographs of lyophilized SF blend hydrogels showed a porous structure with an average pore size of ≈155 which is appropriate for cell penetration, vasculature formation, and wound healing application [52,53]. Water retention of the SF blend after 12 h was measured at 75% as compared to 20% for control collagen (Col) hydrogels. This could be attributed to the long stability of the hydrogel due to the combined effect of hydrogen bonding and hydrophobic interactions connecting AaSF and BmSF proteins. Temperature-dependent inter- and intramolecular interactions, which caused the gelation of the SF blend, could be due to the presence of both hydrophilic and hydrophobic sites between BmSF and AaSF. It is known that hydrophobic β-sheet structures can be form due to the presence of (GAGAGS) protein sequence in BmSF, upon exposure to physical forces such as vortexing and sonication [51,54]. A rheological analysis demonstrated a temperature/concentration-dependent gelation trend for hydrogels as the SF blend gelled in 20 and 45 min at 37 °C and 20 °C, respectively. Furthermore, a significant difference was observed after gelation between G′ (336.42 Pa) and G″ (11.269 Pa) of the SF blend hydrogel (3% w/v). Viscoelastic behavior, which can lead to withstanding shear strain, was also demonstrated for SF gels as the value of the modulus was constant at a frequency range of 0.1–10 rad s^{-1} in the region of 0%–10% shear strain. Compression tests of SF hydrogels (3% w/v) revealed a compressive strength of ≈3 kPa and a compressive modulus of ≈7.4 kPa, suggesting mechanical properties of soft hydrogels. In the compression test, the SF blend reached 20% strain to break down and in the cyclic compression of 10% exhibited recovery up to 15 loading and unloading with reversible deformation. This indicated adequate stability for handling with minimal breakage for wound healing. Moreover, *in vitro* biodegradation analysis showed a significantly higher mass left for SF blend compared to Col gels. After 7 days, 97% and after 14 days, 85% of the initial weight was preserved for SF gel, in comparison with 75% and 65% for Col, respectively. Stable β-sheet networks in addition to the higher molecular weight of SF

protein could be responsible for this higher stability [55]. This stability was also confirmed *in vivo* as SF hydrogel degraded after 4 weeks upon subcutaneous implantation in mice. In a third-degree burn wound model, SF hydrogel showed similar wound healing behavior compared to Col hydrogel. SF was able to firmly attach to ECM, showing comparable wound closure to collagen on day seven, and detaching itself to reveal the underneath native tissue by day 14. At this time point, only 40% of the SF-treated wounds were still open as compared to 80% in the control group. Furthermore, small blood vessels were visible on both SF and Col treated wounds by immunofluorescent staining on day 7. Even when Col hydrogel showed a higher angiogenic potential than SF hydrogels, SF blends still showed a 10-fold increment in vessel density compared to the control group. SF hydrogel also caused a milder immune response as observed by an earlier expression of CD163 (M2 macrophage marker) and a faster decrease in the expression of CD68 (inflammation marker) and TNF-α, compared to Col hydrogel and the control group [51].

The recovery properties of self-healing hydrogels, gel-to-sol, and then sol-to-gel transition make them very attractive for *in situ* application. An injectable self-healing hydrogel composed of benzaldehyde-terminated polyethylene glycol (BAPEG) and dodecyl-modified chitosan (DCS) was fabricated by Chen et al. for wound healing [56]. The hybrid hydrogels exhibited reversible self-healing enabled by a Schiff's base reaction between the benzaldehyde and amino groups in the polymer composite (Fig. 3D) [56]. The rheology analysis showed that DCS/BAPEG with 1/2 M ratios of -CHO and -NH_2 and solid content of 9% exhibited the highest G′ (≈600 Pa) compared to samples with 1/1 and 1/4 M ratios and 13% and 5% solid content. Moreover, the gelation kinetics of the hydrogel showed a consistent G′ until around 100% strain and then collapsed to higher strains for G′, lower than G″, indicating solid to fluid transition of the hydrogel. In addition, the viscosity of the hydrogel decreased when being injected through a syringe, and then recovered its gel state outside the syringe. Furthermore, oscillatory strain (1% and 300%, 10 Hz frequency) applied to the hydrogel showed that the high strain could cause the gel-to-sol transition by breaking the hydrogel network. Thereafter, when the strain is reduced to low values, the hydrogel can regain its normal initial shape, exhibiting the initial G′ value. This behavior can be attributed to the self-healing capability of the hydrogel due to dynamic equilibrium between the Schiff's base and the amine and the aldehyde reactants, which leads to dynamic uncoupling and recoupling of the bonds within the hydrogel networks. The BAPEG/DCS hybrid hydrogels were able to reach a value of 160 mmHg in a bursting pressure test, suggesting their potential application in vessel bleeding repair. These hydrogels also demonstrated their hemostatic capacity in acute wounds in a severe trauma model in mice. Finally, the BAPEG/DCS hybrid hydrogels with encapsulated vascular endothelial growth factor (VEGF) showed better wound healing in a *S. aureus* infected full-thickness skin defect than the hybrid hydrogels without VEGF as assessed by wound area, granulation tissue thickness, and the expression of TNF-α and IL-6 [56].

Besides extrudability and ease of *in situ* gelation, self-healing hydrogels can deliver desired molecules upon injection to the wound site. Another injectable self-healing hydrogel based on a Schiff's base reaction was developed by Wang et al. for wound healing application [57]. In this study, the multifunctional polypeptide-based hydrogel (named as FHE hydrogel) was formed through a reversible Schiff's base reaction between oxidative hyaluronic acid (OHA) and Poly-ε-L-lysine (EPL). FHE hydrogel was capable of releasing loaded bioactive exosomes (for antibacterial purposes) which were loaded through electrostatic bonds with EPL. This pH-dependent release would occur because of the interruption of the Schiff's base bond upon exposure to a weak acidic environment. A full-thickness diabetic wound model was used to assess the healing efficiency of FHE hydrogels. The exosome-loaded FHE hydrogels exhibited complete wound healing by day 21, whilst exosomes, pristine FHE hydrogels, and control groups achieved 76.3%, 64.3%, and 36.3%, respectively. Furthermore, compared to the rest of the treatments, exosome-loaded FHE promoted higher type I and III collagen deposition, cytokeratin and alpha-smooth muscle actin expression, and blood vessel formation [57].

Gao et al. designed an injectable hydrogel, responsive to near-infrared (NIR) light and thermosensitive for drug release into the wound bed [58]. In this study, polydopamine PDA NPs (which could generate local hyperthermia upon exposure to NIR) were loaded with ciprofloxacin (Cip), an antibiotic. Subsequently, the PDA NPs were crosslinked via Schiff's base reaction and/or Michael addition with amine-rich glycol chitosan (GC) to form a NP-Cip/GC injectable hydrogel (Gel-Cip). The shear thinning behavior of the hydrogels, a relevant characteristic for *in situ* application, was demonstrated when, by an increase in shear rate, the viscosity was reduced (from the range of 10^3 to several Pa) for both samples. Photo-thermal behavior of samples exposed to different NIR power densities revealed an increasing trend in accordance with laser power density. Upon NIR light irradiation using laser densities of 1.6, 1.0, and 0.5 W/cm^2, the resulting temperatures of Gel-Cip were 78.1, 59.7, and 46.8 °C, respectively. NIR light irradiation of 0.5 W/cm^2 was further analyzed and showed a remarkable release of Cip compared to Gel-Cip without irradiation. With 3-fold NIR light irradiation during 120 min, ~1.4 μg of Cip were released. In contrast, only ~0.4 μg of Cip were released from Gel-Cip hydrogels without irradiation. Gel-Cip + NIR exhibited 98.9% bactericidal efficacy in *S. aureus*-infected mice, where wounds almost disappeared by day 4 (with only 6.4% of surface area unhealed). Gel-Cip + NIR treated wounds also exhibited higher fibroblast proliferation, thicker epidermis, and more blood vessel and hair follicle formation than the rest of the treatments [58].

Injectable hydrogel solutions can also be used to make microgels. Microgels or hydrogel microspheres are widely used in tissue engineering for different purposes, such as encapsulating different functional components (i.e., cells, growth factors, particles, etc.). Microgels provide a micro-domain with a high surface area-to-volume ratio, which enables a more efficient interaction of the hydrogel with the environment [59]. Microfluidic strategies are the most widely used methods for producing microgels due to their ease of use, high output, and ability to carefully control monodispersity and dimension [60]. The majority of aqueous monodisperse droplets are generated by techniques such as T-junctions, flow focusing, and coaxial capillaries, which recruit constant pressure to produce monodisperse droplets in aqueous solutions. Droplet creation occurs as a result of the interaction between the dispersed phase and the continuous phase in these techniques, and pressure sources are positioned at a distance from the droplet-generating mechanism. Active methods, on the other hand, require an external power supply and may use piezoelectric actuators or electric field techniques to create droplets on demand [59]. Microgels have been used for wound-healing applications because of their specific advantages. Chen et al. used a microfluidic electrospray approach to prepare alginate microgels containing encapsulated copper-/zinc-niacin framework cores for wound healing [60]. The bacterial-responsive degradability of the alginate shells endowed the microcapsules with smart, selective, and programmable release of calcium, copper, and zinc ions in response to different levels of infection. The released ions could kill microorganisms, stimulate the release of nutrients, and activate copper/zinc superoxide dismutase (Cu/ZnSOD) to neutralize oxygen free radicals and protect cells from damage caused by oxidative stress. An *in vivo* study of an infected full-thickness skin defect model showed that microcapsules decrease inflammation and improve angiogenesis, collagen deposition, and phenotypic differentiation of fibroblasts [60]. Cui et al. developed micro-gel ensembles using two different polymers and a Y-channel microfluidic technique [61]. The micro-gel ensembles were composed of a poly(hydroxypropyl acrylate-co-acrylic acid)-magnesium ion (poly-(-HPA-co-AA)-Mg^{2+}) gel and a carboxymethyl chitosan (CMCS) gel, both of which can release and absorb hydrogen ions (H^+) independently at various stages of wound healing in response to changes in the wound microenvironment. *In vitro* and *in vivo* analyses indicated that the

micro-gel ensembles allow for persistent wound pH modulation throughout the four wound-healing stages. The micro-gel ensembles keep the wound milieu at a low pH during the hemostasis and inflammatory stages, thereby inhibiting bacterial development. The acidic environment also stimulates Mg^{2+}, which causes adipocytes to proliferate and migrate, building a wall to shield the wound. The micro-gel ensembles then regulate an ideal alkaline environment for hyperplasia and remodeling, allowing fibroblast proliferation and migration to speed skin healing. Collagen deposition, macrophage polarization, and blood vessel development have also been aided by micro-gel ensembles [61].

Compared to preformed hydrogels, injectable hydrogels are easier to handle and minimally invasive to the adjacent tissues. Their fluid nature allows them to fill irregular and deep cavities in the wounds without wrinkling. They can also deliver drugs and cells in a concentrated manner to the wound bed. Moreover, by crosslinking to the tissue interface during their *in situ* formation, the hydrogels can exhibit appropriate adhesion and engraftment with the host tissue. However, some challenges remain, particularly limitations in cell-friendly extrudability, post-injection fidelity, quick gelation, and safe crosslinking mechanisms that must be overcome to expand and intensify the application of polymers and different bio-additives for *in situ* forming wound dressings.

2.2. 3D printing

In tissue engineering, 3D printing has evolved to precisely fabricate complex geometries with desired porosities and morphologies with computer-aided design (CAD). Using CAD, it will be possible to create structures that fully match the geometry of any type of wound. Three 3D printing technologies have been mainly used for fabricating 3D structures for biomedical applications, including inkjet-based, extrusion-based, and light-based printing [62]. In the inkjet-based technique, via piezoelectric or thermal actuation, droplets of biomaterials are deposited on a platform in a layer-by-layer manner to form the required structure. Inkjet 3D printers have several advantages, such as a wide biomaterial availability, high speed, and accuracy [63]. In extrusion-based 3D printing, mechanical or pneumatic force is applied to extrude biomaterials through the print-head(s). The absence of heat during the process and a broad range of available biomaterials are the main advantages of extrusive bioprinting [63]. In the light-based techniques, by projecting a desired geometric pattern into a bed of hydrogel precursor using light (UV, laser or visible light), 3D hydrogels can be formed [62,64]. In tissue engineering and regenerative medicine, when 3D printing is implemented via cell-laden materials (bioinks), the technique is called bioprinting. Besides the desired geometry and morphology, bioprinted structures could contain co-culture of multiple cells and growth factors based on the target tissue [65]. Extrusion-based and ink jet-based techniques have been far more common for bioprinting [63]. 3D printed or bioprinted hydrogels have been applied in wound dressing application following two general types of fabrication strategies, prefabrication or *in situ* formation.

2.2.1. Prefabricated scaffolds

3D printing enables researchers to combine geometrical precision with different strategies to improve structural properties. This can lead the hydrogel to be beneficial in different structural aspects for proper wound healing and skin regeneration. In a study by Xu et al., a 3D printed (via extrusion-based 3D printing) cellulose nanofibril (CNF) hydrogel was fabricated. Two steps of crosslinking were implemented, using Ca^{2+} solution and chemical crosslinking with 1,4-butanediol diglycidyl ether (BDDE) [66]. Compressive tests showed an increase in the Young's modulus from 3.45 kPa to 7.44 kPa for CNF 1.0 wt% hydrogels before and after secondary crosslinking. The authors observed that NIH-3T3 fibroblast cells could spread in a 3 kPa environment; cell spreading could be further enhanced on 10 kPa substrates [67]. The stress–strain curve showed excellent elasticity, which could be attributed to the Ca^{2+}/carboxylate crosslinking combined with hydrogen bonding [66]. The microporosity of the hydrogels was enhanced after chemical crosslinking by 1,4-butanediol diglycidyl ether (BDDE), which agrees with the higher rigidity of the hydrogel. Human dermal fibroblasts were seeded in these CNF scaffolds. Results showed good cell survival, adhesion, and even higher proliferation in CNF scaffolds than in 2D cell cultures [66]. Using an extrusion-based low temperature 3D printing, Intini et al., developed a hydrogel scaffolds composed of chitosan, which could support 3D skin cell colonization [68]. The thickness of the scaffold was 2.1 mm and the distance between filaments of a grid-shaped hydrogel scaffold was 200 μm with a precise geometry and homogeneity of pore size (Feret diameter of ≈3.5 μm and ≈5 μm for the surface and within the scaffold, respectively) [51]. Keratinocytes and fibroblasts could properly grow within the scaffolds, filling the holes from bottom to top to colonize all the 3D construct. Additionally, by placing a chitosan film at the base of the 3D scaffold, the retention of the cells inside the hydrogel was significantly increased. Tensile testing revealed Young's modulus (YM) of the samples ≈105 kPa which is similar to the elastic modulus of skin tissue specifically in the volar forearm region [69]. The authors assessed the performance of CNF scafolds *in vivo* using an impaired wound healing model in streptozotocin-treated rats. Wounds treated with chitosan scaffolds exhibited a reduction of 50% of total wound area after seven days, and epidermis formation as opposed to the control group. Furthermore, 14 days after the initial injury, the group treated with chitosan showed the presence of hair follicles, blood vessels, sebaceous glands, and arrector pili muscles [68].

Hydrogels must be printable to form the desired complex geometries via 3D printing. After being extruded from the nozzle, hydrogel filaments must maintain their shape. If the filaments collapse after printing, the whole structure will be altered and may not fulfill the expected regenerative functions of the designer [70]. For example, poor shape fidelity may derive on the incomplete filling of the wound area. Moreover, in the case of bioinks, hydrogel solutions should provide performance characteristics that could enable high cell survival (post-printing viability) and normal functionality [71]. The rheological characteristics of a hydrogel play the main role in the printability of hydrogels. However, hydrogel printability and fidelity are related to many additional parameters such as innate features of monomer(s), their concentration and molecular weight, the effect of additives, and the degree of gelation. In a study by Pereira et al., a bioink was made of pectin methacrylate (PECMA) with adjustable mechanical and rheological behavior for skin regeneration [72]. This hydrogel bioink, which was designed for extrusion-based bioprinting, could be crosslinked by a two-step strategy including an ionic mechanism using $CaCl_2$ and UV exposure. The printability of the bioink, PECMA 1.5 wt% supplemented with 0, 1, 3, 5, and 7 mM of $CaCl_2$, were assessed. Only solutions with 5 and 7 mM of $CaCl_2$ were able to form stable, neat filaments extruded from the nozzle. Moreover, the printed constructs did not collapse and showed sufficient integrity to sustain subsequent layers. The 5 mM $CaCl_2$-containing solution was selected as the optimal for further analysis due to the lower yield stress needed to induce flow. Ma et al. designed photo-thermal printable hydrogels composed of calcium silicate (Calsil) nanowires, sodium alginate (SA), Pluronic F127, and L(+)-Glutamic acid (Calsil + SA hydrogels) [73]. Additionally, oligomeric proantho-cyanidin (OPC) was used as the crosslinking and photo-thermal agent, which made the rheological and mechanical properties of the hydrogels tailorable by NIR laser irradiation. Moreover, the temperature of the Calsil + SA + OPC hydrogels could be controlled by altering the NIR laser power density and the concentration of OPC. Rheological assessment showed an increased storage moduli G′, (in the range of 10^2 for Calsil + SA+6% OPC) after 30 min of NIR laser exposure, indicating an increase in hydrogel stiffness. Besides, upon NIR illumination, mechanical spectra of the samples exhibited a 'strong gel' character as demonstrated by parallel G′ and G″ curves, in a frequency independent manner [74]. It

was also shown by amplitude sweeps on different OPC- containing hydrogels that G′ and G″ improved as a function of OPC concentration and/or the NIR exposure time. The compressive mechanical strength was also affected by the concentration of OPC and/or the exposure to NIR. The mechanical strengths of Calsil + SA, Calsil + SA+4%OPC and Calsil + SA+4%OPC after 30 min of NIR exposure were reported ≈2.5 kPa, 4 kPa and 8 kPa, respectively [73]. The *in vivo* performance of these hydrogels was assayed in 10 mm skin wounds inflicted on diabetic C57BL/6 mice. The Calsil + SA + OPC group exhibited a higher wound healing rate (with a relative wound area of 0.2% on day 16), than the Calsil + SA (relative wound area of 0.9%) and the blank group (relative wound area of 5.3%). The Calsil + SA + OPC group also developed more vascular networks than controls and a normal collagen arrangement with no signs of inflammation. These results were attributed to the capability of OPC to promote cell proliferation and angiogenesis, as well as the synergistic effect of Si ions in promoting collagen deposition and re-epithelialization. Mixing different types of polymers can adjust rheological behavior, leading to improved printability and fidelity. For example, it is known that the extracellular matrix (ECM) plays a crucial role as mechanical support and as a promoter of cell attachment and cell-cell interactions [75]. Besides, just like *in situ* injection, extrusion-based bioprinting requires hydrogels with shear thinning properties to flow through the nozzle without compromising cellular viability. In a study by Jorgensen et al., a cell-laden hydrogel construct of cells supplemented with fibrinogen and decellularized human skin-derived extracellular matrix (dsECM) was fabricated via extrusion-based bioprinting [76]. Printability tests revealed that fibrinogen + dsECM materials were suitable for printing applications. Shape fidelity and filament strength were observed to be higher in fibrinogen + dsECM than in controls [76]. The addition of dsECM to the fibrinogen matrix increased the structural stability of the construct after 15 days in culture. Also, a longer structural stability was observed in cell-containing hydrogels than in cell-free ones (≈400 kPa vs 200 kPa). The shear thinning properties of fibrinogen + dsECM were also demonstrated; viscosities of ≈100 Pa s and 0.1 Pa s were determined at low and high shear rates, respectively.

Among different types of 3D printing, digital light processing (DLP) has recently shown great promise in fabricating complex structures with advantages such as fast printing speed and high resolution for biomedical applications. DLP-based 3D printing is based on the movement of the platform containing polymer, being cured by light in a layer-by-layer manner. Zhou et al., developed a 3D printed double-layered skin structure using a biomimetic bioink composed of GelMA, N-(2-aminoethyl)-4-(4-(hydroxymethyl)-2-methoxy-5 nitrosophenoxy) butanamide (NB) linked hyaluronic acid (HA-NB), and lithium phenyl-2,4,6- trimethylbenzoylphosphinate (LAP) as photo-initiator [77]. The authors reported that the mechanical properties of the construct could be adjusted by the presence of HA-NB and by the extent of the reaction between the aldehyde groups and the amine groups of the GelMA chain induced by UV light. Dynamic time-sweep rheology showed very similar gelation points of ≈1.384 s and 1.385 s for GelMA/HA-NB/LAP and GelMA/LAP hydrogels, respectively, upon UV irradiation. In contrast, gelation happened to GelMA/HA-NB without lap after ≈33 s upon UV exposure. The hydrogel was printed in two layers to mimic the epidermal layer (as the dense upper layer) and the corium layer of natural skin (as a porous lower layer containing micro-channels). The aim of the dense upper layer with a thickness of 500 μm has been protection and sustainability against external mechanical stress. On the other hand, the 1.5 mm lower part provided microchannels for proper nutrient transfer, cell migration, and vascularization to facilitate wound healing and skin regeneration. It was seen that increasing the diameter of microchannels has a negative effect on compressive strength. Hydrogels with 200 μm channels showed strength of ≈35 kPa, while samples with 300 μm and 400 μm channels exhibited 30 kPa and 20 kPa, respectively. Moreover, 300 μm and 400 μm channels supported less cell adhesion than samples with 200 μm channels due to a higher surface-volume ration in the later. Therefore, samples with 200 μm microchannels were selected for further experimentation *in vivo*. For *in vivo* evaluation, Sprague-Dawley rats with full-thickness wounds were used. The functional living skin (FLS) was implanted into the wounds and a GelMA/HA-NB/LAP pregel was injected and crosslinked to fill any remaining gaps. FLS-treated wounds exhibited faster healing and advanced skin regeneration than controls, showing follicles and sebaceous glands, as well as the lowest inflammatory response [77]. In another study, Yang et al. developed a bilayer membrane scaffold (BLM) by printing poly (lactic-co-glycolic acid) (PLGA) as the outer layer, and alginate as the lower layer for wound healing application (Fig. 4A) [78]. Mimicking skin's dermis and epidermis, alginate and PLGA layers are intended to promote cell function and conserve moisture, respectively. SEM micrographs showed PLGA nanofibers with an average diameter of 857 nm and a microporous alginate layer. The thickness of the layers was also calculated to be nearly 20 μm for PLGA and 100 μm for the alginate hydrogel. In terms of moisture retention, it was shown that alginate hydrogel lost more than 90% of the water in 24 h, while the BLM scaffold maintained its wetness for 72 h. Consistently, the vapor transmission rate was observed to be much lower for PLGA nanofibers than BLM scaffolds. This lower evaporation rate, which can preserve adequate moisture, is advantageous for the wound bed as it can enhance the viability of epithelial cells and promote migration and proliferation. The experiments also revealed that by adding PLGA to the alginate hydrogel, the mechanical properties of the constructs were enhanced (the tensile stress of ≈231 kPa for alginate hydrogels reached≈ 2753 kPa; the elongation at break increased from ≈139 kPa to ≈304 kPa, and the YM was ≈24 kPa and 531 kPa for alginate hydrogel and BLM scaffold, respectively) [78]. Upon comparing the performance between BLM, PLGA, alginate and untreated wounds in Sprague-Dawley rats, the authors observed that BLM treated wounds healed completely by day 12. However, PLGA, alginate, and untreated wounds only achieved 71.5%, 91.2%, and 66.3% wound closure, respectively. Also on the 12th day, BLM treated wounds showed the highest blood vessel density and collagen deposition.

3D printing is not necessarily used to produce a final functional construct for tissue engineering and wound healing purposes. Using 3D printing, sacrificial structures can be made to act as molds to create hydrogels with desired geometrical features. In a study by Wu et al., a 3D-printed silver nanoparticle (AgNP)-containing polyacrylamide (PAM)/hydroxypropyl methylcellulose (HPMC) hydrogel was fabricated via silver−ethylene interaction [79]. To design this superporous antibacterial hydrogel, first a poly (lactic acid) (PLA) template was 3D printed using fused deposition modeling (FDM), and then the hydrogel precursor was cast into the template (Fig. 4B). N, N′-methylenebisacrylamide (MBAM) monomers was used as the main component of the precursors which can interact with Ag ions through the silver−ethylene interaction, leading to polymerization and forming AgNP-loaded nanocomposite hydrogels. Characterization of lyophilized hydrogels without casting in the 3D printed template showed an average pore diameter of 100 μm for PAM, PAM/HPMC, and AgNP-PAM/HPMC hydrogels. However, the PAM/HPMC and AgNP-PAM/HPMC hydrogels exhibited interconnected and open pores compared to the closed pores of the PAM hydrogel, which indicated the importance of incorporating HPMC into PAM to achieve open pores. SEM micrographs of 3D printed superporous hydrogel also showed an average of 100 μm pore size. However, the porosity of these hydrogels is enhanced by ≈ 37% compared to solid hydrogels, reaching around 91%. In addition, the mechanical strength of the 3D-printed hydrogels remarkably decreased (Young's modulus of less than 0.4 MPa) compared to the control solid hydrogels. This mechanical collapse could be related to the large pores of the 3D printed construct, but still in the suitable range for soft tissue engineering and wound healing application [79]. The wound healing ability of the superporous AgNP-PAM/HPMC hydrogels was assessed in a *S. aureus* infected full-thickness wound model in Sprague Dawley rats. Results demonstrated that even when all groups' wounds were completely closed by day 14, the closure rate was faster with

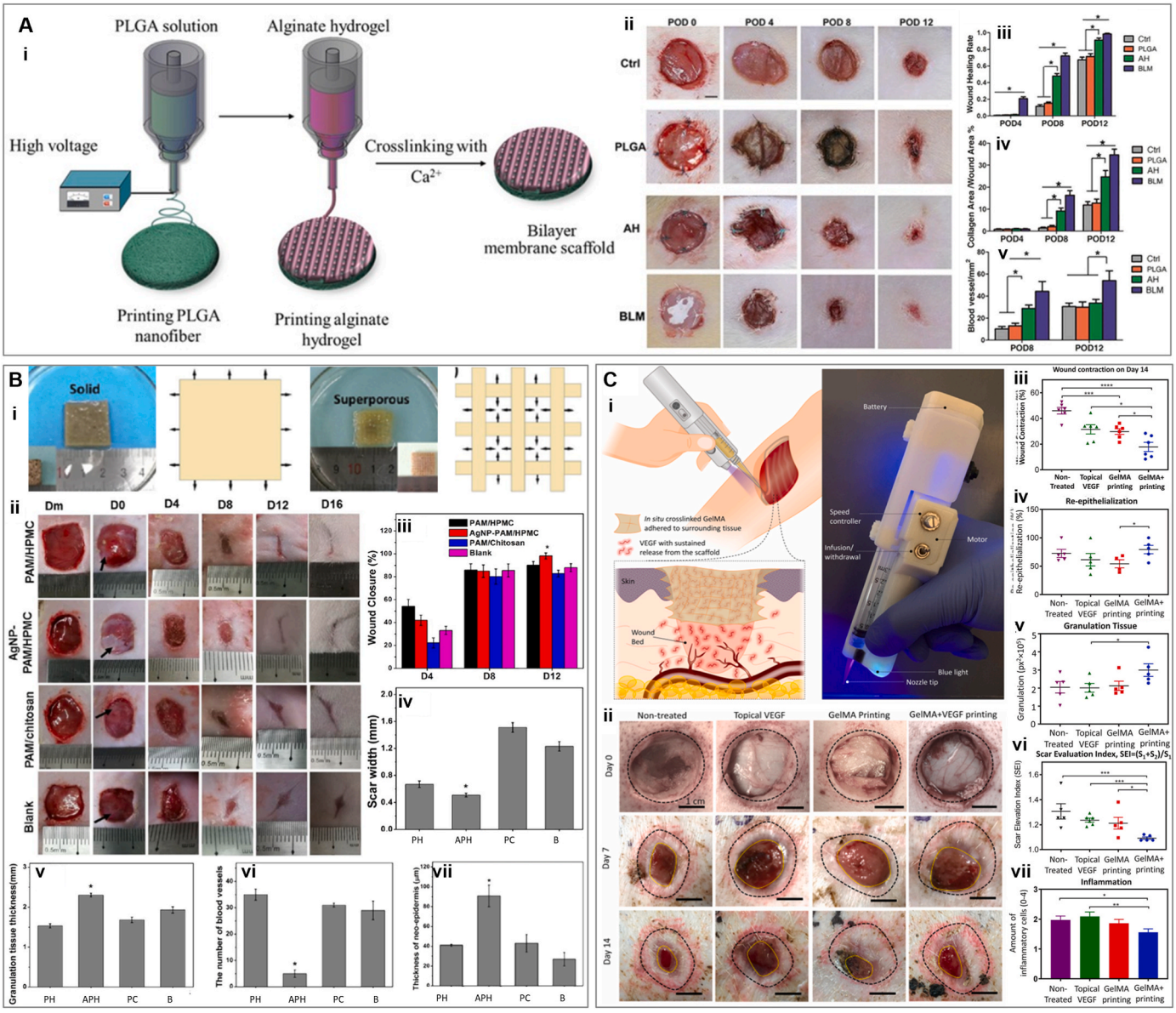

Fig. 4. 3D printing for wound healing application. (A) Poly (lactic-co-glycolic acid) (PLGA)/Alginate hydrogels (i) Schematic process of bilayer PLGA/Alginate membrane scaffold. (ii) *In vivo* wound healing of blank control, PLGA, alginate hydrogel (AH), and bilayer membrane scaffold (BLM) scaffold on days 0, 4, 8, and 12. (iii) Analysis of wound healing rates for different treatments. (iv) Quantification of collagen with trichrome blue staining. (v) Quantification of blood vessel area by analyzing the CD31-positive area. Reprinted and adapted with permission from Yang et al., 2019 [78]. (B). Polyacrylamide (PAM) based hydrogels (i) Swollen state of solid and 3D printed super porous polyacrylamide PAM/hydroxypropyl methylcellulose (HPMC) hydrogels and their schematic representation. (ii) Healing process of wounds treated by PAM/chitosan, (silver nanoparticle) AgNP-PAM/HPMC, or PAM/HPMC over time. (iii) Closure degree of wounds over time. Quantification of scar width (iv) and newborn granulation tissue (v) by H&E staining, and quantification of blood vessels (vi) and thickness of neo-epidermis (vii) by Mason's trichrome staining. Reprinted and adapted with permission from Wu et al., 2019 [79]. (C) Gelatin methacryloyl (GelMA)-vascular endothelial growth factor (VEGF) printing (i) Schematic illustration of *in vivo* printing of GelMA-VEGF hydrogel by a handheld bioprinter. The *in situ* crosslinking process promotes the proper adhesion of the hydrogel to the wound surface. (ii) Representative pictures of the wounds administrated with VEGF, GelMA or GelMA + VEGF on day 7 and day 14 post surgery. (iii) Wound contraction relative to the original wound size. (iv) wound re-epithelialization, calculated based on the area of new epithelium over the total wound area. (v) Amount of granulation tissue. (vi) scar elevation index (SEI) is calculated based on the total area of the healed skin over the area of normal skin below the buildup of hypertrophic scarring. (vii) The degree of inflammation was analyzed by the hematoxylin and eosin (H&E) staining of wound sections to observe the infiltration of inflammatory cells. Reprinted and adapted with permission from Nuutila et al., 2022 [81].

AgNP-PAM/HPMC hydrogels, with a smoother surface and less scarring. It was also observed that this treatment formed the thickest granulation tissue with the smallest scar, as well as the thickest neo-dermis and collagen deposition.

3D printing has brought precision to the architectural design of regenerative constructs or wound dressings. Using this method, it is feasible to make multilayer structures with complex geometry mimicking skin to help wound healing and skin regeneration. However, from the fabrication point of view, there are limitations which should be considered. Printability is the main issue that narrows the range of biomaterials that can be used for 3D printing applications in biomedicine. The challenge is that not only the biomaterial itself, but also the bioactive additives, which are added to the system with the aim of tissue regeneration and wound healing, should not hinder the printability and fidelity properties of the biomaterial. Besides, biomaterials and composites should be shear thinning and have a compatible crosslinking

mechanism with 3D printing. Moreover, talking about bioprinting, in which the living cells undergo a printing process, makes these issues even more complicated. Thus, the state of the art in 3D printed wound dressing is to adjust the functional biomaterials beneficial for wound healing (with or without cells), to be a good fit for the printing procedure.

2.2.2. *In situ* bioprinting

The direct printing of bioinks into the living tissues with the aim of repairing and/or regenerating is called *in situ* bioprinting (also known as "*in vivo*" bioprinting) [80]. The use of this strategy for wound healing minimizes the scaffold preparation time. In addition, more complicated geometries can be fabricated according to the curvature and depth of the wound [80,81]. Two main types of *in situ* bioprinting can be distinguished, robotic [75] and handheld *in situ* printing [82]. Robotic *in situ* bioprinting is highly precise and reliable, but needs complex and expensive instruments not yet widely available. Handheld bioprinters have recently shown great promise in dealing with irregular shapes and curvatures commonly found in real tissues, with the least complexity and being user friendly [81].

One of the major challenges of *in situ* 3D printing is fast delivery and deposition, especially when the intention is delivering cells to the defect site. Commonly, photo-crosslinkable hydrogels are used in *in situ* (bio) printing. Near instantaneous photo-polymerization could occur upon UV exposure of solutions containing thiolated HA, thiolated gelatin, and poly (ethylene glycol) di-acrylate (PEGDA) [83]. GelMA is also a frequently used material for *in situ* bioprinting [84,85]. Next, we describe recent examples. In a study by Skardal et al., a UV cross-linkable heparin-conjugated hyaluronic acid (HA-HP) hydrogel was designed. The authors used a homemade bioprinter, equipped with pressure-driven nozzles, to deliver cells and growth factors for wound healing [86]. The photo-polymerization induced crosslink within a few seconds, ensuring efficient encapsulation of cells for proper *in situ* delivery. Three types of cross-linkers were used in this study in order to modulate structural properties and release kinetics, including linear, four-arm, and eight-arm PEGDA cross-linkers. Results showed a more rapid and cumulatively higher release of bovine serum albumin (BSA) in linear cross-linker HA hydrogels, than that in hydrogels crosslinked with four-arm and eight-arm PEGDA. The microscopic architecture of the hydrogels was also assessed by SEM, indicating an average pore size of ≈100, 50, and 25 μm for linear, 4-armed, and 8-armed PEGDA, respectively. Rheological analysis also exhibited extremely higher G′ for hydrogels crosslinked with 8-armed crosslinker (≈5700 Pa) compared to 4-armed (≈2000 Pa) and linear group (≈200 Pa). Linear crosslinker was selected as the optimal one to have less crosslinking density for more proper delivery of the agents and also an appropriate pore size [86]. The HA-HP hydrogel was used to deliver amniotic fluid-derived stem (AFS) cells to a full-thickness skin wound in a murine model. Many AFS cells appeared in samples taken on day 1, but the amount decreased to 50% on day 7, and by day 14 there were no AFS cells in the harvested tissues. Despite this, HA-HP treated wounds achieved 99.8% closure, whereas HA-treated and control wounds achieved 98.9% and 97.6%, respectively. No significant difference was observed in re-epithelialization, and wound contraction, but the wound aspect ratio was 1.6 and 1.2 for HA-HP and HA treated wounds, respectively, while the control group obtained 2.1. HA-HP + AFS cell treatment also improved vascularization and ECM production and composition.

Besides the fidelity and mechanical stability of 3D printed hydrogels, another obstacle for their application as wound healing constructs is their lack of integration with the defect site. Although *in situ* printing can help to fill irregular cavities, the adhesive interaction of hydrogel with the wound bed is also vital for the proper engraftment and regeneration of tissue. Recently, Nuutila et al. bioprinted *in situ* a GelMA hydrogel containing VEGF using a handheld printer (Fig. 4C) [81]. By adjusting the speed range, the deposition rate of the bioprinter was controllable between 4 and 18 μL/s which is a suitable range to cover either small or large wounds. Moreover, the resolution was tunable by changing the printing speed (hand movement) to achieve fiber diameters ranging from 500 μm to 2500 μm (reduction in diameter by increasing the printing speed). The mechanical analysis of the hydrogels showed that the compressive modulus increased by an increase in the concentration of GelMA; the compressive modulus was determined to be ≈ 1.2, 4.1, and 10.6 kPa, for 6%, 9%, and 12% GelMA, respectively. Furthermore, the adhesion strength of the printed samples to porcine skin was ≈3.7, 6.3, and 10.3 kPa for 6, 9, and 12% GelMA, respectively. The robust GelMA-tissue adhesion observed after *in situ* crosslinking, could be attributed to merely physical interactions (i.e., hydrogen bonding) or even the creation of covalent bonds between the hydrogel and the tissue enabled by the production of free radicals induced by UV *in situ* exposure [87,88]. Both 9% and 12% GelMA printings showed proper shape fidelity. However, the 9% GelMA formulation exhibited lower stiffness, believed to be appropriate for spreading and infiltration of cells [89], with an average pore size of 9.57 μm as determined using SEM. In addition, this porous structure could provide a gradual long-term release of loaded VEGF from the hydrogel (60% in 350 h). For *in vivo* assessment, circular dorsal wounds in a porcine full-thickness wound model were treated with topical VEGF, pristine GelMA, GelMA + VEGF or left untreated. GelMA + VEGF displayed the largest contraction (18% contraction), as compared to 30% in pristine GelMA, 31% in topical VEGF, and 46% in untreated wounds. Microscopic evaluation revealed a higher level of wound re-epithelialization and granulation tissue in GelMA + VEGF treated wounds, as well as a significantly lower scar elevation index. The neoepidermis thickness for GelMA + VEGF treated wounds reached 165 ± 28 μm while the second-best treatment reached 130 ± 14 μm with blank GelMA. The GelMA + VEGF treated wounds also contained the fewest number of inflammatory cells as observed by H&E staining. These results support the use of *in situ* printed GelMA with sustained release of VEGF as an effective treatment for wound healing [81].

The composition of inks could be manipulated for different beneficial purposes besides printability, fidelity, mechanical stability, and integration. Engineering compositions can lead to advantageous properties in terms of wound healing and skin regeneration. For example, formulating a bioink containing interconnected pores up to hundreds of micrometers may enhance cell migration and nutrient transfer in the wound bed. In a study, an emulsion bioink composed of GelMA and polyethylene oxide (PEO) solutions was *in situ* printed by a handheld bioprinter [85]. These two biocompatible aqueous solutions are immiscible, leading to a bioprinted foam with a controllable pore size ranging between 20 μm and about 100 μm. In this emulsion, after forming the hydrogel matrix upon crosslinking of GelMA, PEO droplets leave the system by immersion of the construct in saline or cell culture medium. Not only could the concentration and ratio of the polymers affect the pore size, but also the mixing time was an influential variable. In a constant concentration of 10 wt% for GelMA and 1.6 wt% for PEO, the pore sizes of ≈105, 63, and 32 μm were achieved for the foams produced using mixing times of 5, 10, and 15 s, respectively. As the mixing time increased, the uniformity of the pores was also enhanced. These porous materials induced higher fibroblast proliferation and spreading than standard GelMA hydrogel [85].

Microfluidic techniques can control single or multiple fluids in microscale channels ranging from tens to hundreds of microns [90]. The combination of microfluidic technologies and traditional 3D printing platforms allows for fine control of the compositional and structural features of tissue engineering scaffolds throughout the printing process [90].

Wang et al. produced hollow fibers containing microalgae by quickly polymerizing a fluid containing the microalgae through a coaxial capillary microfluidic chip and then printing them into 3D scaffolds that conformed to irregularly shaped wounds. The inner spindle capillary was pumped with a gelatin inner fluid (5% w/v) with varying $CaCl_2$ concentrations (0.02% w/v). Alginate (2.5% w/v) and GelMA (5.0% w/

v) biopolymers were mixed and poured into the exterior tapering capillary. Depending on the concentration of $CaCl_2$, the channel diameter of the hollow fibers could be adjusted from 150 to 350 μm. Because an oxygenic photosynthetic unicellular microalga (*Chlorella pyrenoidosa*) was introduced during 3D printing, the resulting constructs could continuously supply oxygen under light irradiation, promoting cell proliferation, migration, and differentiation, even under hypoxia. By reducing local hypoxia, enhancing angiogenesis, and encouraging extracellular matrix (ECM) formation, the microalgae-laden scaffolds printed directly into diabetic wounds greatly sped up chronic wound closure [90].

In general, handheld bioprinters, as mentioned before, are user-friendly devices more affordable and user friendly than commercial printers. In addition, they could be designed to overcome common obstacles such as a limited number of inks for 3D bioprinting. In a study by Hakimi et al., a handheld bioprinter containing a microfluidic cartridge was used for *in situ* deposition of different bioinks (alginate and fibrinogen-based) for skin regeneration [82]. Inks were printed simultaneously, the crosslinker was deposited on top of the biomaterial on the wound bed and the thickness of the printed sheets was controlled between 100 and 600 μm via a one-step printing process by adjusting the flow rates. Using systematic turbidity measurements, the kinetics of gelation showed a quicker gelation for the alginate-based layers due to the rapid diffusion of Ca^{2+} ions from above, which is ten times higher than the diffusivity of thrombin (the crosslinker of fibrin-based sheets) at the same viscosity. Fibrin-based sheets with 100, 200, 400, and 600 μm thicknesses showed *in situ* gelation times of ≈44, 64, 110, and 160 s, respectively. Moreover, tensile testing showed a much higher Young's modulus for the alginate-based group than for the fibrin-based group (up to ≈0.25 MPa, compared to ≈0.1 MPa), although the fibrin-based construct exhibited higher elasticity with higher elongation at break than the alginate-group [82]. Preliminary *in vivo* results in a porcine wound model demonstrated possible to stop bleeding post-injury in 5 min after the hydrogel deposition, while untreated wounds bled for 10 min until they reached hemostasis. Also, after 20 days, 3 out of 4 treated wounds achieved complete re-epithelialization, whilst only 1 out of 4 untreated wounds did.

The structural properties of bioinks have been widely investigated in bioprinting for wound healing applications. Several biomaterials have shown a great potential to maintain cell viability and promote certain cell functionalities [91], but they still lack the elasticity of native skin [92]. It would be more complicated to design printable bioinks with high fidelity and optimal elasticity that can provide optimum porosity when the bioinks are going to be more precise.

The recapitulation of native biological features of the skin by including several cell lines and components, such as skin hair follicles, sweat glands, sebaceous glands, among others, increase the challenge of designing printable bioinks with high fidelity and optimal porosity and elasticity. Reducing the cost should be considered as an additional outstanding challenge to overcome to translate bioprinting for wound healing to clinical applications [92].

2.3. Electrospinning

Electrospun nanofibers are one of the most promising and reported micro-/nano scaffolds for wound healing in the last decade [93]. Electrospun hydrogels exhibit both, the characteristics of a fibrous structure and the softness of hydrogels. Nano fibrous constructs can mimic the filamentous network of ECM proteins, leading to proper cell attachment, proliferation, and migration for skin regeneration. These networks, which pose strong interconnectivity and a porosity of 80–95%, also have great potential for vascularization, and could be a promising platform for wound healing application. One of the great advantages of electrospinning is the adjustability of the final architecture by changing parameters of the polymer solution, such as concentration, viscosity, molecular weight, etc. In a study, Sun et al. fabricated a GelMA fibrous hydrogel via electrospinning for skin regeneration [94]. Electrospun UV-crosslinkable GelMA hydrogels with three different degrees of methacrylation (30%, 50%, and 70%) were synthesized and characterized. SEM micrographs showed similar morphology for GelMA and control gelatin electrospun fibers with no significant difference in the average diameters (1.52 and 1.36 μm, respectively). Nevertheless, incubation in PBS for 24 h led to a significant difference in the average diameter in the two groups, reaching ≈2.18 μm for GelMA and ≈1.76 μm for crosslinked (with glutaraldehyde) gelatin samples. This result indicated a higher swelling ratio for GelMA fibers than for pristine gelatin. Moreover, water permeability was reduced by the increase of methacrylation degree. The analysis showed a mean permeability of 2130, 1580, 810, and 680 L m^{-2} h^{-1} atm^{-1} for GelMA-30, GelMA-50, GelMA-70, and crosslinked gelatin, respectively. Thus, the photo-crosslinked GelMA meshes were more appropriate to preserve water content for the wound bed than chemically crosslinked gelatin. The tensile test of fully hydrated fibers showed higher tensile strength for the crosslinked gelatin hydrogel (≈370 kPa) than for GelMA-30 and GelMA-50 (≈230 kPa and 260 kPa respectively), but similar range to GelMA-70. However, elongation at break was observed to be higher in GelMA samples, reaching around 65% for GelMA-70 hydrogel, than in crosslinked gelatin. This suggests more flexibility and elasticity arguably due to a modified chain length and a lower amount of cross linkers in GelMA than in crosslinked gelatin samples. Degradation analysis also exhibited more weight loss for GelMA samples up to 28 days (88% for GelMA-70) than for crosslinked gelatin (63%). This result indicates fast degradability for GelMA samples, which is believed to be more suitable for *in vivo* application. *In vitro* experiments revealed that electrospun GelMA scaffolds support dermal fibroblasts and endothelial cell adhesion, proliferation, and migration. Also, electrospun GelMA membranes used *in vivo* to treat skin flaps in a rat model decreased the formation of necrotic tissue, and allowed better blood perfusion of the skin flap, biodegraded faster, and achieved higher microvessel density 7 days post-implantation than controls [94]. Hydrogel electrospun fibers have also been reported to be promising for wound healing by Zhao et al. [95]. In this study a nano fibrous GelMA scaffold was fabricated with adjustable physical characteristics using electrospinning. Electrospun PLGA and glutaraldehyde-crosslinked gelatin samples were considered as control groups. For all the samples, the fiber diameters were in the range of 700 nm–1400 nm. After 24 h in water, they increased their diameters to 1200 and 2000 nm for the GelMA and gelatin groups, respectively. By increasing the UV exposure time the water permeability was reduced due to a higher degree of photo-crosslinking, and, conversely, the water retention capacity was enhanced. Mechanical properties were also enhanced by an increased exposure to UV light. For 10 min of exposure time, the Young's moduli of GelMA-based mats was reported at around 350 kPa; the tensile strength and elongation at break were 360 kPa and 60%, respectively. In contrast, PLGA mats showed much higher Young's moduli (≈30 MPa) and tensile strengths (≈37 MPa) than GelMA mats; however comparable elongation at break was observed for these scaffolds (≈60% for both PLGA and GelMA with 10 min of UV exposure time). The softer 3D matrixes made of GelMA allowedhigher fibroblast migration and viability compared to control groups [96–98]. The biodegradation properties of GelMA appeared to be advantageous too; they could match the wound healing dynamics by an early mass loss of around 15% in the first 3 days, followed by a gradual degradation up to 90% until day 28 [95,99]. GelMA electrospun scaffolds supported fibroblast survival, proliferation, and migration *in vitro*, better than gelatin and PLGA scaffolds. *In vivo* results comparing GelMA, gelatin, PLGA, and untreated wounds in mice showed that GelMA treated wounds achieved the fastest wound closure and developed a 100 μm thick epidermis on day 21, as well as bundles of organized collagen fibers as observed by Masson's trichrome staining. These results demonstrated the promising performance of GelMA electrospun scaffolds as wound dressing and scaffold for skin model construction [95].

In situ electrospinning of hydrogel fibers has also been investigated in

studies on wound healing and skin regeneration [100]. Koosha et al. used electrospinning to prepare *in situ* glyoxal-crosslinked chitosan/poly (vinyl alcohol) (PVA) hydrogel nanofibers reinforced with halloysite nanotubes (HNTs) without the need for post-treatment stabilization of the nanofibers in an alkaline medium. The incorporation of HNTs into the crosslinked chitosan/PVA nanofibers was confirmed by morphological analyses using SEM/EDX and TEM, and agreed with XRD patterns. The hydrophilic nature of the HNTs caused the nanocomposite nanofibers to swell by almost 400%, whereas crosslinked chitosan/PVA nanofibers showed swelling of only 272%. The addition of 3% and 5% HNTs to the crosslinked nanocomposite nanofibers increased the tensile strength by 2.4 and 3.5 times, respectively, when compared to chitosan/PVA nanofibers. The hydrophilicity of HNT-reinforced nanofibers, demonstrated by a decrease in the water contact angle, favored the attachment of fibroblast cells when HNTs were present in chitosan/PVA nanofibers. The addition of HNTs improved the nanofiber biocompatibility, as demonstrated by AlamarBlue cytotoxicity tests. Glyoxal was also confirmed to have no harmful effects on fibroblast cells and can therefore be utilized safely for crosslinking chitosan/PVA nanofibers [100].

Electrospinning is a versatile and relatively inexpensive method to fabricate micro and nanofibrous scaffolds for tissue regeneration in a reproducible manner. Different numbers of synthetic and natural polymers have been used within this method to fabricate wound dressings. The electrospun mat is highly tailorable as different parameters such as concentration of polymer, applied voltage, etc., can be altered. However, some limitations, such as high voltage application, toxicity of solvents, and difficult handling, could hinder its capability, especially to fabricate hydrated fibrous scaffolds for skin regeneration and wound healing. Innate characteristics of biomaterials are different and could be modulated to be appropriate for wound healing. Moreover, fabrication approaches could modulate their architecture, leading to more sophisticated and versatile scaffolds. Besides the porosity, which is important for nutrient transition and cell migration, one of the most important structural complexities which could be more investigated for wound dressing hydrogels is to design vasculature or tubular-like architectures to allow endothelialization within the hydrogel. This issue is very important, especially for deep wounds that need larger tissue to be regenerated. Furthermore, for structural design, gradient hydrogel constructs could be further evaluated to achieve more advanced regenerative strategies for wound healing and regeneration of injured beneath tissues. For example, a gradient structure in terms of mechanical and physical characteristics may help regeneration of two adjacent tissues (for example, skin and muscle) within the same treatment and 3D hydrogel. Moreover, this gradient could be coupled with a biological gradient to optimize regeneration. A summary of the reviewed studies in this section is represented in Table 1.

3. Engineering the biological environment: additives or enhancers

Besides the engineering of the mechanical and structural properties of a desirable wound dressing, understanding the healing process is key to properly use bioactive agents that could assist healing and regeneration [101]. Wound healing is impaired by different factors like unstable hemostasis, infection, lack of oxygen perfusion, edema and necrosis, which could be controlled by adding different bioagents [102]. Hemostatic, antibacterial, anti-inflammatory or antioxidant molecules could hinder bleeding, infection, inflammation, and oxidative stress to provide a normal path for further steps of wound healing, including proliferation and remodeling [102]. On the other hand, other components such as growth factors, chemokines, electroactive biomaterials, and some metallic ions may contribute directly to regeneration steps. Owing to mild processing conditions, hydrogels can be loaded with various bioactive ingredients and/or cells, and their high porosity and controllable crosslinking density allow them to be delivered in a suitable manner for accelerating wound healing [101,103]. In this section, we elaborate on investigations related to hydrogels impregnated with biomaterials, molecules, drugs, nanoparticles (NPs), and cells for wound healing application.

3.1. Antibacterial agents

Excessive bacterial growth in wounds is detrimental to the healing process. When bacteria proliferate and form a colony, the normal process of wound healing breaks down. Infection is known as a bacterial population of 10^5 per gram of tissue, and it acts as a bioburden as bacteria compete against fibroblasts and macrophages for nutrients [104].

Although any type of wound dressing could be a mechanical barrier to protect tissue from external bacterial attack, it seems crucial to use antibacterial wound dressings to suppress infection or to prevent further bacterial growth. A wide range of antibacterial moieties have been investigated for wound healing, including antibacterial polymers [105,106], peptides [107], NPs [108,109], and antibiotics (Table 2). Alternatively, antibacterial hydrogels can be fabricated from inherently antibacterial polymers. In general, the antimicrobial activity of these antibacterial materials lasts longer than that of composite hydrogels added with antimicrobial agents [105,107]. Among the inherit antibacterial polymers, chitosan (CS) is one of the natural polymers that has been extensively investigated in tissue engineering, especially in wound healing applications, due to its advantageous characteristics such as biocompatibility, high functionality, pain relief, and hemostasis. For example, Miguel et al. fabricated injectable chitosan–agarose hydrogels (CAH) with the aim of skin regeneration and wound healing. CAH hydrogels exhibited proper biocompatibility; confocal microscopy showed fibroblast migration and proliferation within the construct. *In vivo* analysis indicated great wound healing potential of CAH hydrogels; higher re-epithelialization and lower inflammation was observed in CAH treated wounds than in the non-treated group. A minimum inhibitory concentration test (MIC) showed that hydrogels with a chitosan concentration higher than 188 μg/mL, exhibited antibacterial activity against *S. aureus* [110]. Poly-cationic chitosan is able to interact with the electronegative components at the surface of the bacteria's membrane, leading to an increase in cell wall permeability and thus the leakage of cytoplasmic constituents and a loss of ionic gradient through bacterial membranes [111]. In another study, Chen et al. designed an injectable hydrogel composed of chitosan and konjac glucomannan (KGM). These highly adhesive hydrogels exhibited great biocompatibility and dramatically reduced wound healing and re-epithelialization time in an *in vivo* model (Fig. 5A). Moreover, hydrogels inhibited bacterial *S. aureus* and *Escherichia coli* (*E. coli*) growth in 96 and 98%, respectively [105].

Poly-ethylen-imine (PEI) is another antibacterial polymer used for wound healing applications that contains repeated amine units which protonate at physiological pH. These positive charges interact with negatively charged bacteria's surfaces, causing bacterial death via mechanisms including membrane damage or cell depolarization [106]. Giano et al. presented an inherent antibacterial adhesive hydrogel that contained a mixture of poly-dextran aldehyde (PDA) and branched PEI. In this hybrid hydrogel, PDA acts as the adhesive and PEI as a crosslinker and an antibacterial material. The authors observed an *in vitro* antibacterial effect against gram-negative and gram-positive bacteria of the PDA/PEI hydrogels which was also demonstrated *in vivo* in two different infection models with minimal inflammatory response [106].

An aminoacidic-based polymer, ε-poly-L-lysine (EPL), has also been reported as a suitable platform for wound healing applications. This is a biocompatible, biodegradable, and nontoxic homo-poly-amino acid that has exhibited innate antibacterial characteristics [112]. Membrane disruption (resulting in cell lysis) has been hypothesized as the mechanism for the antimicrobial activity of this polymer. Wang et al., designed an injectable dopamine-modified EPL-polyethylene glycol-based hydrogel (PPD hydrogel) that promoted wound healing via faster re-epithelialization than fibrin glue (applied in the control group). The

Table 1
Structural engineering of hydrogel wound dressing.

	Method of fabrication	Material	Crosslinking method	Additives	Study	Structural features	Biological results	Ref
1	Prefabricated casting	GelMA	Photocrosslinking	————	*In vitro*	Compressive modulus up to 200 kPa is dependent on polymer concentration and UV exposure time. Prolonged degradation up to 8 weeks using 20% GelMA.	Over 90% viability of human epidermal keratinocytes (HaCaTs) cultured on the hydrogels. Cellular attachment increases on stiffer hydrogels. Differentiation and stratification of HaCaTs into a multilayered epidermis.	[34]
2	Prefabricated casting	Heparin and PEG-DA	Photocrosslinking	hEGF	*In vitro/ in vivo*	Swelling capacity was higher in heparin-containing hydrogels. Heparin-containing hydrogels have a G′ of 14 kPa and a WVTR of 1010 g/m^2/day. Heparin extended the release of hEGF up to 21 days.	hEGF loaded heparin-based hydrogel enhanced wound closure, granulation tissue formation, epithelialization and capillary formation compared to control groups.	[36]
3	Prefabricated casting	CS, PEG, and PVP	Ionic crosslinking	Tetracycline hydrochloride	*In vitro/ in vivo*	In the presence of PVP, a spherical porous structure was observed, and the swelling rate increased from ~400%–1210%. Tensile strength of 0.8 MPa for 60% humidity and WVTR of ~2230 g/m^2/day were detected for the CS/PEG/PVP sample.	80% of drug was released after 48 h antimicrobial effect was observed *in vitro* against both gram-positive and gram-negative bacteria. Antibiotic containing samples accelerated wound healing with minimum scar formation.	[40]
4	Prefabricated casting	HA	Dynamic coordinate bond between EDTA−Fe^{3+} complexes cross-linked with hyaluronic acid (HA)	Platelet-derived growth factor BB (PDGFBB)	*In vitro/ in vivo*	Higher G′ values than G″ for different ratios of Fe^{3+}−EDTA. G′ ≥ 200 Pa for Fe^{3+}−EDTA complexes and HA units equal to 1:2.	*In vitro* antibacterial effect against *E. coli* and *S. aureus* due to release of Fe^{3+}. Promoted *in vivo* skin regeneration with no inflammation 10 days post implantation.	[42]
5	Prefabricated casting	Pectin & PAA	Interpenetrating network with free-radical polymerization	Lignin-coated Ag NPs & epidermal growth factor (EGF) EGF	*In vitro/ in vivo*	High resilience and stretchability up to 26 times the primary length. NPs-P-PAA hydrogel showed tensile strain of 2660%, ductility of 300 MPa%, fracture energy of 5500 Jm^{-2} and adhesion strengths to porcine skin of 25 kPa for the NPs-P-PAA hydrogel.	High antibacterial activity *in vivo* with increased wound healing and skin tissue regeneration compared to control groups.	[43]
6	*In situ* forming hydrogel	Collagen type I, Poly-D-Lysine (PDL) and chondroitin sulfate	Covalent and ionic bonding	————	*In vitro/ in vivo*	Chondroitin sulfate extended the gelation time to 1 h. A pore size of 10 μm was observed for the collagen/PDL sample. Adding air microbubbles increased the pore size to ≈30–40 μm.	Support for migration of MSTC-derived cells. Bacterial growth inhibition *in vivo* and promoted wound healing.	[47]
7	*In situ* forming hydrogel	Silk fibroin (SF) extracted from two different silkworm	Physical entanglements and crosslinking	————	*In vitro/ in vivo*	Pore size of ≈155 μm, Water retention of 75% for SF blend hydrogel after 12 h compared to 20% for the collagen control group. G′ of 336.42 Pa, compressive modulus of ≈7.4 kPa and 85% of the weight preservation after 14	Proliferation of human dermal fibroblasts and migration keratinocytes *in vitro*. Improved wound healing and more collagen deposition were observed for SF hydrogel compared to the collagen control group.	[51]

(*continued on next page*)

Table 1 (*continued*)

	Method of fabrication	Material	Crosslinking method	Additives	Study	Structural features	Biological results	Ref
						days was observed for SF hydrogel.		
8	*In situ* forming hydrogel	Benzaldehyde-terminated PEG and dodecyl-modified chitosan (DCS)	Reversible Schiff base	VEGF	*In vitro/ in vivo*	Highest G′ was observed ≈600 Pa. Rheological recovery analysis demonstrated self-healing capability.	Strong blood cell coagulation and hemostasis and anti-infective properties. An increase in wound closure, deposition of collagen, angiogenesis, and granulation tissue formation by using a VEGF-loaded hydrogel.	[56]
9	*In situ* forming hydrogel	Oxidative hyaluronic acid (OHA), Poly-ε-L-lysine (EPL) and Pluronic F127 (F127)	Reversible Schiff's base	Adipose mesenchymal stem cells (AMSCs)-derived exosomes	*In vitro/ in vivo*	G′ in the range of 10^3 Pa was observed for all samples at 37 °C, indicating formation of hydrogel. Self-healing capability was shown as G′ of hydrogel was decreased from ~10 kPa to several pascals by an increase of strain up to 1000% and recovered at a strain of 1%.	Exosome-containing hydrogel enhanced proliferation and tube formation ability of HUVECs *in vitro*. *In vivo* analysis showed enhanced wound healing rate, angiogenesis, deposition of collagen and re-epithelialization.	[57]
10	*In situ* forming hydrogel	HA	Dynamic coordination crosslinking	Ag^+ ions	*In vitro/ in vivo*	G′ of ≈400 Pa and G″ of ≈100 Pa. Non-fibrous architecture	Antimicrobial effect against both Gram-positive and Gram-negative bacteria. *In vivo* analysis showed higher wound closure and more complete epithelium layer compared to control group.	[50]
11	*In situ* forming hydrogel	PDA nanoparticles and glycol chitosan (GC)	Schiff's base reaction/Michael addition	Ciprofloxacin	*In vitro/ in vivo*	G′ ≈500 Pa. Photothermal behavior of samples was demonstrated and when exposed to NIR with a power of 0.5 W/cm^2, hydrogels reached 46.8 °C to release antibiotics.	On demand antibacterial effect *In vitro* against *S. aureus*. Antibacterial efficacy and enhanced wound closure *in vivo* without inflammatory responses.	[58]
12	*In situ* forming hydrogel	Quaternized hydroxyethyl cellulose (HEC)/ mesocellular silica foam (MCF)	Radical graft copolymerization	————	*In vitro/ in vivo*	Sol-gel transition characteristics and the highest G′ and viscosity for HEC were up to 10^3 and ≈70 Pa, respectively. By increasing MCF, G′ and viscosity were enhanced to the range of 10^4 and ≈450 Pa, respectively. Swollen composite hydrogel under 37 °C showed G′ in the range of 10^4 Pa.	9.82 w/w% of MCF could trigger the coagulation factors. QHM hydrogel could decrease plasma clotting time to 59% *in vitro* compared to commercially available hemostatic. Great antibacterial and biocompatibility and enhanced wound healing.	[239]
13	*In situ* Injectable/ Microfluidics	Alginate (microcapsules)	Ionic crosslinking	copper-/zinc-niacin	*In vitro/ in vivo*	Size of ~300 μm for alginate capsules containing copper-/ zinc-niacin Smart release of calcium, copper, and zinc ions.	Decreased inflammation and improved angiogenesis and collagen deposition	[60]
14	*In situ* Injectable/ Microfluidics	Poly (hydroxypropyl acrylate-co-acrylic acid)-magnesium ions (poly-(HPA-co-AA) and carboxymethyl chitosan (CMCS) (micro-gel ensemble)	Hydrogen bonding/ amide bonding	Mg^{2+}	*In vitro/ in vivo*	Microfluidics internal/ external flow rate determined microbead size (1–2 mm)	Persistent wound pH modulation Collagen deposition, macrophage polarization, and blood vessel development	[61]
15	Prefabricated 3D printing (Extrusion-based)	Cellulose nanofibril (CNF)	Ionic and chemical (by BDDE) crosslinking	————	*In vitro*	YM of 3.45 kPa for 1 wt % CNF hydrogel and reached 7.44 kPa after	Viability of fibroblast cells. Promoted cell proliferation compared	[66]

(*continued on next page*)

Table 1 (*continued*)

	Method of fabrication	Material	Crosslinking method	Additives	Study	Structural features	Biological results	Ref
						second (chemical crosslinking). No failure at 50% strain, indicating excellent elasticity.	to the 2D structure. Cell proliferation is enhanced with an increase in rigidity of the hydrogel.	
16	Prefabricated 3D printing (Extrusion-based)	Chitosan	Ionic crosslinking	————	*In vitro/ in vivo*	Total thickness of 2.1 mm. Distance between filaments ≈200 μm and a Feret diameter of ≈3.5 μm and 5 μm for the surface and within the structure, respectively. The YM of the samples ≈10^5 kPa.	*In vitro* proliferation of human fibroblasts and keratinocyte. Formation of a skin-like layer. Improved wound closure compared to non-treated groups *in vivo*.	[68]
17	Prefabricated Bioprinting (Extrusion-based	Pectin methacrylate (PECMA)	Ionic crosslinking & Photocrosslinking	Arginylglycylaspartic acid (RGD)	*In vitro*	Range of G′ between ≈79.6 Pa and 2600 Pa based on concentration and DM. After swelling, the elastic modulus of hydrogels (1.5 wt%) decreased significantly from ~1000 Pa to ~400 Pa. Polymer solutions supplemented with 5 mM and 7 mM of $CaCl_2$ were able to form stable, neat filaments.	RGD-PECMA high hydrogels supported metabolic activity of fibroblasts when photocrosslinked for 160 s (G′ of 229.8 ± 44.0 Pa). Although with secondary ionic crosslinking, higher concentration and UV exposure time followed to stiffer hydrogels (160 s: 842.0 ± 97.8 Pa; 300 s: 1210.0 ± 148.5 Pa), spreading of the cells was significantly reduced.	[72]
18	Prefabricated Bioprinting (Extrusion-based)	Calcium silicate (Calsil) nanowires, sodium alginate (SA), Pluronic F127, and L (+)-Glutamic acid (CS + SA hydrogel)	Photothermal & Ionic crosslinking	OPC	*In vitro/ in vivo*	Hydrogels containing OPC exhibited compacted porous structure with a small pore size.Photothermal conversion efficiency was observed by changing NIR power. G′ in the range of 10^2 and mechanical stiffness of 8 kPa for Calsil + SA + 6%OPC after 30 min of NIR laser exposure.	Supported proliferation, and migration of fibroblasts and human umbilical vein endothelial cells (HUVECs). Improved angiogenesis and skin regeneration *in vivo*.	[73]
19	Prefabricated Bioprinting (Extrusion-based)	Fibrinogen and decellularized human skin-derived extracellular matrix (dsECM).	Thrombin-Fibrinogen (Enzymatic) crosslinking	————	*In vitro*	Addition of dsECM to fibrinogen matrix increased G′ reached 452.6 Pa vs. 207.7 Pa for control fibrinogen and after thrombin crosslinking reached ≈800 Pa. 15 days after culture of fibroblasts, G′ was increased compared to cell-free hydrogels, 400 kPa vs 200 kPa. Fibrinogen + dsECM exhibited better shear thinning properties compared to control dsECM and fibrinogen.	Viability of fibroblast was supported till only day 8 for fibrinogen and significantly improved till day 15 in the fibrinogen + dsECM	[76]
20	Prefabricated Bioprinting (DLP 3D printing)	GelMA & HA-NB	Photocrosslinking	————	*In vitro/ in vivo*	Tunable mechanical properties. The compressive modulus was 30–100 kPa based on polymer concentration. The pore size ranged from 200 μm to 400 μm.	Promoted fibroblast and HUVEC migration and proliferation, and Tissue in growth and improved skin regeneration *in vivo*.	[77]
21	Prefabricated 3D printing (FDM) 3D printer	Polyacrylamide (PAM)/ hydroxypropyl methylcellulose (HPMC)	Silver−ethylene interaction	AgNPs	*In vitro/ in vivo*	14 times the dead weight of water uptake capacity was observed for hydrogel. An average pore diameter of 100 μm observed for all samples. The	Enhanced infected wound regeneration and inhibited scar tissue formation *in vivo*.	[79]

(*continued on next page*)

Table 1 (*continued*)

	Method of fabrication	Material	Crosslinking method	Additives	Study	Structural features	Biological results	Ref
						addition of AgNPs and HPMC made pores interconnected. A porosity of 91% and a YM of less than 0.4 MPa were observed for super porous hydrogels.		
22	Prefabricated 3D printing (Extrusion-based) + Electrospinning	Alginate and PLGA	Ionic crosslinking	————	*In vitro/ in vivo*	Bilayer membrane scaffold. Thickness of ~20 μm for PLGA and ~100 μm for alginate hydrogel. PLGA layer enhanced water retention, mechanical properties (YM ≈ 24 kPa and 531 kPa for alginate hydrogel and bilayer scaffold), and decreased degradation rate.	Bilayer membrane improved cell proliferation *in vitro* and promoted, wound closure, collagen deposition, and vascularization *in vivo*.	[78]
23	*In situ* bioprinting (Pressure-driven)	Heparin-conjugated hyaluronic acid (HA-HP)	Photocrosslinking	FGF and VEGF	*In vitro/ in vivo*	Hydrogels crosslinked with four-arm crosslinkers showed a higher release rate compared to eight-arm HA hydrogels. Average pore size of ≈100 μm, 50 μm and 25 μm and G′ of ≈200 Pa, 2000 Pa, and 5700 Pa for linear, 4-armed, and 8-armed, respectively.	Prolonged release of heparin-binding growth factors. Promoted wound closure, ECM production, re epithelialization, and vascularization *in vivo*.	[86]
24	*In situ* bioprinting (handheld Skin Printer with microfluidic cartridge)	Alginate and fibrinogen	Ionic crosslinking and enzymatic crosslinking	————	*In vitro/ in vivo*	Thickness of 100 μm–600 μm via a one-step process. Faster gelation and higher YM for alginate-based compared to fibrin-based hydrogels (≈0.25 MPa vs ≈ 0.1 MPa)	Supported interaction and viability of keratinocytes and fibroblasts. Normal re-epithelialization and wound contraction.	[82]
25	*In situ* bioprinting (handheld)	A two-phase aqueous emulsion bioink made of GelMA and polyethylene oxide (PEO)	Photocrosslinking	————	*In vitro*	The pore size ranged between 20 μm −100 μm based on the concentration and ratio of GelMA and PEO and mixing time.	Improved survival and proliferation of fibroblasts compared to standard GelMA hydrogel.	[85]
26	*In situ* bioprinting (handheld)	GelMA	Photocrosslinking	VEGF	*In vitro/ in vivo*	The fiber diameter ranged from 500 μm to 2500 μm (reduction by increasing the printing speed). Compression modulus of ≈10.6 kPa and adhesion strength to porcine skin of ≈10.3 kPa were reported for samples with GelMA 12% (w/v). The average pore size was 9.57 μm.	Improved migration of endothelial cells *in vitro* due to the sustained release of VEGF. Improved wound closure, neoepidermis formation, angiogenesis, and decreased scar formation compared to control treatments *in vivo*.	[81]
27	3D printing/ Microfluidics	Alginate and GelMA (hollow fibers containing microalgae)	Ionic and photocrosslinking	Chlorella pyrenoidosa	*In vitro/ in vivo*	Depending on $CaCl_2$ concentration, hollow fiber channel diameter could be 150–350 μm.	Promoted cell proliferation, migration, angiogenesis, and wound closure *in vivo*	[90]
28	Electrospinning	GelMA	Photocrosslinking	————	*In vitro/ in vivo*	Average diameters of ≈1.52 μm and 2.18 μm for GelMA for electrospun fibers before and after incubation in PBS. Decrease in permeability was by increase of MD. Tensile	Supported adhesion, migration, and proliferation of endothelial and fibroblast cells. Improved vascularization *in vivo*.	[94]

(*continued on next page*)

Table 1 (*continued*)

	Method of fabrication	Material	Crosslinking method	Additives	Study	Structural features	Biological results	Ref
						strength up to ≈260 kPa.		
29	Electrospinning	GelMA	Photocrosslinking	————	*In vitro/ in vivo*	Average diameter of 1200 nm after 24 h in water. Water retention capacity and YM (350 kPa) improved by an increase in UV exposure time.	Supported adhesion, migration, and proliferation of fibroblast cells. Improved wound closure and collagen deposition *in vivo*.	[95]
30	*In situ* electrospinning	Chitosan/poly (vinyl alcohol) (PVA)	Chemical crosslinking mediated by glyoxal	Halloysite nanotubes (HNT)	*In vitro*	HNT's hydrophilic nature led increase swelling ratio. nanofibers. Nanofibers with 3 and 5% HNT had 2.4 and 3.5 times the tensile strength of chitosan/PVA nanofibers.	HNT increased nanofibers' biocompatibility. Glyoxal does not harm fibroblast cells and can be used to crosslink chitosan/PVA nanofibers.	[100]

antimicrobial properties of PDD conjugates are reported to be dependent on the degree of substitution (DS) of dopamine in the EPL backbone [112]. This characteristic is linked to the higher content of free amino groups and reduced DS in the EPL backbone, which correspond to each other. The EPL was primarily responsible for the ability of the PPD hydrogel to inhibit bacterial growth, and prior investigations had suggested that cell wall/membrane lysis was the mechanism underlying the antibacterial activity [113,114]. Measurements at OD625 nm revealed that PPD hydrogels with the lowest DS had killing abilities against *E. coli* and *S. aureus* of around 95% and 100%, respectively, while fibrin glue, as a control material, showed no antibacterial activity against these microorganisms [112].

Besides biopolymers with intrinsic antimicrobial properties, hydrogels for wound healing applications could be impregnated with different types of antibacterial agents. For instance, curcumin (diferuloylmethane), which is derived from the spice turmeric (*Curcuma longa*), is a yellow pigment with relevant antibacterial, anti-inflammatory, antioxidant, and anticancer properties, as reported by more than 6,000 research articles and more than a hundred clinical studies [115]. Next we briefly discuss several studies associated with curcumin-loaded hydrogels for wound healing applications. Qu et al., designed an injectable micelle/hydrogel hybrid wound dressing composed of quaternized chitosan (QCS) and benzaldehyde terminated Pluronic®F127, loaded with curcumin. An excellent antibacterial rate of over 90% was observed for different hydrogel groups against *S. aureus* and *E. coli*. Besides, the curcumin-incorporated hydrogel exhibited relevant antioxidant activity and pH responsive release profiles. *In vivo* analysis in a full-thickness skin defect model revealed that curcumin within the hydrogel matrix improved the wound healing rate through higher granulation tissue formation (Fig. 5B), collagen deposition, and upregulation of vascular endothelial growth factor (VEGF) [116]. The mechanism behind the antimicrobial activity of curcumin needs to be better understood. However, curcumin killing activity against *Bacillus subtilis* is reported to be related to the inhibition of bacterial cell proliferation by blocking the assembly dynamics of FtsZ in the Z ring [117,118].

Honey is another natural product that has been shown to have great antibacterial activity for wound healing applications. In a study by El-Kased et al., six different formulations of honey hydrogels were prepared using chitosan and carbopol 934 as gelling agents. The antibacterial activity of the six formulations was evaluated against *Pseudomonas aeruginosa* (*P. aeruginosa*), *Klebsiella pneumoniae* (*K. pneumoniae*), *Streptococcus pyogenes* (*S. pyogenes*), *S. aureus*, and *E. coli*. The result of the disc-diffusion-antibiotic-sensitivity assay indicated higher antibacterial activity for hydrogels containing chitosan as a gelling agent and hydrogels with a higher concentration of honey. Among hydrogels containing chitosan, hydrogels with a concentration of 75, 50, and 25% of honey exhibited a minimum bacteria growth inhibition zone of ~8.7, 12.3, and 8.3 mm, respectively. On the other hand, the minimum inhibition zone for bacterial growth for carbopol hydrogels for highest to lowest honey concentration was reported to be 6.8, 6.4, and 5.5 mm. *In vivo* analysis of burn wound treatment also confirmed the highest contraction for the wounds treated with honey 75%-chitosan. The wound diameter for honey 75%-chitosan, pure honey, silver sulphadiazine (a commercial treatment), and normal saline was determined as ~3.8, 5.3, 5.9, and 6.3 mm, respectively, after 9 days of treatment [119]. It is believed that the high content of sugar (that reduced water activity), low pH, and generation of peroxide, nitric oxide, and prostaglandins might be responsible for the antibacterial activity of honey [120]; but more research is needed to fully understand the basis of the antibacterial activity of honey.

Tannic acid (TA), a polyphenolic compound, exhibits antioxidant, anti-inflammatory, and anti-microbial properties which has been used in the clinic in the last decades [121]. For instance, a carboxylated agarose/tannic acid hydrogel was designed by Ninan et al. demonstrating the great potential of TA for wound healing applications. The authors examined cell migration and proliferation in a 2D wound scratch model. They observed that 3T3 fibroblast cells treated with TA-hydrogel conditioned media exhibited remarkably higher migration and proliferation than the control cells exposed to Dulbecco's Modified Eagle Medium (DMEM) with 10% Fetal bovine serum (FBS). The TA-releasing hydrogel showed *in vitro* antimicrobial activity against both *S. aureus* and *E. coli* in an agar diffusion test. The antimicrobial activity of TA could be mediated by mechanisms such as enhanced permeability or disruption of bacterial membranes, or enzyme inhibition through interaction with bacterial proteins [121].

Among the antibacterial molecules used in tissue engineering and wound healing applications, antimicrobial peptides (AMPs) have recently attracted great attention [122]. AMPs are composed of short sequences of cationic amino acids produced by most living creatures [123]. These cationic molecules could be attracted to negatively charged surfaces of bacteria and, as a result, could change the electrostatics of the bacteria surface, disrupt the bacteria membrane, which leads to bacterial lysis [88,107,123]. Annabi et al., developed an antibacterial composite by conjugating the antimicrobial peptide Tet213 to methacryloyl-substituted recombinant human tropoelastin/Gelatin Methacrylate hydrogel (MeTro/GelMA). Colony-forming unit (CFU) assays showed that MeTro/GelMA-AMP hydrogels efficiently inhibited colonization of both methicillin resistant *S. aureus* (MRSA) and *E. coli*, compared to MeTro/GelMA controls. Moreover, antimicrobial evaluation using the LIVE/DEAD™ BacLight™ bacterial viability kit demonstrated the infiltration and colonization of MRSA and *E. coli* within

Table 2
Summary of the reviewed studies involving antibacterial components in hydrogels for wound healing application.

Biomaterials	Antibacterial component	Concentration	Antibacterial Mechanism	Bacterial strains tested	*In vivo*	Main Results	Ref
Chitosan & Agarose	Chitosan	125–400 μg/mL	Electrostatic interaction with bacteria membrane	*S. aureus*	+	Improved re-epithelialization and reduction of inflammation. Hydrogels with CS content higher than 188 μg/mL showed antibacterial activity against *S. aureus*.	[110]
Chitosan and konjac Glucomannan (KGM)	Chitosan	~2.5% w/v	Electrostatic interaction with bacteria membrane	*S. aureus* *E. coli*	+	Enhanced wound healing and re-epithelialization Antibacterial rate against *S. aureus* and *E. coli* was over 95%.	[105]
Polydextran aldehyde/ Polyethylenimine (PDA/PEI)	PEI	6.9% w/v	Electrostatic interaction with bacteria membrane	*S. aureus* *E. coli* *S. pyogenes*	+	Antibacterial activity of hybrid hydrogels was enhanced against *S. pyogenes* by increasing the concentration of PEI	[106]
ε-poly-L-lysine polyethylene glycol based (PPD) hydrogel	ε-poly-l-lysine (EPL)	5% w/v of PPD conjugate	Surface zeta potentials which damage bacteria membrane	*S. aureus* *E. coli*	+	PPD hydrogel promoted antibacterial effect and accelerated rre-epithelialization and wound healing compared to fibrin glue as control group.	[112]
Quaternized chitosan (QCS)/ benzaldehyde terminated Pluronic®F127+Curcumin	QCS/Curcumin	2.7% w/v QCS and 1% w/v curcumin	Blocking the assembly dynamics of FtsZ in the Z ring	*S. aureus* *E. coli*	+	Excellent wound healing rate, granulation tissue formation, and collagen disposition. Proper antioxidant and antibacterial ability against *S. aureus* and *E. coli.*	[116]
Honey-chitosan (CS)	Honey	75%, 50% and 25% w/v of honey.	Low water activity, low pH and generation of peroxide, nitric oxide, and prostaglandin	*P. aeruginosa* *S. aureus* *K. pneumonie* *S. pyogenes*	+	Among honey-CS hydrogels, the sample with highest honey concentration showed strongest antimicrobial effect against four different bacteria species. Higher wound contraction for the wounds treated with 75% honey - chitosan gel compared to control and commercially available wound dressing.	[119]
Carboxylated agarose/tannic acid (TA) hydrogel	TA	0.5% w/v	Enhanced permeability and disruption of the bacteria membrane, enzyme inhibition	*E. coli*	+	Improved cell migration and proliferation for cells exposed to hydrogels containing TA Antimicrobial activity against both *S. aureus* and *E. coli.*	[121]
(GelMA)/(MeTro) hydrogel + AMP Tet213	AMP Tet213	0.1%, 0.3%, and 3 % w/v	Electrostatic interaction with bacteria membrane	*E. coli* *P. aeruginosa* *S. aureus*	+	Hydrogels containing 0.1 and 0.3% w/v AMP showed antibacterial effects similar to 3% (w/v) Zinc Oxide (ZnO) in the same structure.	[88]
Alginate-Chitosan hydrogel/ Tetracycline hydrochloride loaded gelatin microsphere	Tetracycline hydrochloride	1% w/v TH in gelatin microspheres (GM). 30 mg/mL GM.	Protein synthesis inhibition	*S. aureus* *E. coli*	–	Sustained release of TH *in vitro* & strong bacterial growth inhibition effects against *S. aureus* and *E. coli.*	[130]
CS/PVP + silver sulfadiazine	CS + silver sulfadiazine	~1.4% w/v of Cs	Electrostatic interaction with bacteria membrane/ Damaging the cell membrane	*E. coli*	–	Antibacterial activity was observed for all samples (without and with different concentrations of PVP). T6-PVP-0.5 sample exhibited a release profile of 91.2% in PBS within 80 min.	[131]
Guar gum (GG) Gelatin dopamine conjugate (Gel-DA) Silver nanoparticles (Ag NPs)	Silver nanoparticles (Ag NPs)	0.5, 1, 2 mg/mL	Cell wall and cytoplasmic membrane disruption by silver ions, protein synthesis inhibition by ribosomes denaturation	*S. aureus* *E. coli*	+	Inherent antibacterial activity exerted by Ag NPs was enhanced by NIR irradiation. Antibactericidal rates of 96.88% for *S. aureus* and 98.96% for *E. coli.*	[240]
Quaternized chitosan (QCS) Ferric iron (Fe) Protocatechualdehyde (PA),	Quaternized chitosan (QCS)	5% w/v	Electrostatic interaction between the polycationic structure and anionic components of microorganisms	*S. aureus* *E. coli* MRSA	+	MRSA-infected wounds treated with QCS-PA@Fe showed accelerated wound healing and the inherent bactericidal capacity of QCS was enhanced by NIR irradiation. Healed wounds showed less inflammatory response, more blood vessels and hair follicle formation.	[241]
Chitosan and poly (Vinyl alcohol)	Heparinized ZnO nanoparticles	0%, 0.5%, 1.0%, and 2.0% w/v	Infiltrating into the bacteria membrane and	*S. aureus* and *E. coli*	+	Adding heparin to nanoparticles boosts their antibacterial effect. Promoted wound closure, re-	[125]

(*continued on next page*)

Table 2 (*continued*)

Biomaterials	Antibacterial component	Concentration	Antibacterial Mechanism	Bacterial strains tested	*In vivo*	Main Results	Ref
			damaging lipids and proteins [162].			epithelialization, and collagen deposition.	
Sodium alginate and gelatin	Silver nanoparticles	(1.0, 2.0, and 4.0 mM)	Damage to cell membrane and inhibition of DNA replication	*S. aureus* and *P. aeruginosa*	+	Hydrogels with MICs of 0.50 g/mL and 53.0 g/mL were found to have significant bactericidal activity against *S. aureus* and *P. aeruginosa*, respectively. Improved wound closure and granulation tissue for the wounds treated with nanoparticle-containing hydrogels *in vivo*.	[126]
Glycidyl methacrylate functionalized quaternized chitosan (QCSG), gelatin methacrylate (GM)	Graphene oxide	0% to 0.5%, 1%, and 2% w/v	Oxidative stress, membrane stress, and electron transfer [242]	*S. aureus, E. coli,* and MRSA	+	Improved wound closure rate, angiogenesis, and collagen deposition *in vivo* in *S. aureus* infected mice full-thickness treated by hydrogels.	[127]
Bacterial cellulose	Multiwalled carbon nanotubes (MWCNT)	0.1% w/v	Damaging bacteria membrane	*S. aureus*, *E. coli, P. aeruginosa*, MRSA, *S. Typhi*, and *klebsiella sp*	+	Antibacterial activity of the hydrogel against 6 bacteria strains. Faster healing of diabetic wounds in the BC-MWCNT group (99%) vs. negative control (77%) in 21 days. Improved re-epithelialization of the epidermis and healthy granulation tissue.	[128]

MeTro/GelMA hydrogels with no AMP. In contrast, hydrogels containing 0.1 and 0.3% (w/v) AMP induced bacterial dead within the construct. The anti-microbial properties of 0.1 and 0.3% AMP composite hydrogels were similar to those of 3% Zinc Oxide (ZnO) hydrogels.

These results also show that incorporation of antimicrobial peptides into hydrogels could be an alternative strategy to fabricate antibacterial wound dressings and avoid possible side effects associated with other materials to develop safer treatment approaches [88].

Nanomaterials are a large family of antibacterial additives that fall into different categories, such as metallic-based and carbon-based types. Their physicochemical characteristics and dimensions impart multifunctionality for tissue regeneration and wound healing, including antibacterial and anti-inflammatory activity, increased cell–cell interaction, and induction of stem cell differentiation, among others [124]. ZnO nanoparticles [125], silver nanoparticles [126], graphene [127], and carbon nanotubes [128] are the most important nanoparticles used in hydrogels for wound-healing applications. Due to their relevance, we have focused on nanoparticles separately in section 3.5.

As an available and commercialized source for infection treatments, antibiotics have always been attractive as additives in dressing materials. Using antibiotics in wound dressing is advantageous compared to systematic antibiotic treatment, because it decreases the risk of antibiotic resistance and enables controlling local concentrations and sustained release [129,130]. An antibacterial Alginate/Chitosan (Alg/CS) hybrid hydrogel was designed by Chen et al. composed of tetracycline hydrochloride (TH)-loaded gelatin microspheres. Hybrid hydrogels with different microsphere concentrations (10, 20, 30, and 40 mg/mL) were fabricated. By increasing the microsphere ratio, the mechanical stability of the hydrogels increased, and the gelation time decreased. The authors decided to choose hydrogels with a 30 mg/mL microsphere concentration as the optimum sample for further experiments due to homogeneity considerations. Drug release profiles of different samples demonstrated a more extended release for composite gel (Alg/CS/TH-loaded microspheres) than for Alg/CS/TH and TH-loaded gelatin microspheres. Disc diffusion tests revealed bacterial inhibition zones of ~8.00 mm and 8.04 mm after 24 h for Alg/CS/TH-loaded microspheres against *S. aureus* and *E. coli*, respectively. For TH-loaded gelatin microspheres, inhibition zones against of ~10.5 mm and 10 mm against *S. aureus* and *E. coli* were observed, respectively. This result also indicated more sustained release of antibiotics from Alg/CS/TH-loaded microsphere than from TH-loaded gelatin microspheres [130]. Rasool et al. developed a pH sensitive hydrogel based on chitosan-poly (N-vinyl-2-pyrrolidone) (CS/PVP), incorporated with silver sulfadiazine drug (an antibiotic for burnt wounds) for wound healing. Hybrid hydrogels were fabricated in different concentrations of PVP. All samples exhibited antimicrobial activity and the degree of swelling was increased by a reduction in the PVP amount in hydrogels. The release profile of Ag-sulfadiazine loaded in PVP 0.5 hydrogel (CS to PVP ratio of 2:1) showed 91.2% of drug released in a controlled manner during 80 min in PBS [131].

Wounds become non-healing mostly as a consequence of bacterial contamination, which then can lead to severe infections, and these infections are responsible for a high percentage of morbidity and mortality worldwide [132]. Despite numerous studies about antibacterial molecules embedded in hydrogels for wound healing applications, there is still a need for more experiments to find gold standards to be applied in clinic. For example, thousands of antibiotics are known, but only about 1% of them have been used in the clinic, because there are still different concerns about their collateral consequences, such as cytotoxicity and bacterial resistance [133,134]. A better understanding of infection stages and bacteria-killing mechanisms related to each molecule will help researchers and clinicians to design precise and effective wound dressings considering different parameters such as ideal dosage of antibacterial molecules and their release kinetics [135].

3.2. Anti-inflammatory and antioxidant agents

In wound healing processes, if an episode of acute inflammation prolongs for days, it is defined as chronic inflammation. Chronic inflammation occurs through complex mechanisms and impedes the healing process, preventing reaching the proliferation stage. Therefore, it is a rational idea to incorporate anti-inflammatory additives to wound healing constructs for controlling inflammation and accelerate wound healing [136].

Chemokines are known as small signaling proteins that trigger inflammation by recruiting and activating cells. These molecules can bind to several glycosaminoglycans (GAGs) in the ECM such as heparin and heparan sulfate via electrostatic attraction forces between the positively charged amino acids of chemokines and the negative negatively charged sulfate groups of the GAGs. Thus, the amount of sulfate group on GAGs and the GAGs concentration could control binding interactions and thus the transport of chemokines within ECM, that in turn regulates immune cell activation and migration [137]. Arguably, by

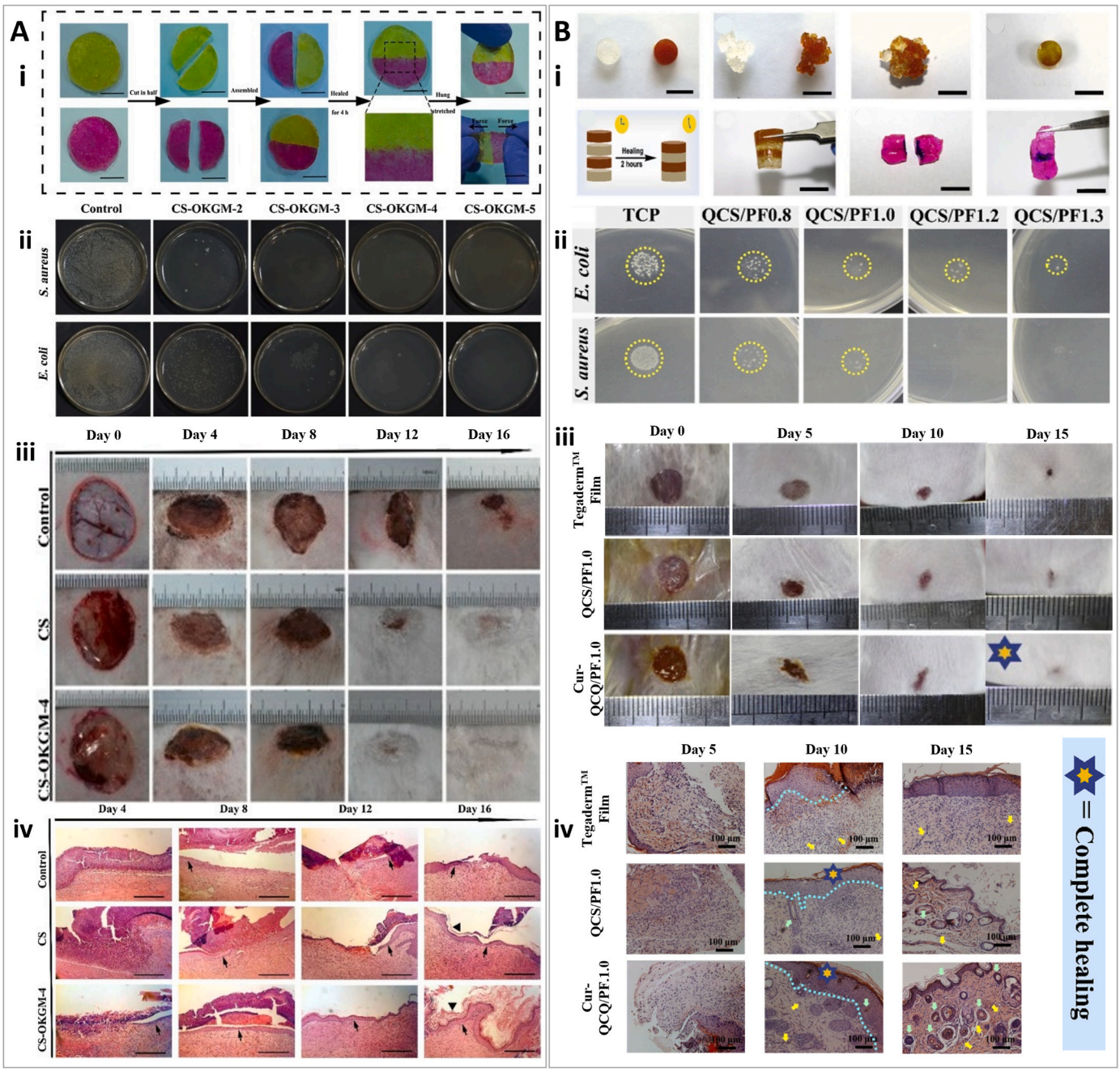

Fig. 5. Wound dressings with antibacterial properties. (A) Chitosan (CS)/konjac glucomannan (KGM) based hydrogels. (i) Self-healing properties of the CS-KGM hydrogels. (ii) Antibacterial efficiency of CS-KGM hydrogels against *S. aureus* and *E. coli*. (iii) Wound healing capacity of CS-KGM hydrogels in a rabbit model compared to CS hydrogels and untreated wounds. (iv) Hematoxylin and eosin (H&E) staining of wounds treated with CS or CS-KGM hydrogels or left untreated. Reprinted and adapted with permission from Chen et al., 2018 [105]. (B) Quaternized chitosan (QCS), Pluronic®F127 (PF) and curcumin (Cur) hydrogels (Cur-QCS/PF). (i) QCS/PF1.0 hydrogel and Cur-QCS/PF1.0 hydrogel disks were cut into pieces, mixed, and self-healed. Scheme and picture of the self-healing capacity with disks and randomly shaped hydrogels. (ii) *E. coli and S. aureus* cell viability when contacting QCS/PF hydrogels with different degrees of cross-linking. (iii) Wound closure from day 0 to day 15 of wounds treated with commercial TegadermTM Film, QCS/PF1.0 hydrogels, or Cur-QCS/PF1.0 hydrogels. (iv) Histomorphological evaluation of wounds treated with commercial TegadermTM Film, QCS/PF1.0 hydrogels, or Cur-QCS/PF1.0 hydrogels; blood vessels: yellow arrows, hair follicles: green arrows, boundary of epithelium and dermis: blue lines, completed epithelium: yellow hexagram. Reprinted and adapted with permission from Qu et al., 2018 [116].

modifying and incorporating GAG-based materials into hydrogels, chemokine concentration. and consequently inflammation in chronic wounds could be controlled [138]. Lohman et al. designed a polyethylene glycol (PEG)/glycosaminoglycan (GAG) heparin in order to control the wound inflammatory response through suppressing chemokines. Enzyme-linked immunosorbent assay (ELISA) results demonstrated that, hydrogels incubated in conditioned medium for 24 h exhibited high cytokine or chemokine binding capacities to the starPEG-GAG hydrogels and approximately no binding capacity to the PEG/PEG control samples. The authors also observed that starPEG-GAG hydrogels showed much higher binding capacity for pro-inflammatory chemokines than for the inflammatory mediators detected in the exudate of chronic wounds. StarPEG-GAG hydrogels incubated in human wound fluids of patients with non-healing chronic wounds

efficiently scavenged the inflammatory chemokines MCP-1 (monocyte chemoattractant protein–1), IL-8 (interleukin-8), MIP-1α (macrophage inflammatory protein–1α) and MIP-1β (macrophage inflammatory protein-1β). Moreover, in a mouse delayed wound healing model, starPEG-GAG hydrogels reduced inflammation, enhanced granulation tissue formation, vascularization, and wound closure [139].

An anti-inflammatory hydrogel composed of KGM, and human hair proteins (KER) was developed by adding an ethanoic extract of *Avena sativa* (OAT). OAT extract is approved by the FDA for local treatment of irritation conditions such as eczema-associated itches. OAT comprises anti-inflammatory and antioxidant molecules such as β-glucans. The results of this study showed complete closure for wounds treated with KGM + KER + OAT hydrogels in 16 days. In contrast, the wounds were healed at 20 and 24 days when treated with KGM + KER and the untreated group, respectively. Moreover, histological analysis indicated no inflammatory cells within 12 days for wounds treated with KGM + KER and KGM + KER + OAT as compared to a large number of them in the control group [140].

One of the reasons that prolonged inflammation is detrimental for wound healing is the excessive amount of reactive oxygen species (ROS) produced by poly-morphonuclear leukocytes and other inflammatory cells. This overproduction of ROS interrupts the balance of cellular oxidant/antioxidant leading to cellular and ECM damage, infection, and slow tissue regeneration [141–143]. Therefore, a compelling argument has been raised for including antioxidants in tissue engineering constructs and wound dressings to boost healing, regeneration, and organ function [144]. An antioxidant is a chemical that, at sufficiently low concentrations, can inhibit oxidation [145]. A vast range of antioxidants, both natural and synthetic, are known. Endogenous antioxidants can be enzymatic or non-enzymatic [146]. The enzymatic forms include glutathione peroxidase, superoxide dismutase, and catalase, whereas non-enzymatic antioxidants include uric acid, lipoic acid, bilirubin, glutathione, and melatonin. Exogenous antioxidants include carotenoids, vitamins E, A, and C, natural flavonoids, and various other substances. Vitamin C is a water-soluble antioxidant that, in conjunction with vitamin E, protects lipids against peroxidation [147].

Alpha-tocopherol (vitamin E) is an antioxidant and anti-inflammatory molecule that has been investigated for wound healing applications. A chitosan/alginate hydrogel containing vitamin E was designed by Ehterami et al. The outcome of this study suggested that Vitamin E incorporated into hydrogels could enhance wound closure in a full-thickness wound model more than Cs/Alg hydrogels and gauze as the control treatments [148]. This result was attributed to the antioxidant activity of Vitamin E via protecting cells from oxidative stress [148]. It is also known that vitamin E plays an important role as an anti-inflammatory agent in skin [149].

Different herbal extracts also have shown relevant antioxidant potential for wound healing applications due to the presence of flavones, polyphenols, and vitamins in their moieties [142]. Illustratively, Red jujube (*Ziziphus jujube*) extract has been reported to relieve the excessive inflammatory responses in wound healing. In a study by Huang et al., a composite hydrogel composed of red jujube (RJ) and GelMA was fabricated as an antioxidant construct for wound healing application [142]. The incorporation of red jujube into GelMA inhibited ROS damage to cells. The result of *in vivo* evaluation also displayed great wound healing properties for GelMA/10%RJ hydrogels; these gels reduced nearly 95% of the wound size at 16 days after implantation on a full-thickness wound model. In contrast, in GelMA and PBS groups, 2 mm and 4 mm of the wound diameter remained unhealed, respectively [142].

Inflammation, as a complex process, stimulates several metabolic cascades and could also cause oxidative stress. Anti-inflammatory and antioxidant molecules could hinder the detrimental effects of inflammation through different mechanisms in different stages (Table 3). There is a need for a better understanding of the underlying mechanisms of inflammation to enable the design of more efficient materials to control inflammation and oxidative stress. Of note, natural anti-inflammatory and antioxidant molecules (i.e., molecules naturally found in fruits and plants) have shown promise to threat wounds; in the near future, wound dressing engineering probably should intensify the study of these natural compounds to leading candidates for deep wound treatment.

3.3. Growth factors

Wound healing is a complex and interactive process that involves several cell types and cellular signals which are regulated by various growth factors (GFs), cytokines, and chemokines [102]. Therefore, the application of GFs in wound healing has been frequent, and many studies have investigated different biomaterials added with GFs to improve bioactive functionality within the wound bed [150,151]. Among the growth factors that could be used to assist wound healing, epidermal growth factor (EGF) accelerates wound healing by inducing proliferation of epithelial cells, fibroblasts, and endothelial cells, and enhancing collagen deposition [152]. Moreover, EGF plays a crucial role in the migration and proliferation of keratinocytes [153]. A heparin-based hydrogel containing EGF was designed by Goh et al. as a platform for wound healing [36]. Results of this study showed more sustained release of EGF from heparin-based hydrogels than from PEG hydrogels. The release of EGF from heparin-based and PEG hydrogels

Table 3
Summary of the reviewed papers about anti-inflammatory and antioxidant agents in hydrogels for wound healing application.

Biomaterials	Anti-inflammatory/ antioxidant agent	Concentration	Mechanism of action	*In vivo*	Main result	Ref
Polyethylene glycol (PEG)/ glycosaminoglycan (GAG) Heparin	(GAG) Heparin	N/A	Electrostatic bond with chemokines	+	Inflammatory chemokines are scavenged in PEG-GAG hydrogels when compared to PEG hydrogels. PEG-GAG hydrogels promoted wound healing via decreasing inflammation and improving vascularization *in vivo*.	[139]
KGM + KER + OAT hydrogel	*Avena sativa* (OAT)	~1% w/v	Inhibition of NF- κ B, proinflammatory cytokines, and histamines	+	OAT containing hydrogels accelerated wound closure compared to the control group. No inflammatory cells in wounds treated with KGM + KER + OAT.	[140]
Chitosan/Alginate-Vitamin E	Vitamin E	200, 400, 800-, and 1600-unit Vit E:10 mL Chit/Alg	Protecting cell membranes from ROS attack by reaction with unstable lipid radicals	+	Vitamin E within the Cs/Alg hydrogels promoted wound closure *in vivo*.	[148]
Red jujube (RJ)/GelMA	Red jujube (which contains flavones, polyphenols, and vitamins)	3%, 5%, 7%, and 10 % w/v.	Donating electrons Protecting cells from ROS attack	+	RJ/GelMA hydrogels protect cells from ROS. Remarkable wound size reduction 8 days after implantation on a wound model compared to control GelMA hydrogel.	[142]

was completed by day 21 and day 5, respectively. This observation was attributed to the high affinities of heparin, as a highly sulfated natural glycosaminoglycan, to various growth factors, which lead to enhanced binding that may extend the half-lives and bioactivity of growth factors. *In vivo* wound healing results also demonstrated higher wound closure, epithelialization, granulation tissue, and capillary formation in wounds treated with heparin-EGF hydrogels than in the rest of the groups of this study (i.e., the groups treated with EGF solution, EGF loaded PEG hydrogels, and the non-treated control group) [36].

Small differences in the chemical nature of growth factors may result in different biological performances. Wu et al. designed heparin-poloxamer (HP) wound healing hydrogels loaded with two different fibroblast growth factors (aFGF and bFGF). These two FGFs possess similar structures and regenerative capacities but exhibited different binding affinities to heparin, leading to different *in vivo* wound healing efficacy when loaded into HP. Isoelectric points of 5.6and 9.6 were determined for aFGF and bFGF, respectively [154]; this suggests that aFGF and bFGF are negatively charged and positively charged, respectively, in physiological conditions. As a result, bFGF may exhibit stronger and easier bonding to HP than aFGF due to more favorable/stronger electrostatic interactions with HP (negatively charged in physiological conditions). The authors experimentally determined the release profile for both growth factors and found remarkable differences. After 10 days, 42.8% of aFGF was released from HP-aFGF. In contrast, only 24.3% of bFGF was released from HP-bFGF during the same period. This result demonstrated the different binding strengths between these two FGF-HP systems and the much slower release of bFGF than aFGF from HP hydrogels. Of note, it has been reported that bFGF alone is 10-100-fold more effective than aFGF in inducing wound related cell proliferation [155], however, *in vivo* wound healing analysis indicated

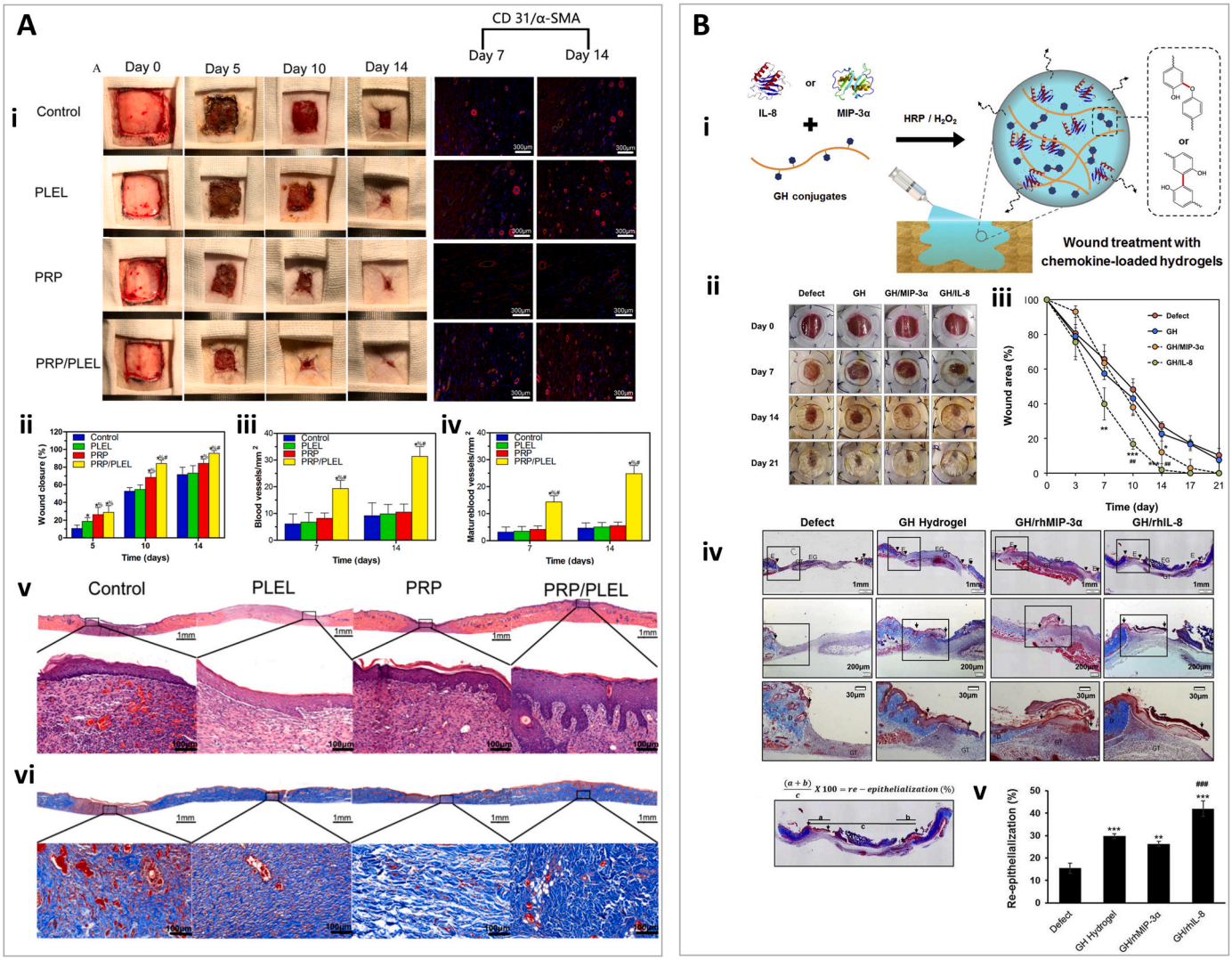

Fig. 6. Wound healing using growth factor-containing hydrogels. (A) (i) Left: Images of full-thickness wounds treated with Poly (D, L-lactide)-poly (ethylene glycol)-poly (D, L-lactide) (PLEL) Platelet-rich plasma (PRP), PRP/PLEL or left untreated at days 0, 5, 10, and 14. Right: Immunofluorescent staining for CD31 and α-SMA shows newly formed blood vessels. (ii) Wound closure rate showing the best performance by PRP/PLEL hydrogels. (iii) Quantification of new blood vessels. (iv) Quantification of mature blood vessels. Hematoxylin and eosin H&E (v) and MT (vi) staining of wounds treated with PLEL, PRP, PRP/PLEL and controls showed better tissue maturation with PRP/PLEL hydrogels. Reprinted and adapted with permission from Qiu et al., 2016 [151]. (B) Hydrogels loaded with chemokines. (i) Schematic illustration of sprayable gelatin hydrogels (GH) loaded with chemokines (IL-8 or MIP-3α) for wound healing. (ii) Pictures of wounds treated with chemokine-loaded GH in STZ-induced diabetic mice on days 0, 7, 14, and 21. (iii) Wound closure rates are presented as a percentage of the initial wound area at day 0. *p < 0.05, **p < 0.01, and ***p < 0.001 vs. defect; ##p < 0.01 vs. GH hydrogel. (iv) Masson's trichrome (MT) stain that shows re-epithelialization of the wounds treated with GH, GH containing MIP-3a or IL-8. D, dermis; E, epidermis; EG, epithelial gap; GT, granulation tissue. (v) Re-epithelialization percentage between treatments and control groups. **p < 0.01, ***p < 0.001 vs. defect; ###p < 0.001 vs. GH hydrogel. Reprinted and adapted with permission from Yoon et al., 2016 [158].

enhanced wound closure, angiogenesis, re-epithelialization, and collagen deposition for wounds treated with HP-aFGF compared to HP-bFGF, which is attributed to the difficulty of release of bFGF from hydrogel [150].

Platelet rich plasma (PRP) is a blood-derived product with a high content of platelets that could easily and inexpensively provide an autologous source of different types of growth factors for for wound healing such as vascular endothelial growth factor (VEGF), PDGF, and transforming growth factor-beta (TGFβ1) [151,156]. Notodihardjo et al. demonstrated that gelatin hydrogel loaded with PRP could decrease wound size after 5, 7, and 14 days. More epithelialization and capillary formation were observed in wounds treated with Gelatin/PRP hydrogels than in those treated with Gelatin hydrogels alone [156]. Using hematoxylin and eosin staining, an epithelium thickness of ~2000 μm was measured for gelatin/PRP treated wounds. In gelatin treated wounds and in the untreated control group, epithelium thickness was determined to be under 1500 and 1000 μm, respectively. Moreover, immuno-histological staining revealed that the capillary area measured ~0.01 μm^2 in wounds treated by gelatin/PRP. In contrast, the capillary area measured ~0.05 μm^2 in wounds treated with pristine gelatin hydrogels [156]. Similar results were observed in a study by Qiu et al.; they treated full-thickness rodent wound models with poly (D, L-lactide)-poly (ethylene glycol)-poly (D, L-lactide) hydrogels containing PRP [151] (Fig. 6A).

Cell-attracting chemokines embedded in hydrogels have also been investigated for wound healing applications. The inhibition of mesenchymal stem cell (MSCs) invasion into wound sites is one of the most critical issues that causes impaired healing in wounds associated to diabetes mellitus. MSCs could cooperate in tissue repair and wound healing via differentiation to different cell lines and by secreting various cytokines and growth factors to improve re-epithelialization, angiogenesis, and collagen deposition [157]. In a study by Yoon et al., two chemokines which are known to be MSCs-attractive (i.e., interleukin-8 [IL-8], macrophage inflammatory protein-3α [MIP-3α]), were loaded into gelatin hydrogels in order to compensate for the lack of cellular signals in the diabetic wound bed. *In vitro* release experiments indicated a constant release of IL-8 and MIP-3α from hydrogels during 7 days. *In vivo* diabetic wound healing studies also demonstrated that chemokine-loaded hydrogels could boost wound healing via an increase in re-epithelialization, neovascularization, and collagen deposition, as compared with pristine gelatin hydrogels [158] (Fig. 6B).

Different growth factors have been demonstrated to be beneficial for the wound healing process in various experiments. However, there is a lack of comparative studies to determine the most efficient growth factor (or the combination of growth factors) to be used in different wound healing scenarios. Moreover, some outstanding limitations, such as the lack of enough clinical trials, preclude from reaching a feasible and reliable therapy for wound healing that considers possible side-effects or long-term effects [159]. Another issue that needs to be considered is the cost of growth factors, which is relatively higher than the cost of other bioactive agents conventionally used in regenerative medicine and wound healing. It seems imperative to develop methodologies to synthetize or isolate growth factors in a low-cost and high-efficient manner, not only for wound healing but also for regenerative medicine and tissue engineering in general. The alternative of using PRP as an autologous source of multiple growth factors is being investigated in clinical trials, and arguably needs further research and refinement to be widely used. Table 4 summarizes recent studies where hydrogels added with growth factors have been used for wound healing applications.

3.4. Electroactive agents

Electroactive biomaterials have drawn attention for wound healing applications in recent years. In mammalian bodies, several tissues are considered electrical signal-sensitive tissues; nerves, muscle, myocardium, bone, and skin, are examples. Skin exhibits a conductivity range from 2.6 mS/cm to 1×10^{-4} mS/cm, varying between different skin layers and components [143]. Cellular processes such as adhesion, proliferation, migration, and differentiation in tissues with electrically excitable cells could be promoted by conductive biomaterials. Therefore, a wide range of electroactive materials can be used in tissue engineering and regenerative medicine, including conductive polymers, metals, and carbon-based biomaterials [160,161].

For wound healing applications, Zhao et al. designed an injectable conductive hydrogel by mixing solutions composed of quaternized chitosan-polyaniline (QCSP) and poly (-ethylene glycol)-co-poly (glycerol sebacate) (PEGS-FA) functionalized with benzaldehyde groups. Polyaniline (PA) is one of the most common conductive polymers that has been widely investigated in biomedicine due to its good biocompatibility and conductivity [143]. *In vivo* wound healing analysis on full-thickness mice wound model showed that conductive QCSP/PEGS hydrogels could promote more effective wound healing than non-conductive QCSP/PEGS hydrogels and commercial dressings (Tegaderm™ film). A more extensive wound contraction, faster re-epithelialization, and thicker granulation and collagen formation was observed in mice wounds treated with conductive than non-conductive hydrogels. Wound contraction for the conductive sample was determined to be 10 and 5% higher than in other groups on day 10 and day

Table 4
Highlights of reviewed studies about growth factor application in hydrogels for wound healing.

Biomaterials	Growth factor	Concentration	*In vivo*	Main result	Ref
Heparin	hEGF	1 cm^2 Hydrogels soaked in PBS containing 100 ng hEGF	+	Accelerated wound closure compared to control group. Improved granulation tissue formation, capillary formation, and epithelialization in Heparin/EGF compared to control	[36]
Heparin-Poloxamer	bFGF/aFGF	N/A	+	About 43% release of aFGF and 24% of bFGF was measured from heparin hydrogel within 10 days associated with stronger binding of bFGF to heparin. Higher wound closure, angiogenesis, re-epithelialization, and collagen deposition were observed for wounds treated with Heparin-aFGF hydrogel compared to control groups.	[150]
Gelatin	PRP	100 μL in 6 mm diameter hydrogel disc	+	More wound contraction, epithelialization, and capillary formation for PRP-Gelatin hydrogel *in vivo* when exposed to a wound model compared to the control group.	[156]
Poly (D, L-lactide)-poly (ethylene glycol)-poly (D, L-lactide) (PLEL)	PRP	10% v/v	+	PRP/PLEL induced EaHy926 proliferation and migration *in vitro*. & Improved wound closure, angiogenesis, and collagen deposition when applied to a rodent wound model compared to PLEL.	[151]
Gelatin	Interleukin 8 (IL-8) & macrophage inflammatory protein-3α (MIP-3α)	10 μg/mL	+	Stable release of chemokines from hydrogels within 7 days. Enhanced re-epithelialization, vascularization, and collagen deposition	[158]

15, respectively. H&E staining revealed the formation of 200 μm thicker granulation tissue for wounds treated by conductive QCSP/PEGS hydrogel than for those treated by non-conductive hydrogel and a commercial dressing. Furthermore, the expression of three genes involved in the wound healing process (i.e., EGF, TGF-β and VEGF) was determined; it was found that all three genes were significantly upregulated in wounds treated by QCSP/PEGS hydrogel as compared to the control groups. This enhanced gene expression induced by the conductive hydrogel could be associated to the activation of cellular processes promoted by the transfer of electrical current from the electroactive hydrogel and the propagation of electrical signals within the wound bed [143]. Electroactive moieties could affect cellular behavior via activation of the calcium/calmodulin pathway [162,163], leading to elevation of calcium levels, then activation of cytoskeletal calmodulin, resulting in enhanced cell proliferation, and increased VEGF and TGF-β expression [143,164]. In another study, aniline tetramer was grafted to oxidized hyaluronic acid (OHA) and mixed with N-carboxyethyl chitosan (CEC) to form a multifunctional electroactive hydrogel for wound healing and skin regeneration [165]. The authors reported that conductive hydrogels containing antibiotics (amoxicillin) not only exhibited proper antibacterial activity, but also accelerated the wound healing process *in vivo*. Conductive hydrogels enhanced granulation tissue formation, and induced higher fibroblast proliferation and angiogenesis in wounds than Tegaderm™ (a commercial wound dressing). In addition, after 10 days of treatment, wounds exposed to aniline tetramer-containing hydrogels showed 18% more contraction than wounds treated with Tegaderm™ [165].

Conductive polymers have been widely investigated for tissue engineering applications and wound healing. This class of polymers has also shown promising results, although some limitations should be considered for their application in biomedical engineering, such as brittleness, non-biodegradability, and toxicity of byproducts [166]. Moreover, alternative classes of conductive moieties, such as metal and carbon-based nanoparticles, are advantageous over conductive polymers due to their multi-functionality and ease of incorporation within polymer matrixes normally used in wound healing applications. Conductive nanomaterials can be embedded in an organic polymer which works as a binder to create a conductive hydrogel [167,168]. In a study by Wang et al., a flexible electrical patch (ePatch) was fabricated using methacrylated alginate (MAA). A silver nanowire (AgNW) was incorporated as electrode material and for its antibacterial properties. *In vitro* results from a scratch assay demonstrated faster cell migration and alignment at specific angles, as well as significantly higher VEGF-A and TGF-β expression due to electrical field (EF) stimulation through the ePatch. The ePatch was also tested, with and without EF stimulation, in a full-thickness wound model in Sprague-Dawley rats. The ePatch with EF stimulation (ePatch/EF) improved directional wound regeneration and minimized scarring. Hematoxylin & Eosin (H&E) and Masson's Trichrome (MT) staining showed more re-epithelialization and longer epidermal tongue, more extensive vessel formation, faster transition through the inflammatory phase with a lower immune cell infiltration in wounds treated with the ePatch/EF than in wounds only covered with the ePatch (but not EF stimulation). In addition, the antibacterial properties of the ePatch were tested both *in vitro* and *in vivo* against *E. coli* and *S. aureus*. In this experiment, no EF stimulation was used. The results suggested that the ePatch could avoid bacterial infection by both gram-positive and negative bacteria [169]. Table 5 shows a summary of the studies discussed in this section.

3.5. Nanoparticles

Nanoparticles (NPs) are nanoscale-dimension materials that exhibit physical and chemical characteristics that can dramatically benefit a wide range of applications in biomedicine and tissue engineering [30,170]. Different classes of NPs, including metal-based and carbon-based NPs, have been incorporated in wound dressing hydrogels to provide nanocomposite hydrogels with a wide range of characteristics such as antibacterial, anti-inflammatory, antioxidant, electroactive, and angiogenic activities (Table 6). One of the most significant advantages of NPs for tissue engineering and wound healing over other additives is their ability to exhibit two or more of these desired characteristics.

Silver NPs (AgNPs) are the most studied nanomaterial for wound dressing applications due to their great biocompatibility and widespread antimicrobial spectrum [171]. In one of the studies using AgNP in hydrogels for wound healing, a composite acrylic acid and N, N′-methylene bisacrylamide/graphene hydrogel loaded with silver NPs was designed. Graphene was used to increase the mechanical properties and water adsorption of the hydrogel and to make it suitable as a wound dressing . An antibacterial study showed the highest bacteria killing ability of hydrogels with the highest Ag to graphene mass ratio (5:1) (Ag5G1) against both *E. coli* and S. *aureus*. Moreover, *in vivo* evaluation of hydrogels showed healing of about 98% for the wounds treated with Ag5G1 after 15 days, as compared to 85% and 53% for Ag1G1 hydrogel and the control groups (without dressing). After 10 days of treatment, histological analysis also showed fewer inflammatory cells, more fibroblast migration, and more collagen fibers in the wound treated with Ag5G1 hydrogels than in wounds in other treatment groups [171].

Zinc (Zn) is another metallic element which has beneficial effects for wound healing. Zn is considered an eco-friendly and non-toxic material [172]. ZnONPs are demonstrated to be antibacterial and Zn^{++} released from this nanomaterial could improve keratinocyte migration toward the wound bed, leading to accelerated wound healing [173,174]. Rakhshaei et al. developed hydrogels composed of carboxymethyl cellulose (CMC) and ZnONP-loaded mesoporous silica (MCM-41) for wound healing treatment. Tetracycline (TC) was also loaded into ZnO-MCM-41 to increase the antibacterial efficiency of the

Table 5
Highlights of reviewed studies of electroactive agents in hydrogels for wound healing.

Biomaterials	Electroactive agent	Concentration	Conductivity	*In vivo*	Main result	Ref
Chitosan-g-polyaniline (QCSP)/ poly (ethylene glycol)-co-poly-glycerol sebacate (PEGS)	Polyaniline (PANI)	~1.5 mg/mL	2.25 mS/cm −3.5 mS/cm	+	Increased wound healing rate was observed for conductive hydrogels via acceleration in wound closure, higher granulation, and collagen formation and faster re-epithelialization compared to non-conductive wound healing dressings as control. Higher expression of VEGF, EGF and TGF-β genes which are involved in wound healing, were observed for wounds treated with conductive hydrogel.	[143]
N-carboxyethyl chitosan (CEC) and oxidized hyaluronic acid-graft-aniline tetramer (OHA-AT)	Aniline tetramer	Theoretical AT content (%): 5, 10, 15, and 20.	0.42 mS/cm	+	*In vivo*, hydrogel demonstrated antibacterial activity and promoted wound healing by increasing granulation tissue formation, fibroblast proliferation, and angiogenesis.	[165]
Methacrylated alginate (MAA) Silver nanowire (AgNW)	Silver nanowire (AgNW)	10% w/v AgNW, 3% w/v MAA	1.54×10^5 S/m	+	ePatch helped wound healing in 7 days, re-epithelialized the skin, grew new blood vessels, regulated the immune response, and stopped infection.	[169]

Table 6
Highlights of reviewed studies related to NPs application in hydrogels for wound healing.

Biomaterials	NP & size	Function	Mechanism of action	Concentration	*In vivo*	Main result	Ref
Acrylic acid	AgNP 39 nm Graphene N/A	Antibacterial	Damage to cell membrane and inhibition of DNA replication	AgNP 12.5 mg/mL Graphene 2.5 mg/mL	+	The highest antibacterial activity for hydrogel with the highest Ag to graphene mass ratio (5:1) (Ag5G1) against *E. coli* and *S. aureus*. Ag5G1 decreased inflammatory cells and enhanced fibroblast migration, collagen deposition, and microlevel formation *in vivo*.	[171]
Carboxymethyl cellulose (CMC)	ZnONPs N/A	Antibacterial and keratinocyte migration	Infiltrating into the bacteria membrane and damaging lipids and proteins [243]	Weight ratio of 10% to CMC	–	ZnONPs promoted loading efficiency of TC within the system and enhanced TC sustained release from the hydrogel.	[172]
Poly- (PEG citrate-co-N-isopropylacrylamide) (PPCN)	Cu framework NPs 285.6 ± 2.7 nm	Angiogenic and ECM protein expression	VEGF triggering and expression and collagen	100 mg/mL	+	Improved migration of HEKa cells, wound closure, angiogenesis, and collagen deposition, compared to PPCN.	[175]
3-(trimethoxysilyl) propyl methacrylate (MPS)MPS	CuNPs 10 nm	Antibacterial and angiogenic	Damaging the bacteria membrane and crosslinking proteins. VEGF triggering	0.5, 1, and 1.5 mg/mL	+	When exposed to near-infrared (NIR) light irradiation, the composite hydrogel showed an antibacterial effect against *S. aureus* and *E. coli*. *In vivo* angiogenesis and wound healing are supported by CuNPs-containing hydrogels compared to the hydrogel control.	[177]
Glycidyl methacrylate functionalized quaternized chitosan (QCSG)	CNT Diameter of 10–20 nm and length of 10–30 μm	Conductivity (1.2×10^{-1} S/m) Hemostatic capability	Transferring electrical signals to activate platelets and growth factors controlling wound healing	2, 4, and 6 mg/mL	+	CNT containing cryogels showed better hemostatic capability response compared with gauze and gelatin hemostatic sponge in different mouse and rabbit injury models, and better wound healing ability and less inflammatory response compared to pristine cryogel and Tegaderm™ dressing.	[181]
Hyaluronic acid-graft-dopamine	rGO N/A	Conductivity (2.5×10^{-4} S/m)	Electrical signals transfer and stimulating excitable skin cells	0.2%, 0.6%, and 1% w/v	+	Photo-thermal antibacterial activity against both *E. coli* and *S. aureus*. Enhanced vascularization, granulation tissue thickness, and collagen deposition *in vivo*.	[186]
Chitosan	Carbon dots (CDs) 4 ± 1 nm	Antibacterial pH-sensitivity	Destroying cell membranes, inducing free radicals [244]	0.25%, 0.5%, 1%, and 2%	+	Antibacterial activity is enhanced with an increase in CD concentration within hydrogels against *S. aureus*. CDs containing hydrogels promoted wound closure.	[188]

nanocomposite hydrogel. The result of the study showed that TC loading within MCM-41 was increased by adding ZnONPs, which could be attributed to electrostatic attraction between positively charged ZnONPs and TC molecules, which possess a negative charge above pH 7.4. In addition, ZnONPs enabled the CMC/MCM-41 hydrogel to release TC more sustainably than CMC and CMC/MCM-41. Finally, based on disk diffusion analysis, CMC/MCM-41 containing TC, exhibited a bacterial inhibition zone of ~10 mm against *E. coli* after 24 h. Hydrogels containing both ZnO and TC generated an inhibition zone of approximately 25 mm. The same trend was observed in experiments against *S. aureus*. The inhibition zone in the presence of TC-containing hydrogel and TC/ZnO-containing hydrogel was 11 and ~29 mm, respectively [172].

Copper (Cu) is another metallic element, which is a key element in many processes related to wound healing, such as induction of VEGF, triggering angiogenesis and expression of skin ECM proteins [175,176]. Furthermore, Cu is widely used as an antibacterial agent to reduce infection in wound bed [177]. In order to have a controlled release of Cu ions, Xiao et al. designed a copper metal organic framework nanoparticle (HKUST-1 NPs) entrapped in poly- (polyethyleneglycol citrate-co-N-isopropylacrylamide) (PPCN) (Fig. 7A). The authors showed that embedding HKUST-1 NPs in PPCN hydrogels enabled the sustained release of Cu ions. *In vitro* analysis indicated that HKUST-1 NPs containing hydrogels improved the migration of human epidermal keratinocytes (HEKa) cells. In addition, in a diabetic rat wound model, these hydrogels enhanced wound closure, angiogenesis, and collagen deposition as compared to PPCN [175]. In another study, CuSNPs were modified with mesoporous silica ($mSiO_2$) and incorporated within 3-(trimethoxysilyl) propyl methacrylate (MPS) for wound healing applications. These composite hydrogels exhibited antibacterial activity against *S. aureus* and *E. coli* when exposed to near-infrared (NIR) light irradiation. *In vivo* animal experiments also revealed that hydrogels containing CuNPs promoted angiogenesis and wound healing as compared to the control group, which was also associated with the release of Cu ions from the hydrogels [177].

Carbon-based nanoparticles have been widely investigated in tissue engineering due to their versatility and multifunctionality. Carbon NPs, such as carbon nano tubes (CNTs), carbon nano fibers (CNFs), and graphene family nano materials (GFNs) with high mechanical strength and electrical conductivity, have shown biocompatibility, antibacterial, antioxidant, and angiogenic potential, and the ability to induce stem cell differentiation [178,179]. These abilities make carbon-based NPs a material with great potential for wound healing application.

Discovered in 1991, CNTs are rolled sheets of carbon atoms that have been widely used to improve the physicochemical properties of tissue engineering constructs [180]. Due to their conductivity, hemostatic, anti-microbial, and anti-inflammatory properties, CNTs have also been used for wound healing application [181]. In a study by Zhao et al., CNT-reinforced (QCSG/CNT) injectable cryogels based on glycidyl methacrylate functionalized quaternized chitosan were fabricated as a platform for hemorrhage hemostasis and wound healing. The incorporation of 6 mg/mL CNT increased in 6-fold the mechanical strength of QCSG cryogels according to compression stress–strain tests. The

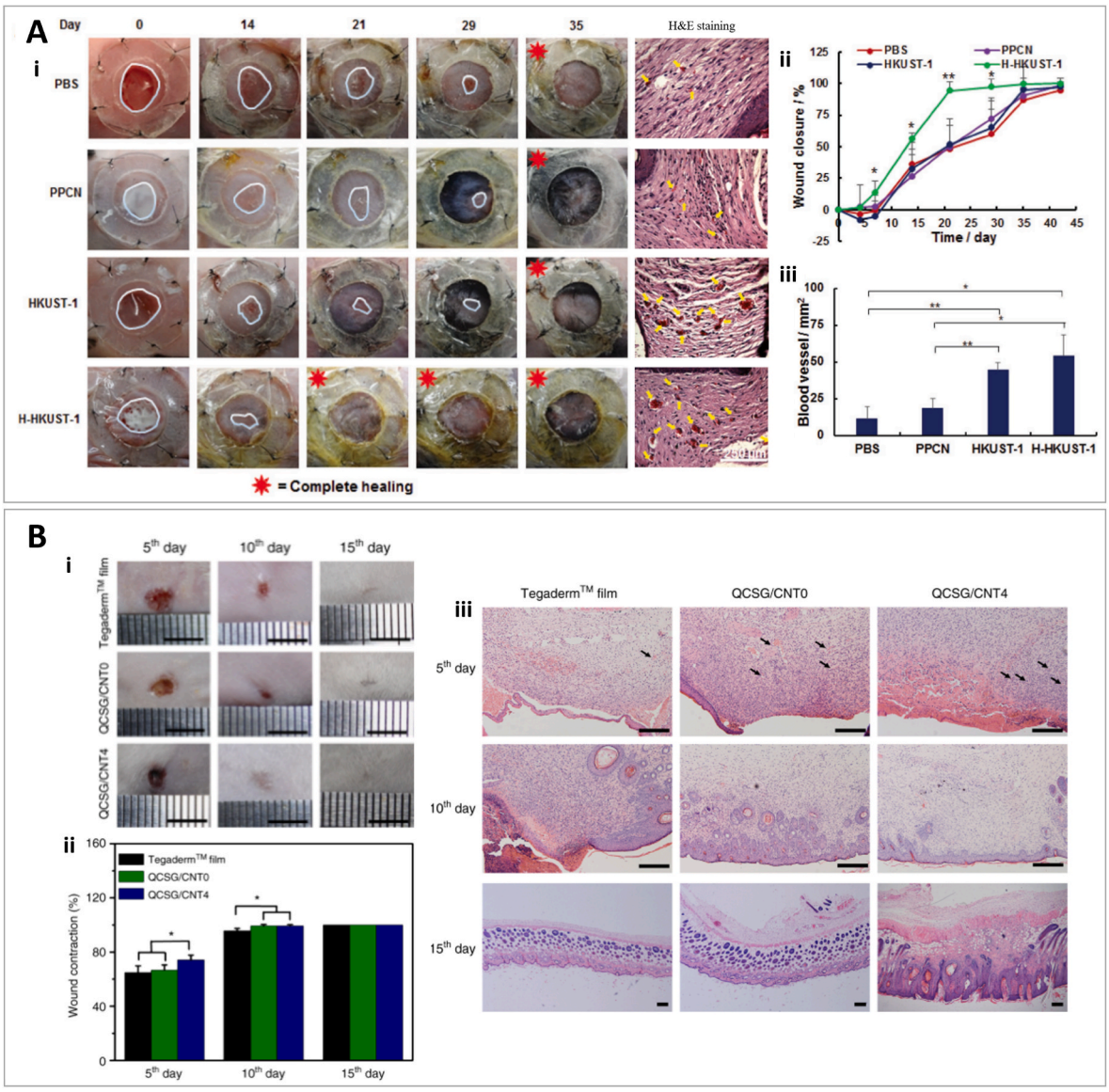

Fig. 7. Nanoparticle-functionalized hydrogels as wound dressings. (A) Effects of copper metal organic framework nanoparticles (HKUST-1 NPs) embedded in poly (polyethyleneglycol citrate-co-N-isopropylacrylamide) (PPCN) on chronic wound healing *in vivo*. (i) Images of wounds treated with phosphate-buffered saline (PBS), PPCN, HKUST-1 NPs, or H-HKUST-1 (e.g., HKUST-1 NPs embedded in PPCN), and blood vessels observed after hematoxylin and eosin (H&E) staining. Quantification of wound closure (ii) and blood vessels (iii) in tissue sections of wounds treated with PBS, PPCN, HKUST-1 NPs, or H-HKUST-1. Reprinted and adapted with permission from Xiao et al., 2018 [175]. (B) Effect of quaternized chitosan functionalized with carbon nanotubes on wound healing. (i) Images of full-thickness wounds of mice treated with Tegaderm™ film (control), glycidyl methacrylate-functionalized quaternized chitosan without carbon nanotubes, and with 4 mg/mL carbon nanotubes (QCSG/CNT4) on days 5, 10, and 15. Scale bar: 5 mm. (ii) Percentage of wound contraction with the three different treatments (iii) H&E staining showed less inflammation and more vascularization after wound treatment with QCSG/CNT4 on days 5, 10, and 15. Reprinted and modified with permission from Zhao et al., 2018 [181].

conductivity of cryogels with CNT concentrations of 2, 4 and 6 mg/mL was measured to be 4.0 × 10^{-2}, 9.5 × 10^{-2} and 1.2 × 10^{-1} S/m, respectively, while wet pure QCSG cryogels exhibited a conductivity of 8.5 × 10^{-3} S/m [181]. CNT containing cryogels exhibited better hemostatic capability than gauze and gelatin hemostatic sponges in different mouse and rabbit injury models. The hemostatic time reported in a mouse-tail amputation model was 117, 107, 91, and 60 s, for QCSG/CNT0, QCSG/CNT2, QCSG/CNT4, and QCSG/CNT6 cryogels, respectively. The hemostatic time was ~120 s for gauze. This result could be associated with the interaction of CNTs with platelets, which possibly activates platelets and induces extracellular Ca^{2+} influx, leading to the release of platelet membrane microparticles [182]. Moreover, in a full-thickness skin defect model, the CNT-loaded construct showed a weaker inflammatory response within 10 days and better wound-healing activity compared to the control cryogel and Tegaderm™ dressing (Fig. 7B). This superiority could be related to the electroactivity of the CNTs in the nanocomposite cryogel, as this would allow electrical signal transfer within the wound bed and then induce cellular activity required for the wound-healing process [143,181].

GFNs, are 2D sheets of carbon that display the thickness of an atom of carbon. In tissue engineering, GFNs have shown great potential due to bio functionality, electroactivity, and high mechanical strength [183]. Graphene oxide (GO) is the oxidized form of this family. Due to the the high amount of oxygen-containing functional groups, GO can be easily dispersed in aqueous solution for biomedical applications. GO increases cell attachment, proliferation, and induces stem cell differentiation [183,184]. The reduced form of GO known as reduced graphene oxide (rGO) exhibits great electroactivity and its use is advantageous in

engineering tissues which contain electrically excitable cells [184]. GFNs as versatile nanomaterials have shown antibacterial properties and antioxidant activity via scavenging ROS [183,185]. Liang et al., developed an injectable conductive hydrogel, based on hyaluronic acid-graft-dopamine (HA-DA), by incorporating rGO. These hybrid hydrogels exhibited appropriate swelling, rheological, and degradation properties. In addition, the authors showed that the conductivity of hydrogels was enhanced by the addition of rGO. Also, HA-DA/rGO hydrogels exhibited photo-thermal antibacterial activity against both *E. coli* and *S. aureus* when exposed to NIR radiation. rGO increased proliferation of L929 cells on hydrogels *in vitro*. When applied to a wound model *in vivo*, better wound contraction, higher collagen deposition, and thicker granulation tissue were observed in wounds treated with HA-DA/rGO hydrogels than with a commercial Tegaderm film or HA-DA hydrogels [186].

Carbon dots (CDs) are a new class of zero-dimensional (0D) nanomaterials with promising potential in various biomedical applications [187]. CDs are biocompatible, exhibit low toxicity, high water solubility, and antibacterial activity [188]. A nanocomposite chitosan/CDs hydrogel was synthesized and evaluated as a wound dressing by Omidi et al. They showed that the incorporation of CD in different percentages yielded an increase in the tensile strength of hydrogels. The tensile strength increased up to ~81 MPa for the highest CD concentration (2% wt), while pristine chitosan scaffold exhibited ~64 MPa. Moreover, composite hydrogels with different CD concentrations (0.25–2% w) showed no increment in toxicity against L929 cells as compared to pure chitosan hydrogel. The antibacterial activity of chitosan/CD hydrogel against *S. aureus* was demonstrated by growth media absorption at 610 nm (OD) compared to chitosan alone. The authors showed that the increase in concentration of CD was proportional to the inhibition of bacterial growth. The bacterial inhibition zone of samples with CD concentration of 5, 10, and 15% v/v was reported to be ~3, 3.6, and 4.5 mm, respectively. The antibacterial activity of CDs has been attributed to their large surface area capable of inducing the generation of reactive oxygen species [189]. *In vivo* analysis on a rat wound model also revealed that the wound closure percentage for the untreated group and the chitosan treated group was 45 and 62% respectively at day 16. In addition, wounds treated with chitosan/CDs nanocomposite completely healed within 16 days [188].

Thanks to their versatility and multifunctionality, NPs have been evolutionary for different biomedical applications such as tissue engineering and wound healing. Although NPs have a wide range of beneficial characteristics for wound healing (i.e., antibacterial, anti-inflammatory, antioxidant, angiogenic, and electroactive), they need to be further investigated to assure safe and secure wound treatments for patients with different types of wounds. Most concerns are related to the dosage that could be considered safe for incorporating them into different wound dressings and, in general, into tissue engineering scaffolds. Moreover, the *in vivo* cytotoxicity and clearance of NPs is another aspect that needs to be clarified; more research is needed to establish standards for clinical trials.

3.6. Cells

Apart from biomaterials, chemical agents, NPs, and growth factors, cells are another crucial component of tissue engineering. Cells could be seeded within scaffolds/hydrogels to develop desired tissue *in vitro* to be further transplanted *in vivo*. Upon proper attachment within a 3D structure, cells are supposed to express ECM, paracrine signals, and growth factors, which lead to an integrated graft and improved tissue regeneration [190]. In wound healing hydrogels, cells could be included (Table 7) with the same purpose, taking advantage of the growth factors and paracrine factors that they secrete [191,192]. Growth factors and paracrine factors contribute to various phenomena and could regulate inflammation and oxidative stress, induce host cell migration, and angiogenesis [191–193].

In a study, an n-isopropylacrylamide (NIPAM)-based thermosensitive hydrogel was designed in order to deliver bone marrow derived MSCs (BMSCs) for healing diabetic chronic wounds. *In vitro* analysis showed that BMSCs could secrete higher amounts of TGF-β1 (fibrosis-promoting factor) and bFGF (inducer of fibroblast proliferation) when embedded within NIPAM hydrogels [192]. When cell-laden-hydrogels were applied to a diabetic rat wound model, they suppressed inflammation, as they inhibited M1 macrophage expression. In addition, they accelerated wound contraction, granulation tissue formation, and angiogenesis as compared to cell-free NIPAM hydrogels. Besides producing TGF-β1 and bFGF, stem cells are capable of secreting other growth factors that are beneficial for wound healing [192]. It is known that MSCs can express pro-angiogenic factors such as VEGF and FGF-2 and interleukin-6 (IL-6) [194,195]. In a study, a UV crosslinked hydrogel composed of GelMA and methacrylated hyaluronic acid (HAMA) was loaded with adipose derived stem cells (ADSC) to improve wound healing. ADSCs remained viable and proliferated for 3 weeks in these hydrogels. The authors showed that ADSC laden hydrogels promoted angiogenesis *in vivo* as compared to cell free hydrogels [191].

Besides cell viability and proliferation in an ECM mimicking matrix, it is also vital that cells, like other bioactive agents, be preserved and exposed to the wound site in a sustained manner to induce proper wound healing. In another study, the angiogenic effect of ADSC-encapsulated chitosan/gelatin was demonstrated by Cheng et al. as a promising platform for wound healing applications. By adding gelatin to chitosan hydrogels, the 5-day viability of ADSCs was improved; live/dead assay results showed an ADSC viability of ~76.5% and 83% for chitosan/2% gelatin and for chitosan/4% gelatin hydrogels, respectively. In contrast, cell viabilities in chitosan hydrogels were reported remarkably lower (at ~47.5% after 5 days) than those observed in chitosan/gelatin. Moreover, *in vitro* analysis showed a gradual degradation of the matrix; thus, ADSCs were released continuously from the composite hydrogel. Consequently, the migration of fibroblasts was also significantly enhanced due to this release. Moreover, more VEGF was found to be released by chitosan/alginate hydrogels than in chitosan gels. A Chick Chorioallantoic Membrane (CAM) assay showed about 152.5 vessel branch points for ADSC-encapsulated in chitosan/gelatin, in comparison with ~64.7 for chitosan hydrogel. Using immunostaining techniques, the co-localization of the HNA and CD31 biomarkers was observed to be

Table 7
Summary of reviewed studies of cell-laden hydrogels for wound healing.

Biomaterials	Cell line	Cell density	*In vivo*	Main result	Ref
GelMA-methacrylated hyaluronic acid (HAMA)	Human Adipose derived stem cell (ADSCs)	0.5×10^6–2×10^6 cells/mL	+	Supported cell proliferation, Enhanced vascularization	[191]
Poly NIPAM- poly (amidoamine)	Mice bone marrow mesenchymal stem cell (BMSC)	1×10^6 cells/mL	+	Secretion of TGF-β1 and bFGF by BMSCs. Inhibition of inflammation, increase in wound contraction, angiogenesis, ECM secretion, and re-epithelialization in *in vivo* wound model for BMSC containing hydrogel.	[192]
Chitosan-Gelatin	Human Adipose derived stem cell (ADSCs)	1×10^6 cells/mL	+	Sustained release of ADSC, enhanced *in vitro* fibroblast migration, and increased capillary formation *in vivo*	[196]

higher in wounds treated with ADSC-encapsulated chitosan/gelatin hydrogels than in wounds treated with ADSC-encapsulated chitosan hydrogels, suggesting an enhanced differentiation of transplanted ASCs toward endothelial lineage [196].

Cell therapy has shown promising results in wound healing applications through two main mechanisms: (i) the use of cells as vehicles secreting paracrine factors, and (ii) stem cell differentiation towards somatic cells of the target tissue. Both mechanisms demand high local cell survival for success, which is challenging in infected wound beds that are high oxidative stress environments. Another important challenge of applying live cells for wound healing is to identify the proper cell source and cell types for clinical trials. Besides cell types, which could be different stem cells and somatic cell lines, the rational use of autograph, allograph, or xenograph sources of the cells should be addressed for further research in this topic.

3.7. Other bioactive agents

Besides the mentioned classes of additives or materials with specific chemical properties, several studies on wound dressing hydrogels are not categorized in these groups (Table 8). In this section, we review studies that have investigated the application of biological molecules, gaseous signaling molecules, inorganic compounds, and living bacteria, among other materials, in wound dressing hydrogels.

3.7.1. Biological macromolecules

Growth factors are an important category of biological macromolecules for tissue engineering and wound healing, but other biological macromolecules, such as DNA, mRNA, active proteins, and stem cell derivatives, have been incorporated into hydrogels for wound healing. Therapeutic nucleic acids (TNAs) are promising new molecules for

Table 8
Summary of other additives used in hydrogels for wound healing.

Biomaterials	Additive	Functionality	Concentration	*In vivo*	Main result	Ref
Hyaluronic Acid	Nonviral DNA pGFPluc & pVEGF	Transfection	N/A	+	Enhanced granulation tissue formation. Improved wound contraction and collagen deposition *in vivo*	[198]
Hyaluronic acid nanoparticles/GelMA	miR-223	Transfection	miR-223 to Hyaluronic acid nanoparticles 1:325 (w:w) ratio 1.3, 2.5, and 5 (w:w) of nanoparticles in GelMA	+	Overexpression of miR-223* in j774A.1 Development of uniformly vascularized skin at the wound site	[199]
Chitosan–collagen	QHREDGS peptide	Support keratinocyte survival and migration	2.2 and 5.9 nmol	+	Enhanced wound closure, re-epithelialization, granulation tissue formation, and blood vessels formation	[201]
Polyethylene glycol-vinyl sulfone	K-peptide (Ac-FKGGERCG-NH2) Q-peptide (-AcNQEQVSPLGGERCG-NH2) RGD (Ac-RGDSPGERCG-NH2)	Type 2 immune response activation	500 μM 500 μM 1 mM	+	Improved wound closure, promoted hair follicle formation, and recruited type 2 immune cells	[202]
Alginate	ADSCs-derived exosomes	Improvement of fibroblasts functionality and synthesis and secretion of collagen and elastin	100 μg/mL	+	Improved wound closure, re-epithelialization, collagen deposition, and angiogenesis *in vivo*	[203]
Alginate generating oxygen	CaO_2 solution	Activating cell proliferation, wound remodeling, etc	Alginate: CaO_2 = 1:1	+	Promoted tissue infiltration, wound closure, and wound repair	[215]
NO-incorporated poly(vinyl alcohol) film/ F127hydrogel	Nitric oxide (NO)	Triggering angiogenesis and inflammatory phases	100 μM GSNO	+	Accelerated wound contraction and increased collagen deposition *in vivo*	[217]
Polyacrylic acid (PAA)	Carbon monoxide (CO)	Increased VEGF and anti-inflammatory effect	1500 μM	+	Enhanced angiogenesis and by increase in VEGF mRNA in wound granulomatous tissues	[218]
Alginate	H_2S	Vasodilation, angiogenesis	0.5, 1, and 10% w/w, to the dry mass of alginate	+	Development of sebaceous glands, hair follicles, and full epithelialization without fibroplasia or inflammation	[231]
Zwitterionic dopamine methacrylamide hydrogels (ZWDO)	Sulfobetaine zwitterionic (ZW)- AgNPs	Nonsticking properties and Antibacterial	ZW: 12.5% w/v AgNPs: N/A	+	Inhibition of cell (MC3T3-E1) attachment. Antimicrobial activity against *E. coli*, *S. aureus*, and *P. auregenosa* due to AgNPs. Accelerated wound contraction and decreased inflammation.	[234]
N, O-carboxymethyl chitosan (nocs)	Fayalite (Fe_2SiO_4, FA)	Promoted angiogenesis	0.5% w/v	+	Promoted angiogenesis and tissue regeneration	[235]
Heparin poloxamer	VEGF-producing *Lactococcus lactis*	VEGF production and M2 macrophage phenotype promotion	1:100	+	Improved wound closure, angiogenesis, and reduced inflammation in diabetic model	[232]
Quaternized chitosan (QCS) Polydopamine-coated reduction Graphene oxide (rGO-PDA) Poly(N-isopropylacrylamide) (PNIPAm)	Polydopamine-coated reduction Graphene oxide (rGO-PDA)	Strengthen tissue adhesiveness, endow antioxidant and photothermal properties	1, 2, 3, 4 mg/mL	+	Assisted wound closure, antibacterial activity, drug release, more collagen deposition, less inflammatory response, more granulation tissue, hair follicle formation, and increased dermal gap.	[236]

healing chronic wounds. Plasmid DNA, small interfering RNAs (siRNAs), microRNA (miRNA) mimics, anti-microRNA oligonucleotides (anti-miR oligos, or AMO), messenger RNAs (mRNAs), and antisense oligonucleotides (ASOs) are examples of TNAs [197]. TNAs can regulate inflammation, protease activities, cell motility, angiogenesis, epithelialization, and oxidative stress to generate a more healing environment at the wound site [197]. The inherent qualities of hydrogels make them ideal carrier systems for transporting TNAs to the wound site while protecting the TNA cargo during delivery [197].

Tokatlian et al., designed a DNA-embedded hyaluronic-based porous hydrogel for wound healing applications. The authors showed that the delivery of plasmid DNA (reporter pGFPluc or proangiogenic pVEGF) enhanced granulation tissue two times more than in the hydrogels without DNA in a splinted mouse wound healing model after 14 days of the application [198]. Three different DNA-loaded hydrogels with different pore sizes were designed in this study: nonporous hydrogels (n-porous), and hydrogels with an average pore size of 60 and 100 μm (60 μm and 100 μm hydrogels). *In vivo* wound healing results showed proper wound closure caused by hydrogels with larger pore size after 14 days, as the remaining wound area was ~20, 30, and 70% for the wounds treated with nonporous hydrogels with 60 and 100 μm pore sizes, respectively [198].

The polarization of macrophages toward the anti-inflammatory (M2) phenotype is driven by an overexpression of miR-223 miRNAs, which may hasten wound healing [199]. However, due to their poor stability, the local-targeted delivery of microRNAs remains complicated. Saleh et al. produced hyaluronic acid nanoparticles coupled with an miR-223 5p mimic (miR-223*) to modulate tissue macrophage polarization during the wound-healing process. *In vitro* results showed that the overexpression of miR-223* in j774A.1 upregulated the expression of the anti-inflammatory gene Arg-1 and downregulated the expression of proinflammatory indicators, including TNF-α, IL-1, and IL-6. Histological evaluation and qPCR analysis after *in vivo* transplantation revealed that localized administration of miR-223* effectively supported the development of uniformly vascularized skin at the wound bed, mainly driven by macrophage polarization to the M2 phenotype [199].

Active peptides are another class of biological molecules that could be added to scaffolds for tissue engineering and wound healing for different purposes [200]. Epithelial cell migration, which mainly involves keratinocytes, is fundamental to wound healing and skin regeneration [201]. Xiao et al., designed an integrin-binding peptide derived from angiopoietin-1, QHREDGS (glutamine-histidine-arginine-glutamic acid-aspartic acid-glycine-serine), as a healing agent which improves migration of primary keratinocytes and stimulates protein kinase B Akt and MAPKp [201]. *In vivo* analysis after 14 days on a mice wound model showed wound closures of about 60% for wounds treated with peptide-containing hydrogels. In contrast, wound closures of less than 40% were observed for both the chitosan/collagen group and the wounds without any treatment. After 14 days, a re-epithelializing percentage of around 80% was observed for the group treated with the QHREDGS peptide. In contrast, this percentage decreased to ~30 and 55% for the wounds treated with chitosan/collagen and the blank group, respectively. It is believed that QHREDGS can interact with receptors which mediate cell attachment and ECM binding leading to improved endothelial metabolism [201].

Regenerative medicine in general requires a balance between tissue formation and biomaterial degradation. To achieve such balance for wound healing application there is a need to enhance the tempo of skin restoration in harmony with the mechanical stability that exist for the engineered skin. Griffin et al., induced type 2 innate and adaptive immune response to enhance skin regeneration [202]. To achieve this goal, they developed a microporous annealed particle (MAP) hydrogel that was tested in a murine splinted excisional wound model in SKH1 mice. They compared the performance of MAP with enantiomeric peptides using either the D or L chirality, or a 1:1 mixture (D-MAP, L-MAP, and 1:1 L/D-MAP, respectively). *In vivo* results showed no differences in wound closure rates or inflammatory signs between treatments. However, a large amount of remaining hydrogel was found in wounds treated with L-MAP, whereas no hydrogel persistence was observed in wounds treated with D-MAP or 1:1 L/D-MAP. Furthermore, wounds treated with D-MAP and 1:1 L/D-MAP displayed thicker skin, new hair follicles, sebaceous glands, and some epidermal cyst formation. These results were confirmed in C57BL/6 mice. Later, they implanted the MAP hydrogels to investigate enhanced immune cell recruitment. L-MAP hydrogels recruited CD11b cells whilst D-MAP and 1:1 L/D-MAP hydrogels recruited CD11b-expressing myeloid cells, a sign of type 2 immunity activation. They also observed an accumulation of individual macrophages with no giant cell formation in D-MAP implants. These results suggested that D-MAP hydrogels induce skin regeneration by recruiting myeloid cells via type 2 immune activation [202].

Exosomes (EXOs) are another biological component which has been successfully included in wound dressing hydrogels [203]. EXOs are a form of lipid membrane vesicle that range in size from 30 to 150 nm [204], and play a critical role in cellular communication and interactions [205]. Stem cell-derived EXOs have the potential to speed up tissue healing because of their many inherent advantages, such as their high stability, non-immune rejection, homing action, and easy regulation of their concentration [206,207]. Through modulating the secretory activity of dermal fibroblasts and enhancing the synthesis and secretion of collagen and elastin, EXOs can stimulate the migration, proliferation, and angiogenesis processes in the wound area, which leads to re-epithelialization [207,208]. In a study by Shafei et al., ADSCs-derived exosomes were loaded into alginate-based hydrogels. Results suggested that this construct was successful in regulating the release of bioactive compounds such as secreted EXO derivatives and growth factors due to the combined effect of the hydrogel degradation and the prolonged release from EXOs. Wound closure, re-epithelialization, collagen deposition, and angiogenesis at the wound sites were greatly enhanced in a full-thickness rat wound model, by using EXO containing alginate hydrogels [203].

3.7.2. Gas signaling molecules

Aerobic organisms require oxygen for survival [209], as oxygen is an important substrate in metabolism, while also serving as a signaling molecule in a variety of biological processes that govern cellular activity and destiny [209–211]. High oxygen tension (characterized as hyperoxia) is well known to stimulate wound-healing activities, such as cell proliferation, wound remodeling, stem or progenitor cell recruitment, and suppression of inflammation [212–214]. An oxygen-generating alginate (OGA) hydrogel reported by Kang et al. was identified as a bioactive acellular matrix that promotes fast wound healing. They produced OGA hydrogels by ionotropic interactions driven by calcium peroxide (CaO_2). The oxygen-releasing activity of the hydrogels could be precisely controlled by adjusting the amount of CaO_2 used. Additionally, the OGA hydrogels were shown to produce oxygen up to hyperoxic levels (over 80% pO2) *in vitro* and *in vivo*, and promoted tissue infiltration, wound closure, and wound repair [215].

Several decades of research have revealed that gaseous signaling molecules, particularly nitric oxide (NO), carbon monoxide (CO), and hydrogen sulfide (H_2S), play critical roles in physiological and pathological states in mammals [216]. These molecules have lower molecular weights than chemical formulations and are more likely to cross the blood–brain barrier and to move between cells [216]. In addition, NO is not simply a gas, but is also a short-lived signaling molecule. NO is a natural molecule produced in the body which plays several vital roles in wound healing processes. NO can improve vasodilation in ulcers, intensify permeability of vasculature, trigger angiogenesis, stimulate fibroblast proliferation, accelerate epithelialization and enhance collagen deposition [217]. In a study, poly (vinyl alcohol) film/F127-hydrogel comprised of NO donor molecule S-nitrosoglutathione (GSNO) was synthesized in order to release NO for wound healing applications. *In vivo* analysis of a mouse wound model showed that NO-releasing

hydrogel enhanced wound contraction by 38% and 80% after 3 and 10 days, respectively, as compared to hydrogel without NO. Ten days after being applied to the wound area, hydrogels without NO exhibited a higher content of neutrophil cells than NO-containing hydrogels. As neutrophils are known as the first cells migrating to the wound bed at the beginning of inflammation, this could be due to a lack of exogenous NO in the wound site, thus extending the inflammatory phase in this group [217].

Carbon monoxide (CO) is an invisible, chemically inert, colorless, and odorless gas [218]. It is a prominent byproduct of the incomplete combustion of carbon-based and carbon-containing chemicals. CO is produced endogenously by heme oxygenase (HO) as a result of heme breakdown, and it plays a role in a variety of physiological and pathological processes, including anti-inflammatory activity [219,220]. CO has a stronger affinity for hemoglobin than oxygen; therefore, CO is considered a particularly hazardous gas. However, multiple studies have shown that exogenous CO has cytoprotective and anti-inflammatory properties in certain circumstances, such as ischemia-reperfusion injury [221–223]. Takagi et al. achieved a sustained release of CO in a mouse full-thickness wound model by employing polyacrylic acid (PAA) as a thickener. The delivery of an aqueous CO-containing PAA solution accelerated wound healing without increasing serum CO levels. The treatment also improved angiogenesis and supported an increased expression of vascular endothelial growth factor mRNA in wound granulomatous tissues [218].

Hydrogen sulfide (H_2S), like CO and NO, has historically been considered a harmful gas in high quantities; nevertheless, H_2S has clear physiological and pathological regulatory effects on many wound-healing processes, including apoptosis, inflammation, proliferation, and differentiation [216]. H_2S participates in various physiological processes, such as vasodilation and angiogenesis, and has a similar inhibitory influence on the death of cardiomyocytes and vascular endothelial cells [224–227] to seen with nitric oxide (NO) and carbon monoxide (CO). Moreover, H_2S has been shown to aid in recovery from burns [228,229] and stomach ulcers [230]. Nazarnezhada et al. developed an H_2S-containing alginate hydrogel (Alg) for use as a wound dressing. Their *in vitro* results indicated that a concentration of 0.5% H_2S was optimal, while concentrations beyond that caused hemolysis and cell toxicity. *In vivo* analysis using a rat full-thickness wound model showed that Alg/H_2S (0.5%) treatment increased wound healing by 98.22%. Histopathological findings also showed that Alg/H_2S therapy induced the development of sebaceous glands, hair follicles, and full epithelialization without causing fibroplasia or inflammation [231].

3.7.3. Living bacteria

A counter-intuitive way of designing hydrogels to promote wound healing is adding living bacteria. A study carried out by Lu et al., 2021 [232] used engineered living lactic bacteria encapsulated in an heparin-poloxamer/HP thermoresponsive hydrogel to produce VEGF (to promote endothelial cell migration, proliferation, and tube formation), as well as to shift macrophages to their anti-inflammatory phenotype by secreting lactic acid. In this work, *Lactococcus lactis* NZ9000 was transformed with an optimized sequence to produce VEGF, as well as an inducible promoter that was able to induce a bacteriostatic environment to inhibit excessive bacterial growth. A heparin poloxamer hydrogel was formed by conjugating heparin with a mono-amine terminated poloxamer. The hydrogel formulation also considered a 20% w/v suspension of *L. lactis*. This probiotic bacterial strain was able to survive and sustain VEGF production for at least 24 h *in vitro* inside the HP hydrogel. Kinetic studies demonstrated a VEGF secretion of up to 10 ng/mL in HP hydrogels as compared to poloxamer without heparin hydrogels, which only reached a VEGF secretion of 4.5 ng/mL. The authors also seeded HUVECs within these hydrogels containing living recombinant bacteria. The proliferation and tube formation of HUVECs was higher in bacteria-containing hydrogels than in the control group. When the HP hydrogel was applied *in vivo*, bacteria were locally restricted to the wound, enhancing VEGF production as well as reducing local inflammation. Furthermore, assays using this hydrogel in diabetic mice with full-thickness skin defects, showed that the number of M1 macrophages decreased whilst the infiltration of M2 macrophages was enhanced. Also, wounds treated with HP hydrogels with VEGF-producing *L. lactis* displayed significantly higher blood perfusion, thicker granulation tissue, higher expression of angiogenesis and wound healing markers, and lower expression of inflammatory markers than control wounds. Results suggested that this hydrogel/probiotic system is suitable to promote wound healing by inhibiting inflammatory microenvironments and enhancing angiogenesis (Fig. 8A) [232].

3.7.4. Antifouling zwitterionic materials

One of the major problems of conventional wound dressings is the undesired adsorption of cells and microorganisms to the dressings. Because the dressing must be typically changed several times, the epithelial cells in contact with the dressing will become detached from the wound site, causing pain for the patients. Antifouling hydrogels, as electroneutral materials, could hinder cell and microorganism attachment to the dressing surface [233,234]. In a study, AgNPs were embedded within a zwitterionic hydrogel composed of hydrophobic dopamine methacrylamide monomer (DMA). The integration of AgNPs within the zwitterionic hydrogel increased its antibacterial activity by 5 folds against *E. coli*, *S. aureus*, and *P. aeruginosa*. Moreover, in an *in vivo* wound model, 15 days post treatment, the wound closure was observed to be 59, 80, and 98% for wounds without treatment, zwitterionic hydrogel, and zwitterionic hydrogel which contains AgNPs, respectively [234].

3.7.5. Mineral compounds

Chronic wounds are caused by disruption of the healing process, especially angiogenesis, which leads to oxygen and nutrient starvation of the injured tissue. Related to this, it is known that hot spring baths yield therapeutic effects due to the trace elements present in the water (such as iron and metalsilicates) and their temperature range of 30–45 °C. Sheng et al. [235] hypothesized that combining mild heat stimuli with bioactive ions would accelerate wound healing, mimicking the hot spring effect. For this purpose, they combined fayalite (Fe_2SiO^4, FA) or calcium silicate with N, O-carboxymethyl chitosan (NOCS) to fabricate FA-NOCS and CS-NOCS hydrogels, respectively. It was observed that FA-NOCS hydrogels continuously released Fe and Si ions for 14 days. Only FA-NOCS hydrogels displayed photo-thermal properties with a laser power-dependent temperature. Using a laser irradiation power of 0.36 W/cm^2 did not affect the ion release. The authors conducted *in vitro* evaluations using FA-NOCS as the test hydrogel and CS-NOCS as the control; HUVECs and human dermal fibroblasts (HDFs) were used in these assays. Photo-thermal treatment at 40 °C did not harm HUVECs, and both cell lines were better stimulated when heat was applied to the FA-NOCS hydrogel. Finally, *in vivo* assessment in a diabetic mouse wound model demonstrated that wounds treated with FA-NOCS, laser irradiation, and FA-NOCS with laser irradiation healed faster than wounds in the CS-NOCS and untreated groups. Furthermore, bioactive Fe and Si ions promoted angiogenesis by enhancing the signaling of VEGF, HIF-1a, and bFGF/bFGFR, and thermal stimulation promoted angiogenesis through the HSP90/eNOS and VEGF pathways (Fig. 8B) [235].

3.7.6. Multimaterial hybrids

Some hydrogels developed to be used as wound dressings cannot be classified into just one category due to their multifunctional qualities provided by multiple components. Research performed by Li et al. developed a biomechanically active and biochemically multifunctional hydrogel to provide accelerated wound closure and healing when used as wound dressing [236]. The hydrogel was made of quaternized chitosan (QCS) to provide strong tissue adhesion, antibacterial activity, and hemostatic capacity; poly (N-isopropylacrylamide) (PNIPAm) as a

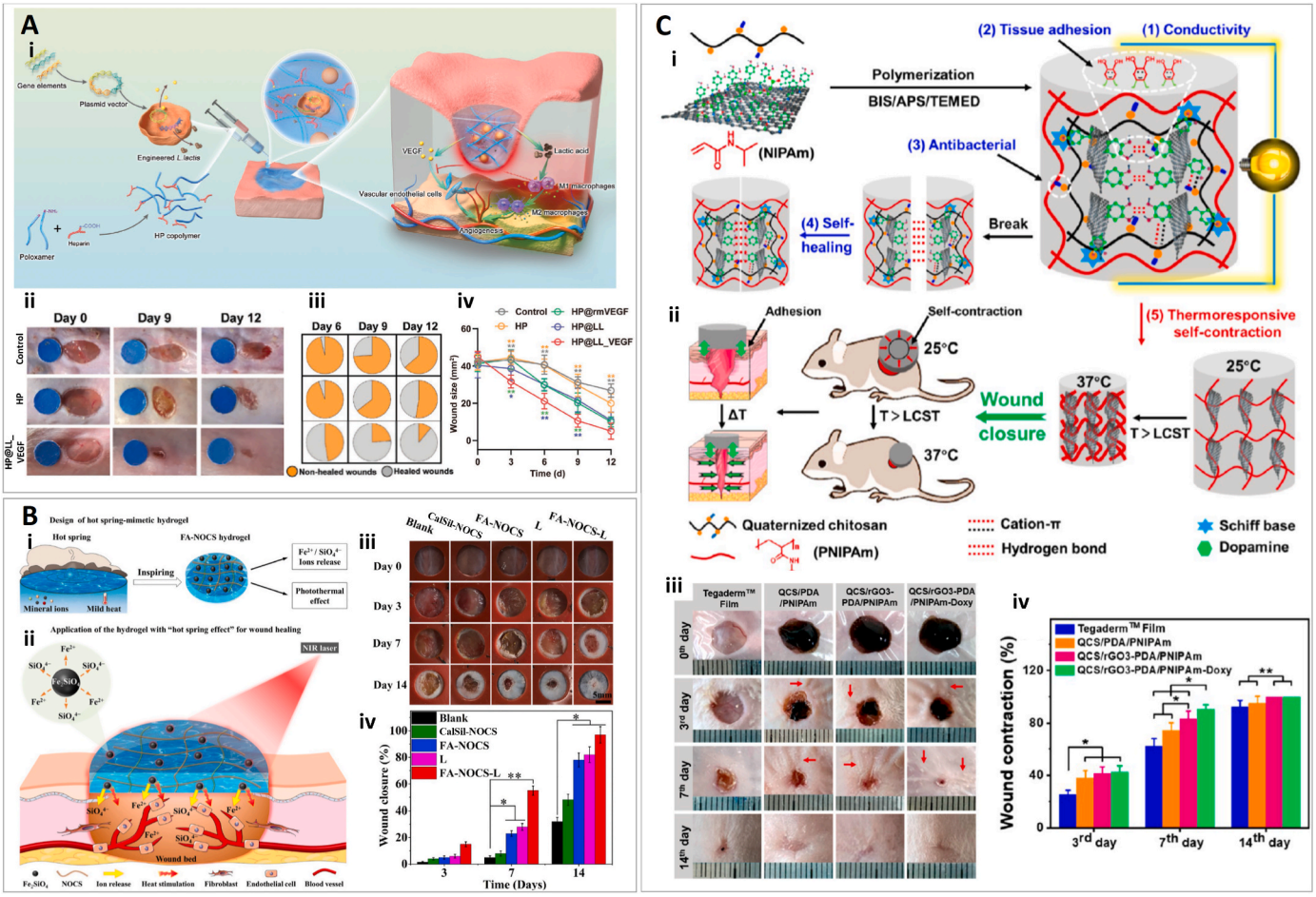

Fig. 8. Wound dressing using other bioactive agents. (A) (i) This graphic represents the accelerating angiogenesis in diabetic wounds by promoting the angiogenic capacity of endothelial cells and inducing macrophages toward M2 polarization. (ii) Representative pictures of the wound area in response to different treatments (HP: heparin poloxamer; HP@rm VEGF: heparin poloxamer with VEGF; HP@LL: heparin poloxamer with *Lactococcus lactis*; HP@LL_VEGF: heparin poloxamer with VEGF-producing *L. lactis*) on days 0, 6, 9, and 12. The blue circle with a 6 mm diameter indicates the initial wound size. (iii) Fractions of the wounds healed with the different treatments. (iv) Quantitative analysis of the wound area for each group (n = 6). Reprinted and adapted with permission from Lu et al., 2021 [232]. (B) (i) Design of a hot spring-mimetic hydrogel, where there is Fe^{2+}/SiO_4^{4-} ion release and photothermal effect provided by fayalite (FA). (ii) Application of the hot spring-mimetic hydrogel for promoting angiogenesis in wound healing due to bioactive ions and heat stimulation. (FA: Fe_2SiO_4; NOCS: N, O-carboxymethyl chitosan. Yellow and red arrow heads denote the release of Fe^{2+}/SiO_4^{4-} ions and the photothermal heating effect of fayalite particles, respectively). (iii) Pictures of wounds treated with FA-NOCS hydrogel, calcium silicate (Calsil)-NOCS hydrogel and/or infrared irradiation (L: laser irradiation only). (iv) Wound closure percentage of different treatments. Reprinted and adapted with permission from Sheng et al., 2021 [235]. (C) (i) Schematic representation of quaternized chitosan (QCS), polydopamine-coated reduction graphene oxide (rGO-PDA), and poly(N-isopropylacrylamide) (PNIPAm) (QCS/rGO-PDA/PNIPAm) hydrogel preparation and its properties. (ii) Schematic diagram of the hydrogels assisting wound closure by thermoresponsive self-contraction. (iii) Pictures of wounds treated with Tegaderm film dressing (control), QCS/PDA/PNIPAm, QCS/rGO3 (containing 3 mg/mL rGO) PDA/PNIPAm, and QCS/rGO3-PDA/PNIPAm-Doxycycline hydrochloride (Doxy) in a murine model on days 0, 3, 7, and 14. (iv) Wound contraction percentage for each treatment. Reprinted and adapted with permission from Sheng et al., 2021 [236].

self-contractive thermoresponsive polymer to assist with wound closure; and polydopamine-coated reduction graphene oxide (rGO-PDA) to provide a conductive component that could strengthen the adhesion ability and give photothermal and antioxidant properties to the hydrogel to enhance wound repair. The resulting hydrogel (QCS/rGO-PDA/PNIPAm) exhibited similar conductivity to human skin (5–5.6 mS/cm) and good hemocompatibility. Only 2% hemolysis was observed in red blood cells. Murine L929 fibroblasts showed 82%–93% viability after being in contact with the hydrogel for 24 h. In addition, QCS/rGO-PDA/PNIPAm effectively released 81%-93% of doxycycline at 37 °C; enhanced release was attributed to theirthermo-responsive self-contraction properties. These hydrogels showed good inherent and photo-thermally induced antibacterial activity. Results demonstrated >85% bactericidal killing ratios in the absence of thermal stimulation and 100% of bacteria were killed after 10 min of near infrared radiation. The hydrogels also exhibited relevant antioxidant properties (i.e., 97.8% free radical removal). Finally, QCS/rGO-PDA/PNIPAm hydrogels demonstrated promising therapeutic effects in wound healing in a full-thickness skin defect model in terms of tissue adhesion capacity, wound contraction, upregulation of collagen production, granulation tissue thickness, mildest inflammatory response, hair follicle formation, dermal gap size, collagen deposition, and faster angiogenesis (Fig. 8C) [236].

4. Outlook

3D hydrogels have shown numerous benefits in promoting wound healing and regeneration of skin tissue. Despite these great achievements, there are still considerations that need to be addressed in the future. In the near future, we envision that the engineering of 3D hydrogels in wound healing will focus on *in situ* injectable hydrogels and/or *in situ* printing approaches. These methods are quick and, most importantly, customizable to the particular needs of the patient. However, more investigations should be conducted to increase the currently

limited number of polymers used for *in situ* fabrication strategies and to make these strategies more holistic, cost-effective, robust, and versatile. Structuring the hydrogels by creating hollow channels [237] or cavities [238], for example, could also significantly facilitate the wound vascularization process. Vascularization remains an enormous challenge yet to be overcome in tissue engineering (in general) and wound healing (in particular). In terms of mechanical properties, hydrogels (particularly those derived from natural sources) seem to need improvement. More evidence is needed to verify successful wound treatment using hydrogels in large animal models. Those types of studies will shed light on the strength and structural stability requirements of hydrogel dressings and enable a smooth and successful translation to their extensive use in clinics.

Various types of bioactive agents have been incorporated into hydrogels with the aim of promoting the wound healing process through different complex mechanisms. Despite promising results in recent years, this field requires further experiments in order to achieve successful therapy which could be translated to the clinic. There are several concerns and challenges for research along this path. An important issue for all additives is the proper dosage that could be considered as an optimum treatment. Here is important to consider that the efficiency and the side-effects of any bioactive agent also depend on their interplay with the hydrogel matrix. Thus, different dosages of a specific bioactive agent could have different therapeutic outcomes based on the type of matrix hydrogel. Besides safety and efficiency, another important consideration is to design a reproducible hydrogel composite, which ideally should also be inexpensive. One of the simplest strategies to have comprehensive wound therapy is recruiting multifunctional agents such as nanoparticles within the hydrogels, which simultaneously exhibit several desirable characteristics such as antibacterial, anti-inflammatory, and electroactivity. Finally, the way additives are released from the designed hydrogel is very important, which is related to the characteristics of the hydrogel in terms of degree of polymerization, crystallization, and bonding, which were not the main focus of this review.

A large number of additives from various sources have been investigated in the last two decades with promising results. However, the need for improved treatments will always motivate the search for more effective and safer additives. Using new types of additives or/and new strategies for promoting the wound healing process could lead to relevant breakthroughs in this field.

Many of these future breakthroughs may be associated with the use of living cells embedded in wound dressings. Cell sourcing for cell laden hydrogels is still a hurdle because the isolation of autologous cells could be invasive for patients with non-healing wounds. Thus, more investigations need to be done to find the solutions to stratified or personalized medicine in wound healing. Wound healing in animals such as rodents (mice) is different from that in humans in many biological aspects. In this regard, the development and use of more precise *in vitro* and *in vivo* models (e.g., wound-on-a-chip systems or large animal models such as canine or porcine, respectively) needs to be addressed. Another crucial aspect that should be considered in wound healing studies is that many of the wound healing impediments are systematic. Organ-on-chip models could help to investigate more systemic implications and interactions. In the end, to ensure a brighter future for 3D hydrogel wound healing, clinical translation capacity and marketing of produced hydrogels should be explored.

Funding

This work was supported by the Consejo Nacional de Ciencia y Tecnología (CONACyT) and Tecnológico de Monterrey. M.H.N, S.C.P.G, and M.G.S.S acknowledge funding received by CONACYT in the form of a Graduate Studies Scholarships. G.T.dS, and M.M.A, gratefully acknowledge the Academic Scholarships provided by CONACyT as members of the National System of Researchers (Sistema Nacional de Investigadores).

Ethical statement

As this article is a review paper, we did not need any “ethics approval” and also there was no need for “consent to participate”.

Declaration of competing interest

The authors declare no conflict of interest.

Appendix A. Supplementary data

Supplementary data to this article can be found online at https://doi.org/10.1016/j.bioactmat.2022.11.019.

References

[1] R.A. Clark, M. Musillo, T. Stransky, Wound repair: basic biology to tissue engineering, in: Princ. Tissue Eng., Elsevier, 2020, pp. 1309–1329.
[2] E. Eriksson, P.Y. Liu, G.S. Schultz, M.M. Martins-Green, R. Tanaka, D. Weir, L. J. Gould, D.G. Armstrong, G.W. Gibbons, R. Wolcott, O.O. Olutoye, R.S. Kirsner, G.C. Gurtner, Chronic wounds: treatment consensus, Wound Repair Regen. 30 (2022) 156–171, https://doi.org/10.1111/wrr.12994.
[3] T.G. Sahana, P.D. Rekha, Biopolymers: applications in wound healing and skin tissue engineering, Mol. Biol. Rep. 45 (2018) 2857–2867, https://doi.org/10.1007/s11033-018-4296-3.
[4] V. Falanga, Bioengineered skin constructs, in: Princ. Tissue Eng., Elsevier, 2020, pp. 1331–1352.
[5] V. Falanga, in: R. Lanza, R. Langer, J.P. Vacanti, A. Atala (Eds.), Chapter 71 - Bioengineered Skin Constructs, fifth ed.Princ. Tissue Eng, Academic Press, 2020, pp. 1331–1352, https://doi.org/10.1016/B978-0-12-818422-6.00073-3.
[6] V. Falanga, Wound healing and its impairment in the diabetic foot, Lancet 366 (2005) 1736–1743, https://doi.org/10.1016/S0140-6736(05)67700-8.
[7] T.M. Honnegowda, P. Kumar, E.G.P. Udupa, S. Kumar, U. Kumar, P. Rao, Role of angiogenesis and angiogenic factors in acute and chronic wound healing, Plast. Aesthetic Res. 2 (2015) 243–249, https://doi.org/10.4103/2347-9264.165438.
[8] H. Brem, T. Jacobs, L. Vileikyte, S. Weinberger, M. Gibber, K. Gill, A. Tarnovskaya, H. Entero, A.J.M. Boulton, Wound-healing protocols for diabetic foot and pressure ulcers, Surg. Technol. Int. 11 (2003) 85–92.
[9] S.G. Keswani, A.B. Katz, F.-Y. Lim, P. Zoltick, A. Radu, D. Alaee, M. Herlyn, T. M. Crombleholme, Adenoviral mediated gene transfer of PDGF-B enhances wound healing in type I and type II diabetic wounds, Wound Repair Regen. 12 (2004) 497–504, https://doi.org/10.1111/j.1067-1927.2004.12501.x.
[10] D. Altavilla, A. Saitta, D. Cucinotta, M. Galeano, B. Deodato, M. Colonna, V. Torre, G. Russo, A. Sardella, G. Urna, G.M. Campo, V. Cavallari, G. Squadrito, F. Squadrito, Inhibition of lipid peroxidation restores impaired vascular endothelial growth factor expression and stimulates wound healing and angiogenesis in the genetically diabetic mouse, Diabetes 50 (2001) 667–674, https://doi.org/10.2337/diabetes.50.3.667.
[11] P.V. Peplow, G.D. Baxter, Gene expression and release of growth factors during delayed wound healing: a review of studies in diabetic animals and possible combined laser phototherapy and growth factor treatment to enhance healing, Photomed. Laser Surg. 30 (2012) 617–636, https://doi.org/10.1089/pho.2012.3312.
[12] D. Stavrou, Neovascularisation in wound healing, J. Wound Care 17 (2008) 298–302, https://doi.org/10.12968/jowc.2008.17.7.30521.
[13] J. Xiang, L. Shen, Y. Hong, Status and future scope of hydrogels in wound healing: synthesis, materials and evaluation, Eur. Polym. J. 130 (2020), 109609, https://doi.org/10.1016/j.eurpolymj.2020.109609.
[14] N. Iqbal, A.S. Khan, A. Asif, M. Yar, J.W. Haycock, I.U. Rehman, Recent concepts in biodegradable polymers for tissue engineering paradigms: a critical review, Int. Mater. Rev. 64 (2019) 91–126, https://doi.org/10.1080/09506608.2018.1460943.
[15] L. Zhang, M. Liu, Y. Zhang, R. Pei, Recent progress of highly adhesive hydrogels as wound dressings, Biomacromolecules 21 (2020) 3966–3983, https://doi.org/10.1021/acs.biomac.0c01069.
[16] J. Lei, L. Sun, P. Li, C. Zhu, Z. Lin, V. Mackey, D.H. Coy, Q. He, The wound dressings and their applications in wound healing and management, Health Sci. J. 8 (2019).
[17] Z. Li, A. Milionis, Y. Zheng, M. Yee, L. Codispoti, F. Tan, D. Poulikakos, C.H. Yap, Superhydrophobic hemostatic nanofiber composites for fast clotting and minimal adhesion, Nat. Commun. 10 (2019) 5562, https://doi.org/10.1038/s41467-019-13512-8.
[18] A. Gupta, M. Kowalczuk, W. Heaselgrave, S.T. Britland, C. Martin, I. Radecka, The production and application of hydrogels for wound management: a review, Eur. Polym. J. 111 (2019) 134–151, https://doi.org/10.1016/j.eurpolymj.2018.12.019.
[19] S. Van Vlierberghe, P. Dubruel, E. Schacht, Biopolymer-based hydrogels as scaffolds for tissue engineering applications: a review, Biomacromolecules 12 (2011) 1387–1408, https://doi.org/10.1021/bm200083n.

[20] N. Asadi, H. Pazoki-Toroudi, A.R. Del Bakhshayesh, A. Akbarzadeh, S. Davaran, N. Annabi, Multifunctional hydrogels for wound healing: special focus on biomacromolecular based hydrogels, Int. J. Biol. Macromol. 170 (2021) 728–750.

[21] Y. Gao, Z. Li, J. Huang, M. Zhao, J. Wu, In situ formation of injectable hydrogels for chronic wound healing, J. Mater. Chem. B. 8 (2020) 8768–8780.

[22] X. Wang, J. Qi, W. Zhang, Y. Pu, R. Yang, P. Wang, S. Liu, X. Tan, B. Chi, 3D-printed antioxidant antibacterial carboxymethyl cellulose/ε-polylysine hydrogel promoted skin wound repair, Int. J. Biol. Macromol. 187 (2021) 91–104, https://doi.org/10.1016/j.ijbiomac.2021.07.115.

[23] L.G. Bracaglia, M. Messina, S. Winston, C.-Y. Kuo, M. Lerman, J.P. Fisher, 3D printed pericardium hydrogels to promote wound healing in vascular applications, Biomacromolecules 18 (2017) 3802–3811, https://doi.org/10.1021/acs.biomac.7b01165.

[24] A. Smandri, A. Nordin, N.M. Hwei, K.-Y. Chin, I. Abd Aziz, M.B. Fauzi, Natural 3D-printed bioinks for skin regeneration and wound healing: a systematic review, Polymers 12 (2020), https://doi.org/10.3390/polym12081782.

[25] J. Koehler, F.P. Brandl, A.M. Goepferich, Hydrogel wound dressings for bioactive treatment of acute and chronic wounds, Eur. Polym. J. 100 (2018) 1–11, https://doi.org/10.1016/j.eurpolymj.2017.12.046.

[26] Y. Luo, Three-dimensional scaffolds, in: Princ. Tissue Eng., Elsevier, 2020, pp. 343–360.

[27] Y. Yang, H. Hu, A review on antimicrobial silver absorbent wound dressings applied to exuding wounds, J. Microb. Biochem. Technol. 7 (2015) 228–233.

[28] M. Gomez-Florit, A. Pardo, R.M.A. Domingues, A.L. Graça, P.S. Babo, R.L. Reis, M.E. Gomes, Natural-based hydrogels for tissue engineering applications, Molecules 25 (2020) 5858, https://doi.org/10.3390/molecules25245858.

[29] S. Mantha, S. Pillai, P. Khayambashi, A. Upadhyay, Y. Zhang, O. Tao, H.M. Pham, S.D. Tran, Smart hydrogels in tissue engineering and regenerative medicine, Materials 12 (2019), https://doi.org/10.3390/ma12203323.

[30] K. Yue, G. Trujillo-de Santiago, M.M. Alvarez, A. Tamayol, N. Annabi, A. Khademhosseini, Synthesis, properties, and biomedical applications of gelatin methacryloyl (GelMA) hydrogels, Biomaterials 73 (2015) 254–271, https://doi.org/10.1016/j.biomaterials.2015.08.045.

[31] M. Buonanno, M. Stanislauskas, B. Ponnaiya, A.W. Bigelow, G. Randers-Pehrson, Y. Xu, I. Shuryak, L. Smilenov, D.M. Owens, D.J. Brenner, 207-nm UV light—a promising tool for safe low-cost reduction of surgical site infections. II: in-vivo safety studies, PLoS One 11 (2016), e0138418, https://doi.org/10.1371/journal.pone.0138418.

[32] B. Trappmann, J.E. Gautrot, J.T. Connelly, D.G. Strange, Y. Li, M.L. Oyen, M.A. C. Stuart, H. Boehm, B. Li, V. Vogel, Extracellular-matrix tethering regulates stem-cell fate, Nat. Mater. 11 (2012) 642–649.

[33] J. Salber, S. Gräter, M. Harwardt, M. Hofmann, D. Klee, J. Dujic, H. Jinghuan, J. Ding, S. Kippenberger, A. Bernd, J. Groll, J.P. Spatz, M. Möller, Influence of different ECM mimetic peptide sequences embedded in a nonfouling environment on the specific adhesion of human-skin keratinocytes and fibroblasts on deformable substrates, Small Weinh. Bergstr. Ger. 3 (2007) 1023–1031, https://doi.org/10.1002/smll.200600596.

[34] X. Zhao, Q. Lang, L. Yildirimer, Z.Y. Lin, W. Cui, N. Annabi, K.W. Ng, M. R. Dokmeci, A.M. Ghaemmaghami, A. Khademhosseini, Photocrosslinkable gelatin hydrogel for epidermal tissue engineering, Adv. Healthc. Mater. 5 (2016) 108–118, https://doi.org/10.1002/adhm.201500005.

[35] H. Joodaki, M.B. Panzer, Skin mechanical properties and modeling: a review, Proc. Inst. Mech. Eng. [H]. 232 (2018) 323–343, https://doi.org/10.1177/0954411918759801.

[36] M. Goh, Y. Hwang, G. Tae, Epidermal growth factor loaded heparin-based hydrogel sheet for skin wound healing, Carbohydr. Polym. 147 (2016) 251–260, https://doi.org/10.1016/j.carbpol.2016.03.072.

[37] M.-H. Lu, W. Yu, Q.-H. Huang, Y.-P. Huang, Y.-P. Zheng, A hand-held indentation system for the assessment of mechanical properties of soft tissues in vivo, IEEE Trans. Instrum. Meas. 58 (2009) 3079–3085, https://doi.org/10.1109/TIM.2009.2016876.

[38] C. Pailler-Mattei, S. Bec, H. Zahouani, In vivo measurements of the elastic mechanical properties of human skin by indentation tests, Med. Eng. Phys. 30 (2008) 599–606, https://doi.org/10.1016/j.medengphy.2007.06.011.

[39] D. Queen, J.D.S. Gaylor, J.H. Evans, J.M. Courtney, W.H. Reid, The preclinical evaluation of the water vapour transmission rate through burn wound dressings, Biomaterials 8 (1987) 367–371, https://doi.org/10.1016/0142-9612(87)90007-X.

[40] S. Anjum, A. Arora, M. Alam, B. Gupta, Development of antimicrobial and scar preventive chitosan hydrogel wound dressings, Int. J. Pharm. 508 (2016) 92–101.

[41] M. Zeng, Z. Fang, C. Xu, Effect of compatibility on the structure of the microporous membrane prepared by selective dissolution of chitosan/synthetic polymer blend membrane, J. Membr. Sci. 230 (2004) 175–181, https://doi.org/10.1016/j.memsci.2003.11.020.

[42] R. Tian, X. Qiu, P. Yuan, K. Lei, L. Wang, Y. Bai, S. Liu, X. Chen, Fabrication of self-healing hydrogels with on-demand antimicrobial activity and sustained biomolecule release for infected skin regeneration, ACS Appl. Mater. Interfaces 10 (2018) 17018–17027.

[43] D. Gan, W. Xing, L. Jiang, J. Fang, C. Zhao, F. Ren, L. Fang, K. Wang, X. Lu, Plant-inspired adhesive and tough hydrogel based on Ag-Lignin nanoparticles-triggered dynamic redox catechol chemistry, Nat. Commun. 10 (2019) 1–10.

[44] G. Lokhande, J.K. Carrow, T. Thakur, J.R. Xavier, M. Parani, K.J. Bayless, A. K. Gaharwar, Nanoengineered injectable hydrogels for wound healing application, Acta Biomater. 70 (2018) 35–47, https://doi.org/10.1016/j.actbio.2018.01.045.

[45] K. Liang, K.H. Bae, M. Kurisawa, Recent advances in the design of injectable hydrogels for stem cell-based therapy, J. Mater. Chem. B. 7 (2019) 3775–3791, https://doi.org/10.1039/C9TB00485H.

[46] L. Yu, J. Ding, Injectable hydrogels as unique biomedical materials, Chem. Soc. Rev. 37 (2008) 1473–1481, https://doi.org/10.1039/B713009K.

[47] C. Lazurko, Z. Khatoon, K. Goel, V. Sedlakova, C. Eren Cimenci, M. Ahumada, L. Zhang, T.-F. Mah, W. Franco, E.J. Suuronen, Multifunctional nano and collagen-based therapeutic materials for skin repair, ACS Biomater. Sci. Eng. 6 (2019) 1124–1134.

[48] P. Kiekkas, D. Aretha, N. Bakalis, I. Karpouhtsi, C. Marneras, G.I. Baltopoulos, Fever effects and treatment in critical care: literature review, Aust. Crit. Care 26 (2013) 130–135.

[49] J. Pupkaite, M. Ahumada, S. Mclaughlin, M. Temkit, S. Alaziz, R. Seymour, M. Ruel, I. Kochevar, M. Griffith, E.J. Suuronen, Collagen-based photoactive agent for tissue bonding, ACS Appl. Mater. Interfaces 9 (2017) 9265–9270.

[50] L. Shi, Y. Zhao, Q. Xie, C. Fan, J. Hilborn, J. Dai, D.A. Ossipov, Moldable hyaluronan hydrogel enabled by dynamic metal–bisphosphonate coordination chemistry for wound healing, Adv. Healthc. Mater. 7 (2018), 1700973.

[51] D. Chouhan, T. Lohe, P.K. Samudrala, B.B. Mandal, In situ forming injectable silk fibroin hydrogel promotes skin regeneration in full thickness burn wounds, Adv. Healthc. Mater. 7 (2018), 1801092.

[52] G. Eke, N. Mangir, N. Hasirci, S. MacNeil, V. Hasirci, Development of a UV crosslinked biodegradable hydrogel containing adipose derived stem cells to promote vascularization for skin wounds and tissue engineering, Biomaterials 129 (2017) 188–198, https://doi.org/10.1016/j.biomaterials.2017.03.021.

[53] X. Zhao, H. Wu, B. Guo, R. Dong, Y. Qiu, P.X. Ma, Antibacterial anti-oxidant electroactive injectable hydrogel as self-healing wound dressing with hemostasis and adhesiveness for cutaneous wound healing, Biomaterials 122 (2017) 34–47, https://doi.org/10.1016/j.biomaterials.2017.01.011.

[54] X. Wang, J.A. Kluge, G.G. Leisk, D.L. Kaplan, Sonication-induced gelation of silk fibroin for cell encapsulation, Biomaterials 29 (2008) 1054–1064, https://doi.org/10.1016/j.biomaterials.2007.11.003.

[55] A.M. Hopkins, L. De Laporte, F. Tortelli, E. Spedden, C. Staii, T.J. Atherton, J. A. Hubbell, D.L. Kaplan, Silk hydrogels as soft substrates for neural tissue engineering, Adv. Funct. Mater. 23 (2013) 5140–5149, https://doi.org/10.1002/adfm.201300435.

[56] G. Chen, Y. Yu, X. Wu, G. Wang, J. Ren, Y. Zhao, Bioinspired multifunctional hybrid hydrogel promotes wound healing, Adv. Funct. Mater. 28 (2018), 1801386.

[57] C. Wang, M. Wang, T. Xu, X. Zhang, C. Lin, W. Gao, H. Xu, B. Lei, C. Mao, Engineering bioactive self-healing antibacterial exosomes hydrogel for promoting chronic diabetic wound healing and complete skin regeneration, Theranostics 9 (2019) 65.

[58] G. Gao, Y.-W. Jiang, H.-R. Jia, F.-G. Wu, Near-infrared light-controllable on-demand antibiotics release using thermo-sensitive hydrogel-based drug reservoir for combating bacterial infection, Biomaterials 188 (2019) 83–95, https://doi.org/10.1016/j.biomaterials.2018.09.045.

[59] M.G.A. Mohamed, P. Ambhorkar, R. Samanipour, A. Yang, A. Ghafoor, K. Kim, Microfluidics-based fabrication of cell-laden microgels, Biomicrofluidics 14 (2020), 021501, https://doi.org/10.1063/1.5134060.

[60] G. Chen, Y. Yu, X. Wu, G. Wang, G. Gu, F. Wang, J. Ren, H. Zhang, Y. Zhao, Microfluidic electrospray niacin metal-organic frameworks encapsulated microcapsules for wound healing, Research (2019) 1–11, https://doi.org/10.34133/2019/6175398, 2019.

[61] T. Cui, J. Yu, C.-F. Wang, S. Chen, Q. Li, K. Guo, R. Qing, G. Wang, J. Ren, Micro-gel ensembles for accelerated healing of chronic wound via pH regulation, Adv. Sci. 9 (2022), 2201254, https://doi.org/10.1002/advs.202201254.

[62] W. Zhu, X. Ma, M. Gou, D. Mei, K. Zhang, S. Chen, 3D printing of functional biomaterials for tissue engineering, Curr. Opin. Biotechnol. 40 (2016) 103–112, https://doi.org/10.1016/j.copbio.2016.03.014.

[63] U. Jammalamadaka, K. Tappa, Recent advances in biomaterials for 3D printing and tissue engineering, J. Funct. Biomater. 9 (2018) 22, https://doi.org/10.3390/jfb9010022.

[64] T. Distler, A.R. Boccaccini, 3D printing of electrically conductive hydrogels for tissue engineering and biosensors – a review, Acta Biomater. 101 (2020) 1–13, https://doi.org/10.1016/j.actbio.2019.08.044.

[65] S.C. Pedroza-González, M. Rodriguez-Salvador, B.E. Pérez-Benítez, M.M. Alvarez, G.T. Santiago, Bioinks for 3D bioprinting: a scientometric analysis of two decades of progress, Int. J. Bioprinting. 7 (2021) 333, https://doi.org/10.18063/ijb.v7i2.337.

[66] C. Xu, B.Z. Molino, X. Wang, F. Cheng, W. Xu, P. Molino, M. Bacher, D. Su, T. Rosenau, S. Willför, G. Wallace, 3D printing of nanocellulose hydrogel scaffolds with tunable mechanical strength towards wound healing application, J. Mater. Chem. B. 6 (2018) 7066–7075, https://doi.org/10.1039/C8TB01757C.

[67] T. Yeung, P.C. Georges, L.A. Flanagan, B. Marg, M. Ortiz, M. Funaki, N. Zahir, W. Ming, V. Weaver, P.A. Janmey, Effects of substrate stiffness on cell morphology, cytoskeletal structure, and adhesion, Cell Motil. 60 (2005) 24–34, https://doi.org/10.1002/cm.20041.

[68] C. Intini, L. Elviri, J. Cabral, S. Mros, C. Bergonzi, A. Bianchera, L. Flammini, P. Govoni, E. Barocelli, R. Bettini, M. McConnell, 3D-printed chitosan-based scaffolds: an in vitro study of human skin cell growth and an in-vivo wound healing evaluation in experimental diabetes in rats, Carbohydr. Polym. 199 (2018) 593–602, https://doi.org/10.1016/j.carbpol.2018.07.057.

[69] X. Liang, S.A. Boppart, Biomechanical properties of in vivo human skin from dynamic optical coherence elastography, IEEE Trans. Biomed. Eng. 57 (2010) 953–959, https://doi.org/10.1109/TBME.2009.2033464.

[70] H. Li, C. Tan, L. Li, Review of 3D printable hydrogels and constructs, Mater. Des. 159 (2018) 20–38, https://doi.org/10.1016/j.matdes.2018.08.023.

[71] V.H.M. Mouser, F.P.W. Melchels, J. Visser, W.J.A. Dhert, D. Gawlitta, J. Malda, Yield stress determines bioprintability of hydrogels based on gelatin-methacryloyl and gellan gum for cartilage bioprinting, Biofabrication 8 (2016), 035003, https://doi.org/10.1088/1758-5090/8/3/035003.

[72] R.F. Pereira, A. Sousa, C.C. Barrias, P.J. Bártolo, P.L. Granja, A single-component hydrogel bioink for bioprinting of bioengineered 3D constructs for dermal tissue engineering, Mater. Horiz. 5 (2018) 1100–1111, https://doi.org/10.1039/C8MH00525G.

[73] H. Ma, Q. Zhou, J. Chang, C. Wu, Grape seed-inspired smart hydrogel scaffolds for melanoma therapy and wound healing, ACS Nano 13 (2019) 4302–4311, https://doi.org/10.1021/acsnano.8b09496.

[74] Polysaccharide Hydrogels, Characterization and biomedical applications, Routledge CRC Press, (n.d.), https://www.routledge.com/Polysaccharide-Hydrogels-Characterization-and-Biomedical-Applications/Matricardi-Alhaique-Coviello/p/book/9789814613613. (Accessed 31 December 2021).

[75] M. Albanna, K.W. Binder, S.V. Murphy, J. Kim, S.A. Qasem, W. Zhao, J. Tan, I. B. El-Amin, D.D. Dice, J. Marco, J. Green, T. Xu, A. Skardal, J.H. Holmes, J. D. Jackson, A. Atala, J.J. Yoo, In situ bioprinting of autologous skin cells accelerates wound healing of extensive excisional full-thickness wounds, Sci. Rep. 9 (2019), https://doi.org/10.1038/s41598-018-38366-w.

[76] A.M. Jorgensen, Z. Chou, G. Gillispie, S.J. Lee, J.J. Yoo, S. Soker, A. Atala, Decellularized skin extracellular matrix (dsECM) improves the physical and biological properties of fibrinogen hydrogel for skin bioprinting applications, Nanomaterials 10 (2020) 1484, https://doi.org/10.3390/nano10081484.

[77] F. Zhou, Y. Hong, R. Liang, X. Zhang, Y. Liao, D. Jiang, J. Zhang, Z. Sheng, C. Xie, Z. Peng, X. Zhuang, V. Bunpetch, Y. Zou, W. Huang, Q. Zhang, E.V. Alakpa, S. Zhang, H. Ouyang, Rapid printing of bio-inspired 3D tissue constructs for skin regeneration, Biomaterials 258 (2020), 120287, https://doi.org/10.1016/j.biomaterials.2020.120287.

[78] S. Wang, Y. Xiong, J. Chen, A. Ghanem, Y. Wang, J. Yang, B. Sun, Three dimensional printing bilayer membrane scaffold promotes wound healing, Front. Bioeng. Biotechnol. 7 (2019) 348, https://doi.org/10.3389/fbioe.2019.00348.

[79] Z. Wu, Y. Hong, Combination of the silver–ethylene interaction and 3D printing to develop antibacterial superporous hydrogels for wound management, ACS Appl. Mater. Interfaces 11 (2019) 33734–33747, https://doi.org/10.1021/acsami.9b14090.

[80] S. Singh, D. Choudhury, F. Yu, V. Mironov, M.W. Naing, In situ bioprinting – bioprinting from benchside to bedside? Acta Biomater. 101 (2020) 14–25, https://doi.org/10.1016/j.actbio.2019.08.045.

[81] K. Nuutila, M. Samandari, Y. Endo, Y. Zhang, J. Quint, T.A. Schmidt, A. Tamayol, I. Sinha, In vivo printing of growth factor-eluting adhesive scaffolds improves wound healing, Bioact. Mater. 8 (2022) 296–308, https://doi.org/10.1016/j.bioactmat.2021.06.030.

[82] N. Hakimi, R. Cheng, L. Leng, M. Sotoudehfar, P.Q. Ba, N. Bakhtyar, S. Amini-Nik, M.G. Jeschke, A. Günther, Handheld skin printer:: in situ formation of planar biomaterials and tissues, Lab Chip 18 (2018) 1440–1451, https://doi.org/10.1039/c7lc01236e.

[83] S.V. Murphy, A. Skardal, A. Atala, Evaluation of hydrogels for bio-printing applications, J. Biomed. Mater. Res. A. 101A (2013) 272–284, https://doi.org/10.1002/jbm.a.34326.

[84] M. Xie, Y. Shi, C. Zhang, M. Ge, J. Zhang, Z. Chen, J. Fu, Z. Xie, Y. He, In situ 3D bioprinting with bioconcrete bioink, Nat. Commun. 13 (2022) 3597, https://doi.org/10.1038/s41467-022-30997-y.

[85] G. Ying, J. Manríquez, D. Wu, J. Zhang, N. Jiang, S. Maharjan, D.H. Hernández Medina, Y.S. Zhang, An open-source handheld extruder loaded with pore-forming bioink for in situ wound dressing, Mater. Today Bio. 8 (2020), 100074, https://doi.org/10.1016/j.mtbio.2020.100074.

[86] A. Skardal, S.V. Murphy, K. Crowell, D. Mack, A. Atala, S. Soker, A tunable hydrogel system for long-term release of cell-secreted cytokines and bioprinted in situ wound cell delivery, J. Biomed. Mater. Res. B Appl. Biomater. 105 (2017) 1986–2000, https://doi.org/10.1002/jbm.b.33736.

[87] A. Assmann, A. Vegh, M. Ghasemi-Rad, S. Bagherifard, G. Cheng, E.S. Sani, G. U. Ruiz-Esparza, I. Noshadi, A.D. Lassaletta, S. Gangadharan, A. Tamayol, A. Khademhosseini, N. Annabi, A highly adhesive and naturally derived sealant, Biomaterials 140 (2017) 115–127, https://doi.org/10.1016/j.biomaterials.2017.06.004.

[88] N. Annabi, D. Rana, E. Shirzaei Sani, R. Portillo-Lara, J.L. Gifford, M.M. Fares, S. M. Mithieux, A.S. Weiss, Engineering a sprayable and elastic hydrogel adhesive with antimicrobial properties for wound healing, Biomaterials 139 (2017) 229–243, https://doi.org/10.1016/j.biomaterials.2017.05.011.

[89] J.W. Nichol, S.T. Koshy, H. Bae, C.M. Hwang, S. Yamanlar, A. Khademhosseini, Cell-laden microengineered gelatin methacrylate hydrogels, Biomaterials 31 (2010) 5536–5544, https://doi.org/10.1016/j.biomaterials.2010.03.064.

[90] X. Wang, C. Yang, Y. Yu, Y. Zhao, In situ 3D bioprinting living photosynthetic scaffolds for autotrophic wound healing, Research (2022) 1–11, https://doi.org/10.34133/2022/9794745, 2022.

[91] W. Hassan, Y. Dong, W. Wang, Encapsulation and 3D culture of human adipose-derived stem cells in an in-situ crosslinked hybrid hydrogel composed of PEG-based hyperbranched copolymer and hyaluronic acid, Stem Cell Res. Ther. 4 (2013) 32, https://doi.org/10.1186/scrt182.

[92] P. He, J. Zhao, J. Zhang, B. Li, Z. Gou, M. Gou, X. Li, Bioprinting of skin constructs for wound healing, Burns Trauma 6 (2018), https://doi.org/10.1186/s41038-017-0104-x.

[93] A.D. Juncos Bombin, N.J. Dunne, H.O. McCarthy, Electrospinning of natural polymers for the production of nanofibres for wound healing applications, Mater. Sci. Eng. C 114 (2020), 110994, https://doi.org/10.1016/j.msec.2020.110994.

[94] X. Sun, Q. Lang, H. Zhang, L. Cheng, Y. Zhang, G. Pan, X. Zhao, H. Yang, Y. Zhang, H.A. Santos, W. Cui, Electrospun photocrosslinkable hydrogel fibrous scaffolds for rapid in vivo vascularized skin flap regeneration, Adv. Funct. Mater. 27 (2017), 1604617, https://doi.org/10.1002/adfm.201604617.

[95] X. Zhao, X. Sun, L. Yildirimer, Q. Lang, Z.Y. (William) Lin, R. Zheng, Y. Zhang, W. Cui, N. Annabi, A. Khademhosseini, Cell infiltrative hydrogel fibrous scaffolds for accelerated wound healing, Acta Biomater. 49 (2017) 66–77, https://doi.org/10.1016/j.actbio.2016.11.017.

[96] P. Soman, J.A. Kelber, J.W. Lee, T.N. Wright, K.S. Vecchio, R.L. Klemke, S. Chen, Cancer cell migration within 3D layer-by-layer microfabricated photocrosslinked PEG scaffolds with tunable stiffness, Biomaterials 33 (2012) 7064–7070, https://doi.org/10.1016/j.biomaterials.2012.06.012.

[97] A. Buxboim, I.L. Ivanovska, D.E. Discher, Matrix elasticity, cytoskeletal forces and physics of the nucleus: how deeply do cells 'feel' outside and in? J. Cell Sci. 123 (2010) 297–308, https://doi.org/10.1242/jcs.041186.

[98] T.S. Panetti, D.F. Hannah, C. Avraamides, J.P. Gaughan, C. Marcinkiewicz, A. Huttenlocher, D.F. Mosher, Extracellular matrix molecules regulate endothelial cell migration stimulated by lysophosphatidic acid, J. Thromb. Haemostasis 2 (2004) 1645–1656, https://doi.org/10.1111/j.1538-7836.2004.00902.x.

[99] J. Patterson, J.A. Hubbell, Enhanced proteolytic degradation of molecularly engineered PEG hydrogels in response to MMP-1 and MMP-2, Biomaterials 31 (2010) 7836–7845, https://doi.org/10.1016/j.biomaterials.2010.06.061.

[100] M. Koosha, M. Raoufi, H. Moravvej, One-pot reactive electrospinning of chitosan/PVA hydrogel nanofibers reinforced by halloysite nanotubes with enhanced fibroblast cell attachment for skin tissue regeneration, Colloids Surf. B Biointerfaces 179 (2019) 270–279, https://doi.org/10.1016/j.colsurfb.2019.03.054.

[101] E. Caló, V.V. Khutoryanskiy, Biomedical applications of hydrogels: a review of patents and commercial products, Eur. Polym. J. 65 (2015) 252–267, https://doi.org/10.1016/j.eurpolymj.2014.11.024.

[102] R. Ogawa, Total Scar Management: from Lasers to Surgery for Scars, Keloids, and Scar Contractures, Springer Nature, 2019.

[103] L.P. da Silva, R.L. Reis, V.M. Correlo, A.P. Marques, Hydrogel-based strategies to advance therapies for chronic skin wounds, Annu. Rev. Biomed. Eng. 21 (2019).

[104] M.C. Robson, T.J. Krizek, J.P. Heggers, Biology of surgical infection, Curr. Probl. Surg. 10 (1973) 1–62, https://doi.org/10.1016/S0011-3840(73)80010-3.

[105] H. Chen, J. Cheng, L. Ran, K. Yu, B. Lu, G. Lan, F. Dai, F. Lu, An injectable self-healing hydrogel with adhesive and antibacterial properties effectively promotes wound healing, Carbohydr. Polym. 201 (2018) 522–531, https://doi.org/10.1016/j.carbpol.2018.08.090.

[106] M.C. Giano, Z. Ibrahim, S.H. Medina, K.A. Sarhane, J.M. Christensen, Y. Yamada, G. Brandacher, J.P. Schneider, Injectable bioadhesive hydrogels with innate antibacterial properties, Nat. Commun. 5 (2014) 4095, https://doi.org/10.1038/ncomms5095.

[107] J. Zhu, H. Han, F. Li, X. Wang, J. Yu, X. Qin, D. Wu, Peptide-functionalized amino acid-derived pseudoprotein-based hydrogel with hemorrhage control and antibacterial activity for wound healing, Chem. Mater. 31 (2019) 4436–4450, https://doi.org/10.1021/acs.chemmater.9b00850.

[108] Z. Fan, B. Liu, J. Wang, S. Zhang, Q. Lin, P. Gong, L. Ma, S. Yang, A novel wound dressing based on Ag/graphene polymer hydrogel: effectively kill bacteria and accelerate wound healing, Adv. Funct. Mater. 24 (2014) 3933–3943, https://doi.org/10.1002/adfm.201304202.

[109] M.R. Reithofer, A. Lakshmanan, A.T.K. Ping, J.M. Chin, C.A.E. Hauser, In situ synthesis of size-controlled, stable silver nanoparticles within ultrashort peptide hydrogels and their anti-bacterial properties, Biomaterials 35 (2014) 7535–7542, https://doi.org/10.1016/j.biomaterials.2014.04.102.

[110] S.P. Miguel, M.P. Ribeiro, H. Brancal, P. Coutinho, I.J. Correia, Thermoresponsive chitosan–agarose hydrogel for skin regeneration, Carbohydr. Polym. 111 (2014) 366–373, https://doi.org/10.1016/j.carbpol.2014.04.093.

[111] H. Hamedi, S. Moradi, S.M. Hudson, A.E. Tonelli, Chitosan based hydrogels and their applications for drug delivery in wound dressings: a review, Carbohydr. Polym. 199 (2018) 445–460, https://doi.org/10.1016/j.carbpol.2018.06.114.

[112] R. Wang, J. Li, W. Chen, T. Xu, S. Yun, Z. Xu, Z. Xu, T. Sato, B. Chi, H. Xu, A biomimetic mussel-inspired ε-Poly-l-lysine hydrogel with robust tissue-anchor and anti-infection capacity, Adv. Funct. Mater. 27 (2017), 1604894, https://doi.org/10.1002/adfm.201604894.

[113] C. Zhou, P. Li, X. Qi, A.R.M. Sharif, Y.F. Poon, Y. Cao, M.W. Chang, S.S.J. Leong, M.B. Chan-Park, A photopolymerized antimicrobial hydrogel coating derived from epsilon-poly-L-lysine, Biomaterials 32 (2011) 2704–2712, https://doi.org/10.1016/j.biomaterials.2010.12.040.

[114] R. Wang, D. Xu, L. Liang, T. Xu, W. Liu, P. Ouyang, B. Chi, H. Xu, Enzymatically crosslinked epsilon-poly-l-lysine hydrogels with inherent antibacterial properties for wound infection prevention, RSC Adv. 6 (2016) 8620–8627, https://doi.org/10.1039/C5RA15616E.

[115] M. Khamrai, S.L. Banerjee, S. Paul, S. Samanta, P.P. Kundu, Curcumin entrapped gelatin/ionically modified bacterial cellulose based self-healable hydrogel film: an eco-friendly sustainable synthesis method of wound healing patch, Int. J. Biol. Macromol. 122 (2019) 940–953, https://doi.org/10.1016/j.ijbiomac.2018.10.196.

[116] J. Qu, X. Zhao, Y. Liang, T. Zhang, P.X. Ma, B. Guo, Antibacterial adhesive injectable hydrogels with rapid self-healing, extensibility and compressibility as wound dressing for joints skin wound healing, Biomaterials 183 (2018) 185–199, https://doi.org/10.1016/j.biomaterials.2018.08.044.

[117] D. Rai, J.K. Singh, N. Roy, D. Panda, Curcumin inhibits FtsZ assembly: an attractive mechanism for its antibacterial activity, Biochem. J. 410 (2008) 147–155, https://doi.org/10.1042/BJ20070891.
[118] S. Kaur, N.H. Modi, D. Panda, N. Roy, Probing the binding site of curcumin in Escherichia coli and Bacillus subtilis FtsZ – a structural insight to unveil antibacterial activity of curcumin, Eur. J. Med. Chem. 45 (2010) 4209–4214, https://doi.org/10.1016/j.ejmech.2010.06.015.
[119] R.F. El-Kased, R.I. Amer, D. Attia, M.M. Elmazar, Honey-based hydrogel: in vitro and comparative in vivo evaluation for burn wound healing, Sci. Rep. 7 (2017) 9692, https://doi.org/10.1038/s41598-017-08771-8.
[120] N.S. Al-Waili, K. Salom, G. Butler, A.A. Al Ghamdi, Honey and microbial infections: a review supporting the use of honey for microbial control, J. Med. Food 14 (2011) 1079–1096, https://doi.org/10.1089/jmf.2010.0161.
[121] N. Ninan, A. Forget, V.P. Shastri, N.H. Voelcker, A. Blencowe, Antibacterial and anti-inflammatory pH-responsive tannic acid-carboxylated agarose composite hydrogels for wound healing, ACS Appl. Mater. Interfaces 8 (2016) 28511–28521, https://doi.org/10.1021/acsami.6b10491.
[122] M. Kazemzadeh-Narbat, H. Cheng, R. Chabok, M.M. Alvarez, C. de la Fuente-Nunez, K.S. Phillips, A. Khademhosseini, Strategies for antimicrobial peptide coatings on medical devices: a review and regulatory science perspective, Crit. Rev. Biotechnol. 41 (2021) 94–120, https://doi.org/10.1080/07388551.2020.1828810.
[123] J.M. Ageitos, A. Sánchez-Pérez, P. Calo-Mata, T.G. Villa, Antimicrobial peptides (AMPs): ancient compounds that represent novel weapons in the fight against bacteria, Antibiot. - Meet. Chall. 21st Century Health Care Part I. 133 (2017) 117–138, https://doi.org/10.1016/j.bcp.2016.09.018.
[124] N.K. Rajendran, S.S.D. Kumar, N.N. Houreld, H. Abrahamse, A review on nanoparticle based treatment for wound healing, J. Drug Deliv. Sci. Technol. 44 (2018) 421–430, https://doi.org/10.1016/j.jddst.2018.01.009.
[125] M.T. Khorasani, A. Joorabloo, H. Adeli, P.B. Milan, M. Amoupour, Enhanced antimicrobial and full-thickness wound healing efficiency of hydrogels loaded with heparinized ZnO nanoparticles: in vitro and in vivo evaluation, Int. J. Biol. Macromol. 166 (2021) 200–212, https://doi.org/10.1016/j.ijbiomac.2020.10.142.
[126] F.R. Diniz, R.C.A.P. Maia, L. Rannier Andrade, L.N. Andrade, M. Vinicius Chaud, C.F. da Silva, C.B. Corrêa, R.L.C. de Albuquerque Junior, L. Pereira da Costa, S. R. Shin, S. Hassan, E. Sanchez-Lopez, E.B. Souto, P. Severino, Silver nanoparticles-composing alginate/gelatine hydrogel improves wound healing in vivo, Nanomaterials 10 (2020) 390, https://doi.org/10.3390/nano10020390.
[127] Y. Liang, B. Chen, M. Li, J. He, Z. Yin, B. Guo, Injectable antimicrobial conductive hydrogels for wound disinfection and infectious wound healing, Biomacromolecules 21 (2020) 1841–1852, https://doi.org/10.1021/acs.biomac.9b01732.
[128] A. Khalid, A. Madni, B. Raza, M. ul Islam, A. Hassan, F. Ahmad, H. Ali, T. Khan, F. Wahid, Multiwalled carbon nanotubes functionalized bacterial cellulose as an efficient healing material for diabetic wounds, Int. J. Biol. Macromol. 203 (2022) 256–267, https://doi.org/10.1016/j.ijbiomac.2022.01.146.
[129] J.J. Elsner, I. Berdicevsky, M. Zilberman, In vitro microbial inhibition and cellular response to novel biodegradable composite wound dressings with controlled release of antibiotics, Acta Biomater. 7 (2011) 325–336, https://doi.org/10.1016/j.actbio.2010.07.013.
[130] H. Chen, X. Xing, H. Tan, Y. Jia, T. Zhou, Y. Chen, Z. Ling, X. Hu, Covalently antibacterial alginate-chitosan hydrogel dressing integrated gelatin microspheres containing tetracycline hydrochloride for wound healing, Mater. Sci. Eng. C 70 (2017) 287–295, https://doi.org/10.1016/j.msec.2016.08.086.
[131] A. Rasool, S. Ata, A. Islam, Stimuli responsive biopolymer (chitosan) based blend hydrogels for wound healing application, Carbohydr. Polym. 203 (2019) 423–429, https://doi.org/10.1016/j.carbpol.2018.09.083.
[132] M. Mühlstädt, C. Thomé, C. Kunte, Rapid wound healing of scalp wounds devoid of periosteum with milling of the outer table and split-thickness skin grafting, Br. J. Dermatol. 167 (2012) 343–347, https://doi.org/10.1111/j.1365-2133.2012.10999.x.
[133] S. Hogg, Essential Microbiology, John Wiley & Sons, 2013.
[134] B.N. Green, C.D. Johnson, J.T. Egan, M. Rosenthal, E.A. Griffith, M.W. Evans, Methicillin-resistant Staphylococcus aureus: an overview for manual therapists, J. Chiropr. Med. 11 (2012) 64–76, https://doi.org/10.1016/j.jcm.2011.12.001.
[135] D. Simões, S.P. Miguel, M.P. Ribeiro, P. Coutinho, A.G. Mendonça, I.J. Correia, Recent advances on antimicrobial wound dressing: a review, Eur. J. Pharm. Biopharm. 127 (2018) 130–141, https://doi.org/10.1016/j.ejpb.2018.02.022.
[136] M.D. Hadagali, L.S. Chua, The anti-inflammatory and wound healing properties of honey, Eur. Food Res. Technol. 239 (2014) 1003–1014, https://doi.org/10.1007/s00217-014-2297-6.
[137] D.D. Patel, W. Koopmann, T. Imai, L.P. Whichard, O. Yoshie, M.S. Krangel, Chemokines have diverse abilities to form solid phase gradients, Clin. Immunol. 99 (2001) 43–52, https://doi.org/10.1006/clim.2000.4997.
[138] U. Freudenberg, Y. Liang, K.L. Kiick, C. Werner, Glycosaminoglycan-based biohybrid hydrogels: a sweet and smart choice for multifunctional biomaterials, Adv. Mater. 28 (2016) 8861–8891, https://doi.org/10.1002/adma.201601908.
[139] N. Lohmann, L. Schirmer, P. Atallah, E. Wandel, R.A. Ferrer, C. Werner, J. C. Simon, S. Franz, U. Freudenberg, Glycosaminoglycan-based hydrogels capture inflammatory chemokines and rescue defective wound healing in mice, Sci. Transl. Med. 9 (2017), eaai9044, https://doi.org/10.1126/scitranslmed.aai9044.
[140] P.K. Veerasubramanian, P. Thangavel, R. Kannan, S. Chakraborty, B. Ramachandran, L. Suguna, V. Muthuvijayan, An investigation of konjac glucomannan-keratin hydrogel scaffold loaded with Avena sativa extracts for diabetic wound healing, Colloids Surf. B Biointerfaces 165 (2018) 92–102, https://doi.org/10.1016/j.colsurfb.2018.02.022.
[141] B. Halliwell, J.M.C. Gutteridge, C.E. Cross, Free radicals, antioxidants, and human disease: where are we now? J. Lab. Clin. Med. 119 (1992) 598–620, https://doi.org/10.5555/uri:pii:002221439290284R.
[142] J. Huang, L. Chen, Z. Gu, J. Wu, Red jujube-incorporated gelatin methacryloyl (GelMA) hydrogels with anti-oxidation and immunoregulation activity for wound healing, J. Biomed. Nanotechnol. 15 (2019) 1357–1370, https://doi.org/10.1166/jbn.2019.2815.
[143] X. Zhao, H. Wu, B. Guo, R. Dong, Y. Qiu, P.X. Ma, Antibacterial anti-oxidant electroactive injectable hydrogel as self-healing wound dressing with hemostasis and adhesiveness for cutaneous wound healing, Biomaterials 122 (2017) 34–47, https://doi.org/10.1016/j.biomaterials.2017.01.011.
[144] P. Marrazzo, C. O'Leary, Repositioning natural antioxidants for therapeutic applications in tissue engineering, Bioengineering 7 (2020) 104, https://doi.org/10.3390/bioengineering7030104.
[145] R. Sarangarajan, S. Meera, R. Rukkumani, P. Sankar, G. Anuradha, Antioxidants: friend or foe? Asian Pac. J. Trop. Med. 10 (2017) 1111–1116, https://doi.org/10.1016/j.apjtm.2017.10.017.
[146] J.A. Morales-Gonzalez, Á. Morales-González, E.O. Madrigal-Santillan, A Master Regulator of Oxidative StressThe Transcription Factor Nrf2, BoD – Books on Demand, 2016.
[147] K. Neha, M.R. Haider, A. Pathak, M.S. Yar, Medicinal prospects of antioxidants: a review, Eur. J. Med. Chem. 178 (2019) 687–704, https://doi.org/10.1016/j.ejmech.2019.06.010.
[148] A. Ehterami, M. Salehi, S. Farzamfar, H. Samadian, A. Vaez, S. Ghorbani, J. Ai, H. Sahrapeyma, Chitosan/alginate hydrogels containing Alpha-tocopherol for wound healing in rat model, J. Drug Deliv. Sci. Technol. 51 (2019) 204–213, https://doi.org/10.1016/j.jddst.2019.02.032.
[149] F. Nachbar, H.C. Korting, The role of vitamin E in normal and damaged skin, J. Mol. Med. 73 (1995) 7–17, https://doi.org/10.1007/BF00203614.
[150] J. Wu, J. Zhu, C. He, Z. Xiao, J. Ye, Y. Li, A. Chen, H. Zhang, X. Li, L. Lin, Y. Zhao, J. Zheng, J. Xiao, Comparative study of heparin-poloxamer hydrogel modified bFGF and aFGF for in vivo wound healing efficiency, ACS Appl. Mater. Interfaces 8 (2016) 18710–18721, https://doi.org/10.1021/acsami.6b06047.
[151] M. Qiu, D. Chen, C. Shen, J. Shen, H. Zhao, Y. He, Platelet-rich plasma-loaded poly(d,l-lactide)-poly(ethylene glycol)-Poly(d,l-lactide) hydrogel dressing promotes full-thickness skin wound healing in a rodent model, Int. J. Mol. Sci. 17 (2016) 1001, https://doi.org/10.3390/ijms17071001.
[152] G. Gainza, D.C. Bonafonte, B. Moreno, J.J. Aguirre, F.B. Gutierrez, S. Villullas, J. L. Pedraz, M. Igartua, R.M. Hernandez, The topical administration of rhEGF-loaded nanostructured lipid carriers (rhEGF-NLC) improves healing in a porcine full-thickness excisional wound model, J. Contr. Release 197 (2015) 41–47, https://doi.org/10.1016/j.jconrel.2014.10.033.
[153] Y. Ando, P.J. Jensen, Epidermal growth factor and insulin-like growth factor I enhance keratinocyte migration, J. Invest. Dermatol. 100 (1993) 633–639, https://doi.org/10.1111/1523-1747.ep12472297.
[154] M. Klagsbrun, Y. Shing, Heparin affinity of anionic and cationic capillary endothelial cell growth factors: analysis of hypothalamus-derived growth factors and fibroblast growth factors, Proc. Natl. Acad. Sci. USA 82 (1985) 805, https://doi.org/10.1073/pnas.82.3.805.
[155] M.A. Fonder, G.S. Lazarus, D.A. Cowan, B. Aronson-Cook, A.R. Kohli, A. J. Mamelak, Treating the chronic wound: a practical approach to the care of nonhealing wounds and wound care dressings, J. Am. Acad. Dermatol. 58 (2008) 185–206, https://doi.org/10.1016/j.jaad.2007.08.048.
[156] P.V. Notodihardjo, N. Morimoto, N. Kakudo, M. Matsui, M. Sakamoto, P.H. Liem, K. Suzuki, Y. Tabata, K. Kusumoto, Gelatin hydrogel impregnated with platelet-rich plasma releasate promotes angiogenesis and wound healing in murine model, J. Artif. Organs 18 (2015) 64–71, https://doi.org/10.1007/s10047-014-0795-8.
[157] Y. Wu, L. Chen, P.G. Scott, E.E. Tredget, Mesenchymal stem cells enhance wound healing through differentiation and angiogenesis, Stem Cell. 25 (2007) 2648–2659, https://doi.org/10.1634/stemcells.2007-0226.
[158] D.S. Yoon, Y. Lee, H.A. Ryu, Y. Jang, K.-M. Lee, Y. Choi, W.J. Choi, M. Lee, K. M. Park, K.D. Park, J.W. Lee, Cell recruiting chemokine-loaded sprayable gelatin hydrogel dressings for diabetic wound healing, Acta Biomater. 38 (2016) 59–68, https://doi.org/10.1016/j.actbio.2016.04.030.
[159] F. Zarei, M. Soleimaninejad, Role of growth factors and biomaterials in wound healing, Artif. Cell Nanomed. Biotechnol. 46 (2018) 906–911, https://doi.org/10.1080/21691401.2018.1439836.
[160] A. Saberi, F. Jabbari, P. Zarrintaj, M.R. Saeb, M. Mozafari, Electrically conductive materials: opportunities and challenges in tissue engineering, Biomolecules 9 (2019) 448, https://doi.org/10.3390/biom9090448.
[161] M. Gajendiran, J. Choi, S.-J. Kim, K. Kim, H. Shin, H.-J. Koo, K. Kim, Conductive biomaterials for tissue engineering applications, J. Ind. Eng. Chem. 51 (2017) 12–26, https://doi.org/10.1016/j.jiec.2017.02.031.
[162] H. Cui, L. Cui, P. Zhang, Y. Huang, Y. Wei, X. Chen, In situ electroactive and antioxidant supramolecular hydrogel based on cyclodextrin/copolymer inclusion for tissue engineering repair, Macromol. Biosci. 14 (2014) 440–450, https://doi.org/10.1002/mabi.201300366.
[163] H. Cui, Y. Liu, M. Deng, X. Pang, P. Zhang, X. Wang, X. Chen, Y. Wei, Synthesis of biodegradable and electroactive tetraaniline grafted poly(ester amide) copolymers for bone tissue engineering, Biomacromolecules 13 (2012) 2881–2889, https://doi.org/10.1021/bm300897j.
[164] R. Gharibi, H. Yeganeh, A. Rezapour-Lactoee, Z.M. Hassan, Stimulation of wound healing by electroactive, antibacterial, and antioxidant polyurethane/siloxane

dressing membranes: in vitro and in vivo evaluations, ACS Appl. Mater. Interfaces 7 (2015) 24296–24311, https://doi.org/10.1021/acsami.5b08376.
[165] J. Qu, X. Zhao, Y. Liang, Y. Xu, P.X. Ma, B. Guo, Degradable conductive injectable hydrogels as novel antibacterial, anti-oxidant wound dressings for wound healing, Chem. Eng. J. 362 (2019) 548–560, https://doi.org/10.1016/j.cej.2019.01.028.
[166] R. Balint, N.J. Cassidy, S.H. Cartmell, Conductive polymers: towards a smart biomaterial for tissue engineering, Acta Biomater. 10 (2014) 2341–2353, https://doi.org/10.1016/j.actbio.2014.02.015.
[167] J. Liang, K. Tong, Q. Pei, A water-based silver-nanowire screen-print ink for the fabrication of stretchable conductors and wearable thin-film transistors, Adv. Mater. 28 (2016) 5986–5996, https://doi.org/10.1002/adma.201600772.
[168] C.-Y. Chen, H. Yin, X. Chen, T.-H. Chen, H.-M. Liu, S.-S. Rao, Y.-J. Tan, Y.-X. Qian, Y.-W. Liu, X.-K. Hu, M.-J. Luo, Z.-X. Wang, Z.-Z. Liu, J. Cao, Z.-H. He, B. Wu, T. Yue, Y.-Y. Wang, K. Xia, Z.-W. Luo, Y. Wang, W.-Y. Situ, W.-E. Liu, S.-Y. Tang, H. Xie, Ångstrom-scale silver particle–embedded carbomer gel promotes wound healing by inhibiting bacterial colonization and inflammation, Sci. Adv. 6 (2020), https://doi.org/10.1126/sciadv.aba0942 eaba0942.
[169] C. Wang, X. Jiang, H.-J. Kim, S. Zhang, X. Zhou, Y. Chen, H. Ling, Y. Xue, Z. Chen, M. Qu, L. Ren, J. Zhu, A. Libanori, Y. Zhu, H. Kang, S. Ahadian, M.R. Dokmeci, P. Servati, X. He, Z. Gu, W. Sun, A. Khademhosseini, Flexible patch with printable and antibacterial conductive hydrogel electrodes for accelerated wound healing, Biomaterials 285 (2022), 121479, https://doi.org/10.1016/j.biomaterials.2022.121479.
[170] A. Hasan, M. Morshed, A. Memic, S. Hassan, T.J. Webster, H.E.-S. Marei, Nanoparticles in tissue engineering: applications, challenges and prospects, Int. J. Nanomed. 13 (2018) 5637–5655, https://doi.org/10.2147/IJN.S153758.
[171] Z. Fan, B. Liu, J. Wang, S. Zhang, Q. Lin, P. Gong, L. Ma, S. Yang, A novel wound dressing based on Ag/graphene polymer hydrogel: effectively kill bacteria and accelerate wound healing, Adv. Funct. Mater. 24 (2014) 3933–3943, https://doi.org/10.1002/adfm.201304202.
[172] R. Rakhshaei, H. Namazi, A potential bioactive wound dressing based on carboxymethyl cellulose/ZnO impregnated MCM-41 nanocomposite hydrogel, Mater. Sci. Eng. C 73 (2017) 456–464, https://doi.org/10.1016/j.msec.2016.12.097.
[173] A. Chaturvedi, A.K. Bajpai, J. Bajpai, S.K. Singh, Evaluation of poly (vinyl alcohol) based cryogel–zinc oxide nanocomposites for possible applications as wound dressing materials, Mater. Sci. Eng. C 65 (2016) 408–418, https://doi.org/10.1016/j.msec.2016.04.054.
[174] G. Rath, T. Hussain, G. Chauhan, T. Garg, A.K. Goyal, Development and characterization of cefazolin loaded zinc oxide nanoparticles composite gelatin nanofiber mats for postoperative surgical wounds, Mater. Sci. Eng. C 58 (2016) 242–253, https://doi.org/10.1016/j.msec.2015.08.050.
[175] J. Xiao, S. Chen, J. Yi, H.F. Zhang, G.A. Ameer, A cooperative copper metal–organic framework-hydrogel system improves wound healing in diabetes, Adv. Funct. Mater. 27 (2017), 1604872, https://doi.org/10.1002/adfm.201604872.
[176] G. Borkow, J. Gabbay, R. Dardik, A.I. Eidelman, Y. Lavie, Y. Grunfeld, S. Ikher, M. Huszar, R.C. Zatcoff, M. Marikovsky, Molecular mechanisms of enhanced wound healing by copper oxide-impregnated dressings, Wound Repair Regen. 18 (2010) 266–275, https://doi.org/10.1111/j.1524-475X.2010.00573.x.
[177] M. Li, X. Liu, L. Tan, Z. Cui, X. Yang, Z. Li, Y. Zheng, K.W.K. Yeung, P.K. Chu, S. Wu, Noninvasive rapid bacteria-killing and acceleration of wound healing through photothermal/photodynamic/copper ion synergistic action of a hybrid hydrogel, Biomater. Sci. 6 (2018) 2110–2121, https://doi.org/10.1039/C8BM00499D.
[178] S.H. Ku, M. Lee, C.B. Park, Carbon-based nanomaterials for tissue engineering, Adv. Healthc. Mater. 2 (2013) 244–260, https://doi.org/10.1002/adhm.201200307.
[179] D. Maiti, X. Tong, X. Mou, K. Yang, Carbon-based nanomaterials for biomedical applications: a recent study, Front. Pharmacol. 9 (2019) 1401, https://doi.org/10.3389/fphar.2018.01401.
[180] E.L. Hopley, S. Salmasi, D.M. Kalaskar, A.M. Seifalian, Carbon nanotubes leading the way forward in new generation 3D tissue engineering, Biotechnol. Adv. 32 (2014) 1000–1014, https://doi.org/10.1016/j.biotechadv.2014.05.003.
[181] X. Zhao, B. Guo, H. Wu, Y. Liang, P.X. Ma, Injectable antibacterial conductive nanocomposite cryogels with rapid shape recovery for noncompressible hemorrhage and wound healing, Nat. Commun. 9 (2018) 2784, https://doi.org/10.1038/s41467-018-04998-9.
[182] S.H. De Paoli Lacerda, J. Semberova, K. Holada, O. Simakova, S.D. Hudson, J. Simak, Carbon nanotubes activate store-operated calcium entry in human blood platelets, ACS Nano 5 (2011) 5808–5813, https://doi.org/10.1021/nn2015369.
[183] S. Goenka, V. Sant, S. Sant, Graphene-based nanomaterials for drug delivery and tissue engineering, J. Contr. Release 173 (2014) 75–88, https://doi.org/10.1016/j.jconrel.2013.10.017.
[184] M.H. Norahan, M. Pourmokhtari, M.R. Saeb, B. Bakhshi, M. Soufi Zomorrod, N. Baheiraei, Electroactive cardiac patch containing reduced graphene oxide with potential antibacterial properties, Mater. Sci. Eng. C 104 (2019), 109921, https://doi.org/10.1016/j.msec.2019.109921.
[185] G. Choe, S.-W. Kim, J. Park, J. Park, S. Kim, Y.S. Kim, Y. Ahn, D.-W. Jung, D. R. Williams, J.Y. Lee, Anti-oxidant activity reinforced reduced graphene oxide/alginate microgels: mesenchymal stem cell encapsulation and regeneration of infarcted hearts, Biomaterials 225 (2019), 119513, https://doi.org/10.1016/j.biomaterials.2019.119513.
[186] Y. Liang, X. Zhao, T. Hu, B. Chen, Z. Yin, P.X. Ma, B. Guo, Adhesive hemostatic conducting injectable composite hydrogels with sustained drug release and photothermal antibacterial activity to promote full-thickness skin regeneration during wound healing, Small 15 (2019), 1900046, https://doi.org/10.1002/smll.201900046.
[187] V. Georgakilas, J.A. Perman, J. Tucek, R. Zboril, Broad family of carbon nanoallotropes: classification, chemistry, and applications of fullerenes, carbon dots, nanotubes, graphene, nanodiamonds, and combined superstructures, Chem. Rev. 115 (2015) 4744–4822, https://doi.org/10.1021/cr500304f.
[188] M. Omidi, A. Yadegari, L. Tayebi, Wound dressing application of pH-sensitive carbon dots/chitosan hydrogel, RSC Adv. 7 (2017) 10638–10649, https://doi.org/10.1039/C6RA25340G.
[189] M.J. Hajipour, K.M. Fromm, A.A. Ashkarran, D. Jimenez de Aberasturi, I.R. de Larramendi, T. Rojo, V. Serpooshan, W.J. Parak, M. Mahmoudi, Antibacterial properties of nanoparticles, Trends Biotechnol. 30 (2012) 499–511, https://doi.org/10.1016/j.tibtech.2012.06.004.
[190] R. Lanza, R. Langer, J.P. Vacanti, A. Atala, Principles of Tissue Engineering, Academic Press, 2020.
[191] G. Eke, N. Mangir, N. Hasirci, S. MacNeil, V. Hasirci, Development of a UV crosslinked biodegradable hydrogel containing adipose derived stem cells to promote vascularization for skin wounds and tissue engineering, Biomaterials 129 (2017) 188–198, https://doi.org/10.1016/j.biomaterials.2017.03.021.
[192] S. Chen, J. Shi, M. Zhang, Y. Chen, X. Wang, L. Zhang, Z. Tian, Y. Yan, Q. Li, W. Zhong, M. Xing, L. Zhang, L. Zhang, Mesenchymal stem cell-laden anti-inflammatory hydrogel enhances diabetic wound healing, Sci. Rep. 5 (2015), 18104, https://doi.org/10.1038/srep18104.
[193] W.-S. Kim, B.-S. Park, J.-H. Sung, The wound-healing and antioxidant effects of adipose-derived stem cells, Expet Opin. Biol. Ther. 9 (2009) 879–887, https://doi.org/10.1517/14712590903039684.
[194] P. Schumann, F. Tavassol, D. Lindhorst, C. Stuehmer, K.-H. Bormann, A. Kampmann, R. Mülhaupt, M.W. Laschke, M.D. Menger, N.-C. Gellrich, M. Rücker, Consequences of seeded cell type on vascularization of tissue engineering constructs in vivo, Microvasc. Res. 78 (2009) 180–190, https://doi.org/10.1016/j.mvr.2009.06.003.
[195] A. Kampmann, D. Lindhorst, P. Schumann, R. Zimmerer, H. Kokemüller, M. Rücker, N.-C. Gellrich, F. Tavassol, Additive effect of mesenchymal stem cells and VEGF to vascularization of PLGA scaffolds, Microvasc. Res. 90 (2013) 71–79, https://doi.org/10.1016/j.mvr.2013.07.006.
[196] N.-C. Cheng, W.-J. Lin, T.-Y. Ling, T.-H. Young, Sustained release of adipose-derived stem cells by thermosensitive chitosan/gelatin hydrogel for therapeutic angiogenesis, Acta Biomater. 51 (2017) 258–267, https://doi.org/10.1016/j.actbio.2017.01.060.
[197] A.G. Berger, J.J. Chou, P.T. Hammond, Approaches to modulate the chronic wound environment using localized nucleic acid delivery, Adv. Wound Care 10 (2021) 503–528, https://doi.org/10.1089/wound.2020.1167.
[198] T. Tokatlian, C. Cam, T. Segura, Porous hyaluronic acid hydrogels for localized nonviral DNA delivery in a diabetic wound healing model, Adv. Healthc. Mater. 4 (2015) 1084–1091, https://doi.org/10.1002/adhm.201400783.
[199] B. Saleh, H.K. Dhaliwal, R. Portillo-Lara, E. Shirzaei Sani, R. Abdi, M.M. Amiji, N. Annabi, Local immunomodulation using an adhesive hydrogel loaded with miRNA-laden nanoparticles promotes wound healing, Small 15 (2019), 1902232, https://doi.org/10.1002/smll.201902232.
[200] K. Klimek, G. Ginalska, Proteins and peptides as important modifiers of the polymer scaffolds for tissue engineering applications—a review, Polymers 12 (2020) 844, https://doi.org/10.3390/polym12040844.
[201] Y. Xiao, L.A. Reis, N. Feric, E.J. Knee, J. Gu, S. Cao, C. Laschinger, C. Londono, J. Antolovich, A.P. McGuigan, M. Radisic, Diabetic wound regeneration using peptide-modified hydrogels to target re-epithelialization, Proc. Natl. Acad. Sci. USA 113 (2016) E5792, https://doi.org/10.1073/pnas.1612277113.
[202] D.R. Griffin, M.M. Archang, C.-H. Kuan, W.M. Weaver, J.S. Weinstein, A.C. Feng, A. Ruccia, E. Sideris, V. Ragkousis, J. Koh, M.V. Plikus, D. Di Carlo, T. Segura, P. O. Scumpia, Activating an adaptive immune response from a hydrogel scaffold imparts regenerative wound healing, Nat. Mater. 20 (2021) 560–569, https://doi.org/10.1038/s41563-020-00844-w.
[203] S. Shafei, M. Khanmohammadi, R. Heidari, H. Ghanbari, V. Taghdiri Nooshabadi, S. Farzamfar, M. Akbariqomi, N.S. Sanikhani, M. Absalan, G. Tavoosidana, Exosome loaded alginate hydrogel promotes tissue regeneration in full-thickness skin wounds: an in vivo study, J. Biomed. Mater. Res. A. 108 (2020) 545–556, https://doi.org/10.1002/jbm.a.36835.
[204] M. Record, K. Carayon, M. Poirot, S. Silvente-Poirot, Exosomes as new vesicular lipid transporters involved in cell–cell communication and various pathophysiologies, Biochim. Biophys. Acta BBA - Mol. Cell Biol. Lipids. 1841 (2014) 108–120, https://doi.org/10.1016/j.bbalip.2013.10.004.
[205] C. Bang, T. Thum, Exosomes: new players in cell–cell communication, Int. J. Biochem. Cell Biol. 44 (2012) 2060–2064, https://doi.org/10.1016/j.biocel.2012.08.007.
[206] S.R. Baglio, D. Pegtel, N. Baldini, Mesenchymal stem cell secreted vesicles provide novel opportunities in (stem) cell-free therapy, Front. Physiol. 3 (2012) accessed October 6, 2022, https://www.frontiersin.org/articles/10.3389/fphys.2012.00359.
[207] S. Sahoo, D.W. Losordo, Exosomes and cardiac repair after myocardial infarction, Circ. Res. 114 (2014) 333–344, https://doi.org/10.1161/CIRCRESAHA.114.300639.
[208] K. Rilla, A.-M. Mustonen, U.T. Arasu, K. Härkönen, J. Matilainen, P. Nieminen, Extracellular vesicles are integral and functional components of the extracellular matrix, Matrix Biol. (2019) 75–76, https://doi.org/10.1016/j.matbio.2017.10.003, 201–219.
[209] Life with oxygen | science, n.d. https://www.science.org/doi/10.1126/science.1147949. (Accessed 6 October 2022).

[210] K.L. Covello, M.C. Simon, HIFs, hypoxia, and vascular development, in: Curr. Top. Dev. Biol., Academic Press, 2004, pp. 37–54, https://doi.org/10.1016/S0070-2153(04)62002-3.
[211] S. Schreml, R.m. Szeimies, L. Prantl, S. Karrer, M. Landthaler, P. Babilas, Oxygen in acute and chronic wound healing, Br. J. Dermatol. 163 (2010) 257–268, https://doi.org/10.1111/j.1365-2133.2010.09804.x.
[212] Q. Zhang, Q. Chang, R.A. Cox, X. Gong, L.J. Gould, Hyperbaric oxygen attenuates apoptosis and decreases inflammation in an ischemic wound model, J. Invest. Dermatol. 128 (2008) 2102–2112, https://doi.org/10.1038/jid.2008.53.
[213] S.R. Thom, V.M. Bhopale, O.C. Velazquez, L.J. Goldstein, L.H. Thom, D.G. Buerk, Stem cell mobilization by hyperbaric oxygen, Am. J. Physiol. Heart Circ. Physiol. 290 (2006) H1378–H1386, https://doi.org/10.1152/ajpheart.00888.2005.
[214] S.R. Thom, T.N. Milovanova, M. Yang, V.M. Bhopale, E.M. Sorokina, G. Uzun, D. S. Malay, M.A. Troiano, K.R. Hardy, D.S. Lambert, C.J. Logue, D.J. Margolis, Vasculogenic stem cell mobilization and wound recruitment in diabetic patients: increased cell number and intracellular regulatory protein content associated with hyperbaric oxygen therapy, Wound Repair Regen. 19 (2011) 149–161, https://doi.org/10.1111/j.1524-475X.2010.00660.x.
[215] J.I. Kang, K.M. Park, K.D. Park, Oxygen-generating alginate hydrogels as a bioactive acellular matrix for facilitating wound healing, J. Ind. Eng. Chem. 69 (2019) 397–404, https://doi.org/10.1016/j.jiec.2018.09.048.
[216] B. Wang, C. Huang, L. Chen, D. Xu, G. Zheng, Y. Zhou, X. Wang, X. Zhang, The emerging roles of the gaseous signaling molecules NO, H2S, and CO in the regulation of stem cells, ACS Biomater. Sci. Eng. 6 (2020) 798–812, https://doi.org/10.1021/acsbiomaterials.9b01681.
[217] F.S. Schanuel, K.S. Raggio Santos, A. Monte-Alto-Costa, M.G. de Oliveira, Combined nitric oxide-releasing poly(vinyl alcohol) film/F127 hydrogel for accelerating wound healing, Colloids Surf. B Biointerfaces 130 (2015) 182–191, https://doi.org/10.1016/j.colsurfb.2015.04.007.
[218] T. Takagi, T. Okayama, J. Asai, K. Mizushima, Y. Hirai, K. Uchiyama, T. Ishikawa, Y. Naito, Y. Itoh, Topical application of sustained released-carbon monoxide promotes cutaneous wound healing in diabetic mice, Biochem. Pharmacol. 199 (2022), 115016, https://doi.org/10.1016/j.bcp.2022.115016.
[219] V. Vijayan, F.A.D.T.G. Wagener, S. Immenschuh, The macrophage heme-heme oxygenase-1 system and its role in inflammation, Biochem. Pharmacol. 153 (2018) 159–167, https://doi.org/10.1016/j.bcp.2018.02.010.
[220] T. Takagi, Y. Naito, K. Uchiyama, T. Yoshikawa, The role of heme oxygenase and carbon monoxide in inflammatory bowel disease, Redox Rep. 15 (2010) 193–201, https://doi.org/10.1179/174329210X12650506623889.
[221] H. Fujimoto, M. Ohno, S. Ayabe, H. Kobayashi, N. Ishizaka, H. Kimura, K. Yoshida, R. Nagai, Carbon monoxide protects against cardiac ischemia—reperfusion injury in vivo via MAPK and akt—eNOS pathways, Arterioscler. Thromb. Vasc. Biol. 24 (2004) 1848–1853, https://doi.org/10.1161/01.ATV.0000142364.85911.0e.
[222] T. Kaizu, A. Ikeda, A. Nakao, A. Tsung, H. Toyokawa, S. Ueki, D.A. Geller, N. Murase, Protection of transplant-induced hepatic ischemia/reperfusion injury with carbon monoxide via MEK/ERK1/2 pathway downregulation, Am. J. Physiol. Gastrointest. Liver Physiol. 294 (2008) G236–G244, https://doi.org/10.1152/ajpgi.00144.2007.
[223] M.C. Ott, J.R. Scott, A. Bihari, A. Badhwar, L.E. Otterbein, D.K. Gray, K.A. Harris, R.F. Potter, Inhalation of carbon monoxide prevents liver injury and inflammation following hind limb ischemia/reperfusion, Faseb. J. 19 (2005) 106–108, https://doi.org/10.1096/fj.04-2514fje.
[224] S.A. Coavoy-Sánchez, S.K.P. Costa, M.N. Muscará, Hydrogen sulfide and dermatological diseases, Br. J. Pharmacol. 177 (2020) 857–865, https://doi.org/10.1111/bph.14699.
[225] J. Schleifenbaum, C. Köhn, N. Voblova, G. Dubrovska, O. Zavarirskaya, T. Gloe, C. S. Crean, F.C. Luft, Y. Huang, R. Schubert, M. Gollasch, Systemic peripheral artery relaxation by KCNQ channel openers and hydrogen sulfide, J. Hypertens. 28 (2010) 1875–1882, https://doi.org/10.1097/HJH.0b013e32833c20d5.
[226] P.W. Henderson, S.P. Singh, D. Belkin, V. Nagineni, A.L. Weinstein, J. Weissich, J. A. Spector, Hydrogen sulfide protects against ischemia-reperfusion injury in an in vitro model of cutaneous tissue Transplantation1, J. Surg. Res. 159 (2010) 451–455, https://doi.org/10.1016/j.jss.2009.05.010.
[227] R.M. Osipov, M.P. Robich, J. Feng, Y. Liu, R.T. Clements, H.P. Glazer, N.R. Sodha, C. Szabo, C. Bianchi, F.W. Sellke, Effect of hydrogen sulfide in a porcine model of myocardial ischemia-reperfusion: comparison of different administration regimens and characterization of the cellular mechanisms of protection, J. Cardiovasc. Pharmacol. 54 (2009) 287–297, https://doi.org/10.1097/FJC.0b013e3181b2b72b.
[228] A. Papapetropoulos, A. Pyriochou, Z. Altaany, G. Yang, A. Marazioti, Z. Zhou, M. G. Jeschke, L.K. Branski, D.N. Herndon, R. Wang, C. Szabó, Hydrogen sulfide is an endogenous stimulator of angiogenesis, Proc. Natl. Acad. Sci. USA 106 (2009) 21972–21977, https://doi.org/10.1073/pnas.0908047106.
[229] W.-J. Cai, M.-J. Wang, P.K. Moore, H.-M. Jin, T. Yao, Y.-C. Zhu, The novel proangiogenic effect of hydrogen sulfide is dependent on Akt phosphorylation, Cardiovasc. Res. 76 (2007) 29–40, https://doi.org/10.1016/j.cardiores.2007.05.026.
[230] M. Magierowski, K. Magierowska, S. Kwiecien, T. Brzozowski, Gaseous mediators nitric oxide and hydrogen sulfide in the mechanism of gastrointestinal integrity, protection and ulcer healing, Molecules 20 (2015) 9099–9123, https://doi.org/10.3390/molecules20059099.
[231] S. Nazarnezhada, G. Abbaszadeh-Goudarzi, H. Samadian, M. Khaksari, J. M. Ghatar, H. Khastar, N. Rezaei, S.R. Mousavi, S. Shirian, M. Salehi, Alginate hydrogel containing hydrogen sulfide as the functional wound dressing material: in vitro and in vivo study, Int. J. Biol. Macromol. 164 (2020) 3323–3331, https://doi.org/10.1016/j.ijbiomac.2020.08.233.
[232] Y. Lu, H. Li, J. Wang, M. Yao, Y. Peng, T. Liu, Z. Li, G. Luo, J. Deng, Engineering bacteria-activated multifunctionalized hydrogel for promoting diabetic wound healing, Adv. Funct. Mater. 31 (2021), 2105749, https://doi.org/10.1002/adfm.202105749.
[233] Y. Tang, X. Cai, Y. Xiang, Y. Zhao, X. Zhang, Z. Wu, Cross-linked antifouling polysaccharide hydrogel coating as extracellular matrix mimics for wound healing, J. Mater. Chem. B. 5 (2017) 2989–2999, https://doi.org/10.1039/C6TB03222B.
[234] A. GhavamiNejad, C.H. Park, C.S. Kim, In situ synthesis of antimicrobial silver nanoparticles within antifouling zwitterionic hydrogels by catecholic redox chemistry for wound healing application, Biomacromolecules 17 (2016) 1213–1223, https://doi.org/10.1021/acs.biomac.6b00039.
[235] L. Sheng, Z. Zhang, Y. Zhang, E. Wang, B. Ma, Q. Xu, L. Ma, M. Zhang, G. Pei, J. Chang, A novel "hot spring"-mimetic hydrogel with excellent angiogenic properties for chronic wound healing, Biomaterials 264 (2021), 120414, https://doi.org/10.1016/j.biomaterials.2020.120414.
[236] M. Li, Y. Liang, J. He, H. Zhang, B. Guo, Two-pronged strategy of biomechanically active and biochemically multifunctional hydrogel wound dressing to accelerate wound closure and wound healing, Chem. Mater. 32 (2020) 9937–9953, https://doi.org/10.1021/acs.chemmater.0c02823.
[237] E.J. Bolívar-Monsalve, C.F. Ceballos-González, C. Chávez-Madero, B.G. de la Cruz-Rivas, S. Velásquez Marín, S. Mora-Godínez, L.M. Reyes-Cortés, A. Khademhosseini, P.S. Weiss, M. Samandari, A. Tamayol, M.M. Alvarez, G. Trujillo-de Santiago, One-step bioprinting of multi-channel hydrogel filaments using chaotic advection: fabrication of pre-vascularized muscle-like tissues, Adv. Healthc. Mater. n/a (2022), 2200448, https://doi.org/10.1002/adhm.202200448.
[238] G. Ying, N. Jiang, C. Parra-Cantu, G. Tang, J. Zhang, H. Wang, S. Chen, N.-P. Huang, J. Xie, Y.S. Zhang, Bioprinted injectable hierarchically porous gelatin methacryloyl hydrogel constructs with shape-memory properties, Adv. Funct. Mater. 30 (2020), 2003740, https://doi.org/10.1002/adfm.202003740.
[239] C. Wang, H. Niu, X. Ma, H. Hong, Y. Yuan, C. Liu, Injectable Bioinspired, Quaternized hydroxyethyl cellulose composite hydrogel coordinated by mesocellular silica foam for rapid, noncompressible hemostasis and wound healing, ACS Appl. Mater. Interfaces 11 (2019) 34595–34608, https://doi.org/10.1021/acsami.9b08799.
[240] H. Zhang, X. Sun, J. Wang, Y. Zhang, M. Dong, T. Bu, L. Li, Y. Liu, L. Wang, Multifunctional injectable hydrogel dressings for effectively accelerating wound healing: enhancing biomineralization strategy, Adv. Funct. Mater. 31 (2021), 2100093, https://doi.org/10.1002/adfm.202100093.
[241] Y. Liang, Z. Li, Y. Huang, R. Yu, B. Guo, Dual-dynamic-bond cross-linked antibacterial adhesive hydrogel sealants with on-demand removability for post-wound-closure and infected wound healing, ACS Nano 15 (2021) 7078–7093, https://doi.org/10.1021/acsnano.1c00204.
[242] P. Kumar, P. Huo, R. Zhang, B. Liu, Antibacterial properties of graphene-based nanomaterials, Nanomaterials 9 (2019) 737, https://doi.org/10.3390/nano9050737.
[243] K.S. Siddiqi, A. ur Rahman, Tajuddin, A. Husen, Properties of zinc oxide nanoparticles and their activity against microbes, Nanoscale Res. Lett. 13 (2018) 141, https://doi.org/10.1186/s11671-018-2532-3.
[244] K. Rajendiran, Z. Zhao, D.-S. Pei, A. Fu, Antimicrobial activity and mechanism of functionalized quantum dots, Polymers 11 (2019) 1670, https://doi.org/10.3390/polym11101670.